Keele University

Investigating the effects of nicergoline on calcium signalling in human platelets and megakaryocytes

Dr Abdullah Mohammed Alghannam

Institute for Science and Technology in Medicine, Keele University

Thesis submitted to Keele University for the degree of Master of Philosophy

October 2017

Table of contents

1. Introduction

2. Materials and Methods

3. Results

5. Discussion

Table of figures

Abbreviation List

$[Ca^{2+}]_{cyt}$	Cytosolic Ca^{2+} concentration
$[Ca^{2+}]_{ext}$	Extracellular Ca^{2+} concentration
$[Ca^{2+}]_{st}$	Intracellular store Ca^{2+} concentration
5-HT	Serotonin
[w/v]	weight per volume
ACD	Acid Citrate Dextrose
ADP	Adenosine diphosphate
APC	Allophycocyanin
ARD1-NAT1	N-acetyltransferase 1 (arylamine N-acetyltransferase)
ATA	Aurintricarboxylic acid
ATP	Adenosine Triphosphate
BSA	Bovine serum albumin
Ca^{2+}	Calcium
CD	Cluster of differentiation
CMB	Cortical microtubule bundle
CRP	Collagen-related peptide
DAG	1,2-diacylglycerol
DM-BAPTA	Dimethyl BAPTA
DMS	Demarcation membrane system
DMSO	Dimethyl sulphoxide
DNAse	deoxyribonuclease
DTS	Dense Tubular System

EGTA	Ethylene glycol-bis(β-aminoethyl ether)-N,N,N',N'-tetraacetic acid
ER	Endoplasmic Reticulum
FITC	Fluorescein isothiocyanate
FL	Flt-3 Ligand
GPIb-IX-V	Glycoprotein Ib-IX-V complex
GPVI	Glycoprotein VI
HBS	HEPES-buffered saline
HDAC	Histone deacetylase
IL	Interleukin
IP_3	Inositol 1,4,5-trisphophate
IP_3R	Inositol 1,4,5-triphosphate receptor
L_{max}	Maximum Luminescence
MC	Membrane complex
NAADP	Nicotinic acid adenine dinucleotide phosphate
NCX	Na+/Ca^{2+} exchanger
OCS	Open Canalicular System
Orai1	Calcium release activated calcium channel protein 1
PAR	Protease-activated receptor
PBS	Phosphate-buffered saline
PIP_2	Phosphatidylinositol 4,5-bisphosphate
PLC	Phospholipase C
PMCA	Plasma membrane Ca^{2+} ATPase
PRP	Platelet-rich plasma
PTM	Posttranslational modification
SCF	Stem cell factor

SEM Standard error of the mean

SERCA Sarco/endoplasmic reticulum Ca^{2+}-ATPase

SIRT2 Sirtuin deacetylase2

SOCE Store-operated Ca^{2+} entry

STIM1 Stromal interaction molecule 1

TBHQ 2,5-di –(t-butyl)-1,4-hydroquinone

Thr Thrombin

TPO Thrombopoietin

TSA Trichostatin A

vWF von Willebrand factor

Acknowledgements

First and foremost, I would like to thank God for giving me the opportunity to study at ISTM, Keele University. I am highly indebted to my supervisor Dr Alan Harper for his guidance and constant supervision as well as for providing necessary information regarding the project & also for his support in completing the project. I would like to express my gratitude towards my parents and my wife who have willingly helped me out with their abilities and encouragement. I would like to acknowledge Dr Carmen Coxon for lending the Light Transmission Chronolog Aggregometer. I have taken efforts in this project. However, it would not have been possible without the support and help of my colleagues Faiza Musa, Peter son Anand and kind cooperation of all the blood donors. I would like to extend my sincere thanks to all of them.

Abstract

Recent study suggested that the anti-platelet effect of nicergoline is caused by inhibiting agonist-evoked Ca^{2+} signalling by disrupting the normal localization of the dense tubular system in human platelets. This effect is brought about by the disruption of the cortical microtubule bundle which plays a role in holding the dense tubular system in its normal location. However, these previous studies did not define the mechanism by which nicergoline induces this disruption of the cortical microtubule bundle. In this study we aimed to further elucidate the mechanism by which nicergoline could disrupt the localization of the microtubules in human platelets. To do this we have examined the effect of inhibitors of microtubule motor proteins such as kinesin, dyneins and myosin, as well as inhibitors of microtubule deacetylases to see whether these can mimic or modulate the effects of nicergoline on platelet Ca^{2+} signalling and functional responses. These experiments have demonstrated that myosin, dyneins and histone deacetylases are not the targets of nicergoline due to inhibitors of these targets failing to recreate the effects of nicergoline in both Ca^{2+} signalling and platelet function assays. In contrast, our data does demonstrate the potential for kinesins to be a target of nicergoline's action, as an inhibitor of these motor proteins recapitulates the effect of this drug on thrombin-evoked Ca^{2+} signalling and platelet function assays. In addition, combined treatment with both drugs does not produce cumulative effects suggesting that they are working through the same pathway. These data give further insight towards the mechanism underling the anti-platelet effect of nicergoline and suggest an important role for the platelet molecular motor proteins in regulating platelet function and to be a possible target of action for a novel anti-platelet therapy in future.

1. Introduction

1.1 Basic Principles of Haemostasis

Haemostasis involves a set of interrelated mechanisms which are triggered by damage to blood vessels that helps the circulation maintain its functional integrity (Furie *et al*., 2008). Upon damage to the vessel wall, a coordinated sequence of events elicited by the local activation of platelets helps the blood vessel to prevent further bleeding and allow it to regain its normal structure and function (**Fig 1.1**). In the undamaged vessel, platelets are quiescent and unable to aggregate. The intact endothelial lining of the vessel wall helps keep platelets from activation by producing a number of substances which inhibit platelet activation, such as prostacyclin and nitric oxide (Ignarro *et al*., 1987; Palmer *et al*., 1987; Marcus *et al*., 2002). Endothelial cells further prevent blood clotting through expression of the ectonucleotidase, CD39, on their cell surface, which reduces autocrine signalling between platelets (Marcus *et al*., 2005).

Upon damage to the blood vessel, the inhibitory endothelial lining is removed and platelets are activated by their exposure to the subendothelial matrix, which contains adhesive ligands such as collagen, which can directly bind and activate platelets (Furie *et al*., 2008) as well as tissue factor which activates the extrinsic coagulation pathway leading to local production of the platelet agonist, thrombin (Vu *et al*., 1991). This initial stage of activation includes the adhesion of platelets to the subendothelial matrix at the site of injury (*adhesion*), triggering platelet activation which causes platelets to spread and secrete their granules to recruit other circulating platelets (*recruitment)*.

Platelet stimulation also triggers the activation of the platelet fibrinogen receptor, integrin $\alpha_{IIb}\beta 3$, which allows platelets to create an aggregate through binding to one another via fibrinogen (*Cohesion*; Brass *et al*., 2011). This initial clot is then stabilized further by the activation of the clotting cascade leading to creation of a fibrin scaffold that mechanically supports the thrombus against the effects of flowing blood (*Stabilization*; Brass *et al.,* 2011). Clot retraction is the final event of thrombus formation which helps to bring the damaged vessel wall together and allow the final wound to begin to heal (Feghhi & Sniadecki, 2011).

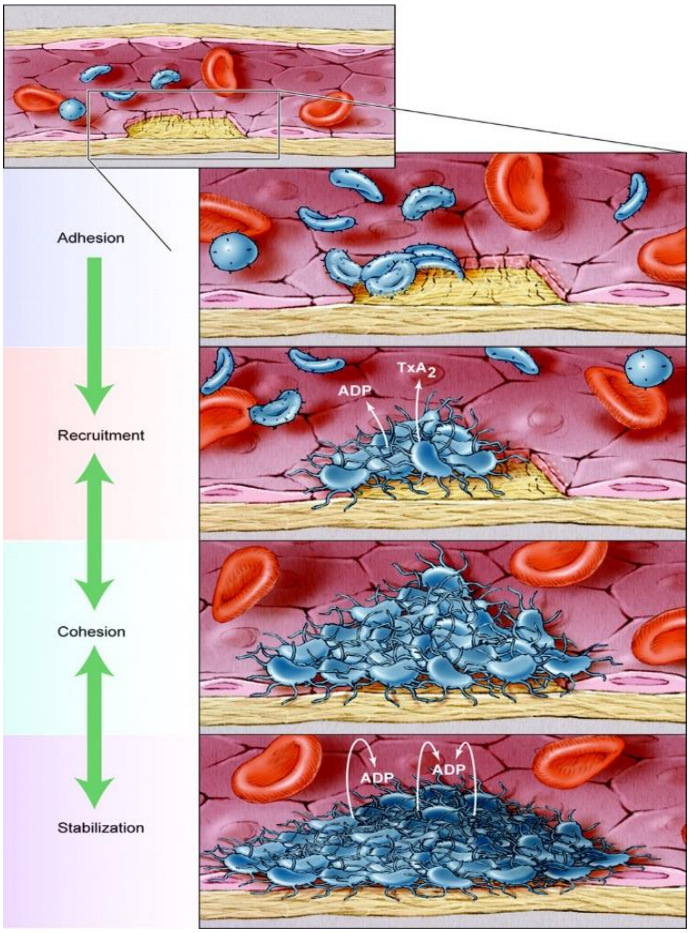

Figure 1.1: **Fundamental steps of haemostasis**: The intact endothelium prevents activation of resting platelets through secretion of inhibitory messengers such as prostacyclin and nitric oxide. Upon vascular damage, platelets are exposed to the subendothelial collagen and/or locally-formed thrombin which triggers their activation so they can adhere at the site of damage. This initial layer of activated platelets releases autocrine messengers such as ADP and thromboxane A_2 which help activate and recruit more platelets to the forming thrombus, where they are able cohere with each other via fibrinogen and the activated integrin $\alpha_{IIb}\beta_3$ (Figure reproduced from Brass et al., 2006).

1.2 Inappropriate platelet activation elicits pathological blood clotting responses

The normal haemostatic pathway is principally controlled by platelet activation responses – thus when platelets have an insufficient reaction to vessel injury, this can lead to a tendency for the affected individual to have a propensity to suffer from excessive bleeding in response to injury (called a bleeding diathesis). The complex, multi-step nature of platelet activation can be seen in the human conditions that result from molecular defects in each of the basic steps of haemostasis identified above. This includes failure to adhere to the damaged subendothelial matrix (e.g. Von Willebrand's disease, Bernard Soulier syndrome), failure to recruit circulating platelets (e.g. storage pool disorders, Hermansky-Pudlak syndrome), failure to aggregate (e.g. Glanzmann's thrombasthenia) and failure to stabilize the thrombus (e.g. Haemophilia, Scott's syndrome). In contrast, platelet activation in undamaged vessels or uncontrolled thrombus formation can lead to vascular obstruction. Such unwanted platelet activation underlies a range of cardiovascular disorders such as myocardial infarction, stroke or deep vein thrombosis (Furie *et al*., 2008). Thus by understanding the normal cell biology of platelets it may be possible to uncover new ways of treating patients with overactive or underactive clotting responses.

1.3 Platelet structure

Platelets are the smallest blood cells in the body, with 150-400 $x10^9$ platelets found in each litre of blood. Unstimulated platelets are disc-shaped cells of about 2-3 µm in diameter and 6-8 fL in volume (Zucker-Franklin, 1997). Platelets are anucleate cells which also lack a number of other core cellular organelles such as the mitotic apparatus

and Golgi apparatus (Gibbins, 2004; Zucker-Franklin, 1997). As shown in **Fig 1.2**, platelets have a number of other key ultrastructural features which are the presence of a thick glycocalyx (Zucker-Franklin & Petursson, 1984), an invagination of their plasma

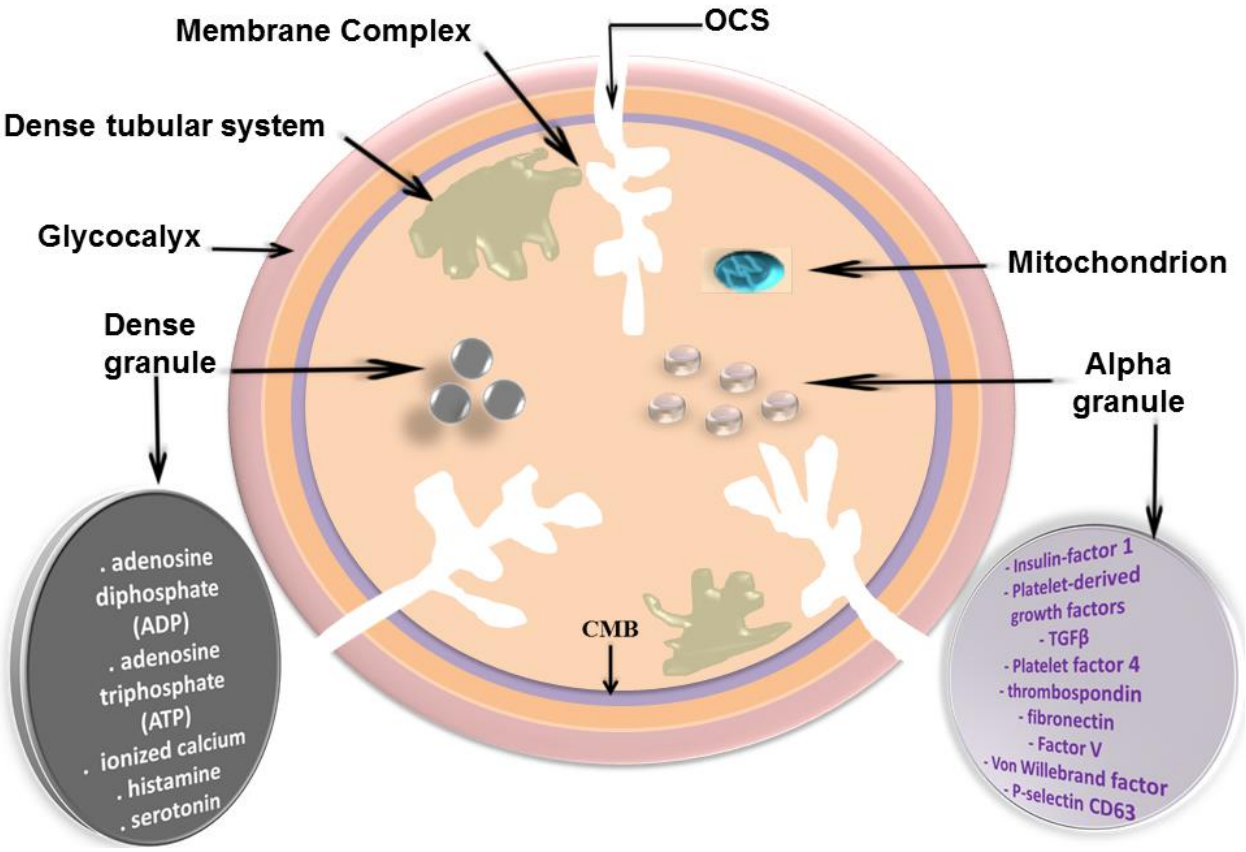

Figure 1.2: Diagram showing the basic structure of a resting platelet: Platelets are discoid cells maintained by the presence of a submembrane cortical microtubule bundle (CMB) These cells also possess a specialized invagination of their plasma membrane called the open canalicular system (OCS). The OCS spreads throughout the cell and comes into close contact with the main platelet Ca^{2+} store, the dense tubular system (DTS) – this structure is called the membrane complex. In addition to this platelets possess a number of different secretory granules (α-granules, dense granules and lysosomes) which possess a range of biologically-active molecules which can contribute to haemostasis and inflammatory processes within the body. The platelet is also notable amongst blood cells for possessing a thick glycocalyx, which includes a range of glycoproteins important for platelet activation.

membrane system called the open canalicular system (OCS) and the presence of a number of characteristic organelles such as the dense tubular system (DTS), the alpha and dense granules.

1.3.1 Platelet discoid shape and the cytoskeleton

1.3.1.1 The cortical microtubule bundle

The resting platelets discoid appearance is a characteristic feature of these blood cells and is thought to be maintained by the presence of a cortical microtubule bundle which lies directly under the platelet plasma membrane (Behnke, 1965; Italiano *et al*., 2003; White & Krivit, 1967; White, 1968a; White & Rao, 1998). Microtubules are made up of heterodimers of globular α-tubulin and β-tubulin polypeptides (Downing and Nogales, 1998; Sullivan, 1988). The platelet cortical microtubule bundle is thought to consist of a single microtubule chain made up of significant quantities of β_1 tubulin (Schwer *et al*., 2001). The cortical microtubule polymer is rolled up into 8-12 coils giving the appearance of a bundle of closely associated filaments when observed in cross section (White & Krivit, 1967; White & Rao, 1998; Italiano *et al*., 1999). The loose coiling of the cortical microtubule bundle has been shown to be influenced by kinesin and dynein molecular motors, which work antagonistically in the resting platelet to prevent the contraction of the cortical microtubule ring (Diagouraga *et al*., 2014).

It has been found that β_1-tubulin is the predominant isoform of β-tubulin present in platelets (Wang et al., 1986; Lewis *et al*., 1987; Lecine *et al*., 2000) and its expression is largely restricted to the megakaryocyte lineage (Schwer *et al.,* 2001). It has been found that mice deficient in the platelet-specific β_1-tubulin protein had reduced numbers of

platelets due to an effect of this loss on thrombopoiesis, as well as spherical platelets due to the reduced number of microtubule coilings observed in these cells (Schwer *et al.* 2001). Interestingly these platelets showed a reduction in some (but not all) responses to *in vitro* stimulation with thrombin (Schwer *et al.,* 2001; Italiano *et al.,* 2003). These data suggest that the maintenance of the normal cortical microtubule bundle may play a role in eliciting normal platelet function (Schwer *et al*., 2001).

1.3.1.2 The cortical actin cytoskeleton

Platelets also contain an actin microfilamentous system. Actin filaments (F-actin) are made of polymers of globular actin proteins. In resting platelets, around 30-40% of actin molecules are assembled into the microfilaments, with the rest available for polymerization u;2pon platelet activation (Fox *et al.*, 1984). In the resting platelet, much of the F-actin is found congregated in a cortical actin ring (Rosado *et al*., 2000). However disassembly of the cortical actin ring has been shown to have limited effect on resting platelet shape (White & Rao, 1998). In the resting state the actin microfilaments have all the cellular organelles arranged in a way that they are away from the plasma membrane as well as separate from each other. However when the cell is activated, the actin filaments start to form filaments within the cell periphery and also within the developing filopodia (Fox, 1993). The actin filaments assemble into parallel bundles which allows the platelet to spread over the exposed subendothelial matrix (Fox, 1993). The actin cytoskeleton has been shown to bind indirectly to the cytoplasmic tails of Glycoprotein Ib-IX-V (GPIb-IX-V) and the integrin $\alpha_{IIb}\beta_3$ indirectly via a number of actin-binding proteins as well as elements of the contractile system including myosin and

calmodulin. Collectively this contractile system helps translocate these receptors to the external surface of the resting platelet (Michelson, 2013).

1.3.2 Platelet membrane organization

Platelet membrane structure is principally made up of two highly-organised membrane systems; the open canalicular system (OCS; which is originated from the platelet surface; **Fig 1.3**; Behnke, 1967; Behnke, 1968) and the dense tubular system (DTS; which is derived from the smooth endoplasmic reticulum of the megakaryocytes; White, 1972).

1.3.2.1 The open canalicular system

The OCS is known to derive from the remnants of the megakaryocyte's demarcation membrane system (DMS; Zucker-Franklin, 1989). The OCS is made up of a complex series of invaginations of the plasma membrane of the platelet – and can be seen in electron microscopic cross-sections as glycocalyx-lined clear vacuoles between the other cytoplasmic elements (Figure 4), which appear to have a similar composition to the platelet plasma membrane (White, 1972; van Nispen tot Pannerden *et al*., 2010). The channels of the OCS can be seen connected with the platelet exterior and remain open during platelet activation, cell shape change and release (White, 1973; White, 1974). The OCS serves to increase the surface area of the platelet exposed to plasma

.

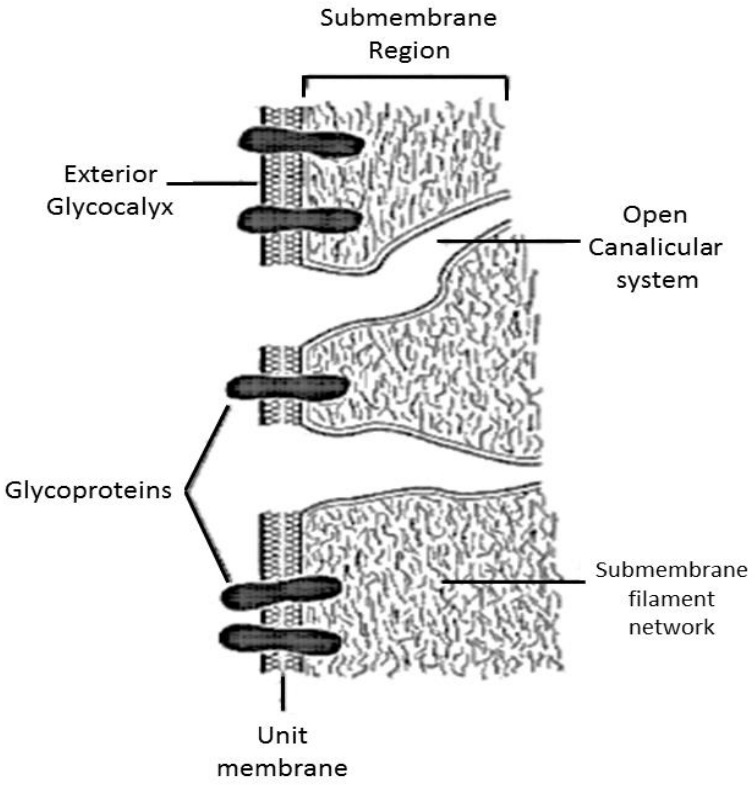

Figure 1.3:**The structure of the platelet plasma membrane.** Figure showing glycocalyx and invaginations of plasma membrane to form Open canalicular system (Modified from Frederick & Richard, 1997).

and allows communication of the deepest region of the platelet with the extracellular space (White, 1968a). Previous work has shown that the OCS acts as a two way channel both allowing for plasma-derived substances to be taken-up and stored in platelet secretory vesicles but also to allow the release of granule contents into the plasma during platelet activation (White, 1972). As such the OCS is considered a key channel for transport around the platelet.

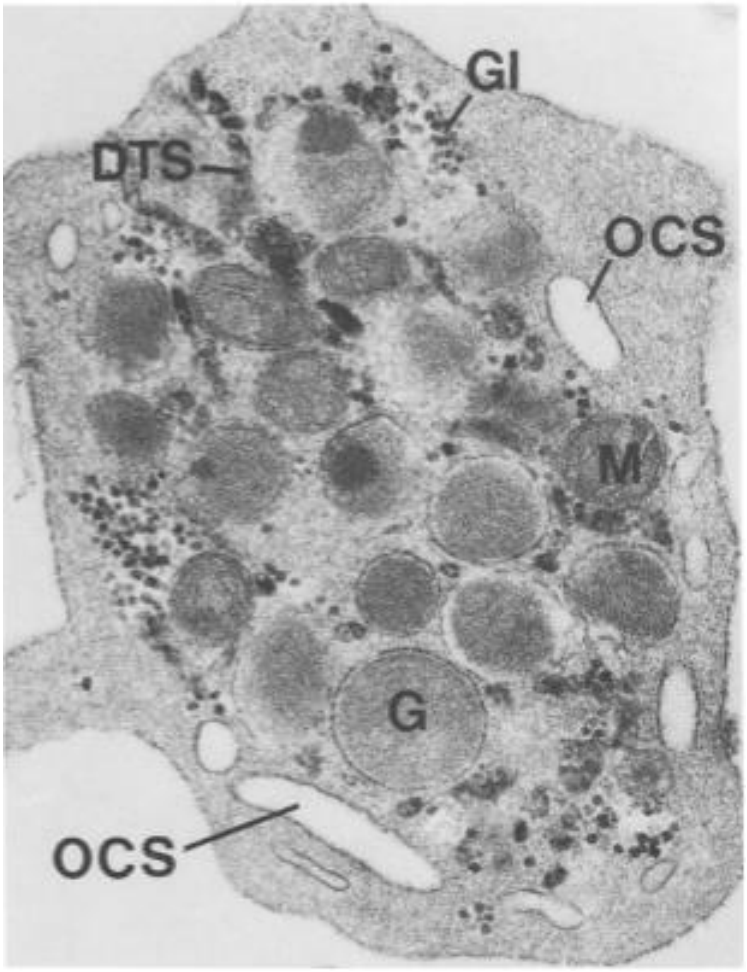

Figure 1.4: **Electron micrograph showing a cross-section through a platelet demonstrating the structural arrangements of the major membrane systems**: DTS; dense tubular system, OCS; Open canalicular system, GI; glycogen and M; mitochondrion (Reproduced from Zucker-Franklin, 1997).

1.3.2.2 The dense tubular system

The other major membrane structure found within platelets is called the dense tubular system (**Fig 1.4**). The DTS is derived from the residual endoplasmic reticulum of the megakaryocyte (Behnke, 1968). Like the endoplasmic reticulum of other cells, the DTS stores large amounts of Ca^{2+} (Gerrard *et al*., 1978) and is known to be the principal site of agonist-evoked Ca^{2+} release upon platelet activation (Sage *et al*., 2011; See section 1.5.). The DTS also contains the enzymes required for the synthesis of prostaglandins

(Cutler *et al*., 1978; Kaser-Glanzmann *et al.*, 1978; Gerrard *et al*., 1976). The DTS can be selectively labelled in electron microscopic slices by cytochemically labelling this compartment utilizing a reaction catalyzed by the peroxidase activity associated with prostaglandin synthesis in the DTS (Gerrard *et al*., 1976). The DTS can also be characterized by the presence of proteins containing the endoplasmic reticulum retention signal, KDEL, which are selectively found in this location (van Nispen tot Pannerden *et al*., 2010).

The DTS has been shown to closely associate with the cortical microtubule bundle in a number of electron microscopy studies – suggesting that the cortical microtubule bundle may be anchored to the DTS and may be responsible for its distribution in the platelet (Behnke, 1965; White, 1969; White, 1968b). Interestingly, the DTS has been shown to be rapidly reorganized upon platelet activation – suggesting that there are active mechanisms that control the distribution of this organelle within the platelet (Ebbeling *et al*., 1992).

1.3.2.3 The membrane complex

Although the OCS and DTS are observed to form distinct membrane systems within the platelet, they can also be to be closely apposed to one another in a specific subregion of the platelet known as the membrane complex (White, 1972; van Nispen tot Pannerden *et al*., 2010; **Fig 1.5**).

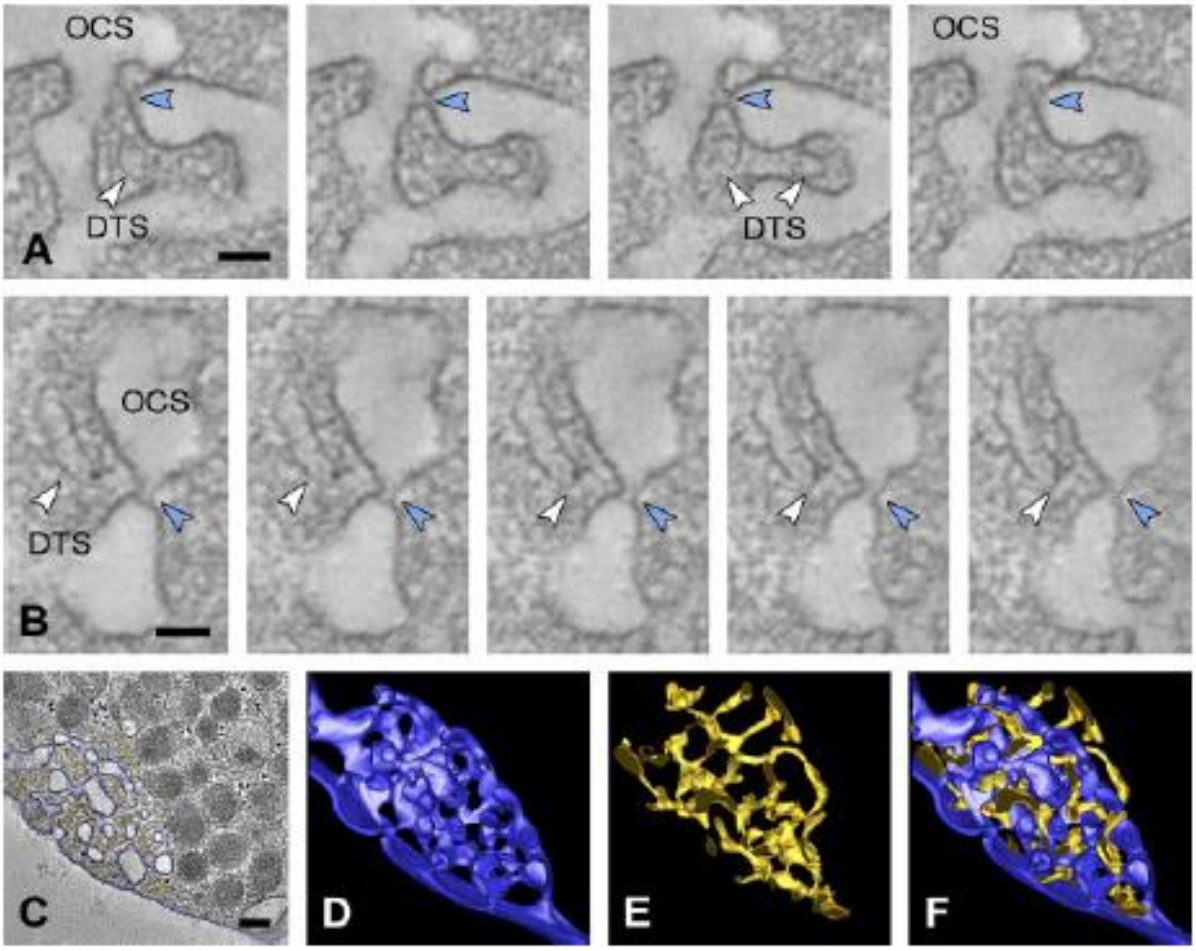

Figure 1.5: Structure of the membrane complex. Cross section tomography scanning showing the two components of the platelet membrane system: (A and B) Continuities of the surface membrane forming the OCS (blue arrowheads) come in close contact with DTS membrane (white arrowheads) at the OCS neck regions. (C) The two components in 3D-imaging showing the association representing the membrane system. (D and E) Three-dimensional imaging showing the structure of the OCS (blue) and DTS (yellow). (F) 3D reconstruction showing the close apposition between the OCS and DTS (Reproduced from van Nispen tot Pannerden et al., 2010).

The close apposition of these two membrane systems is unique among blood cells and the only equivalent structures in the human body are the nanojuctions created between the T-tubule and sarcoplasmic reticulum of striated muscles (Ezerman & Ishikawa, 1967; Hagopian & Spiro, 1967), and the sarcoplasmic reticulum and plasma membrane in smooth muscle cells (van Breemen *et al*., 2013). This similarity in platelet and muscle

structure has long been established (Grette, 1962; White, 1967), yet despite the membrane complex having being hypothesized to play a role in platelet Ca^{2+} signalling in an analogous manner to its role in striated muscle (White, 1972), the significance of this structure remains uncertain. In other cell types these nanometer-scale interactions of membranes are referred to as nanojunctions (van Breemen *et al*., 2013). The close interaction of transporters and channels involved in Ca^{2+} signalling here allow these nanojunctions to have Ca^{2+} signals which are isolated from the bulk cytosol and thus can create a specialized nanodomain which can allow Ca^{2+} to independently control a range of Ca^{2+}-sensitive processes within the same cell type (van Breemen *et al*., 2013).

1.3.3 Other key platelet organelles

Platelets also have a range of other membrane-bound organelles inside them including α-granules, dense granules and lysosomes (Figure 2). Platelets can also be seen to contain glycogen granules and mitochondria randomly distributed in the cytoplasm - the presence of both mitochondria and glycogen suggested that oxidative phosphorylation and glycolysis both are an energy source for the cells (Zucker-Franklin, 1981).

1.3.3.1 α-granules

The α-granules are the most abundant type of granule present within platelets, with around 40-80 α-granules seen in each cell (Harrison and Cramer, 1993; Reed, 2007). The α-granules are oval in shape and around 200-500nm in diameter (Fox, 1993). The α-granules contain zones of distinct electron density – including an electron-dense nucleoid where β-thromboglobulin, platelet factor 4 and proteoglycans are concentrated,

and an adjacent translucent area containing key proteins involved in haemostasis such as von Willebrand factor (vWF), factor V and fibrinogen (White, 1993; Maynard *et al*., 2007; McRedmand, 2007). A range of other proteins (e.g. coagulation factors, adhesive proteins, chemokines, protease inhibitors, vascular endothelial growth factor and endostatin) are also found within the alpha granules either due to the biosynthesis of those proteins and packaging into the alpha granules in the megakaryocytes or by their uptake from the plasma by endocytosis (George, 1990; George, 1991). Previous work has suggested that contents of α-granules can be differentially released upon activation of the PAR-1 or PAR-4 thrombin receptors (Harrison and Cramer, 1993) although this is controversial and more recent evidence has disputed this claim (Sehgal & Storrie, 2007,2009). The exocytosis of α-granules upon platelet activation allows the release of adhesive proteins (such as fibronectin and chemokines) that can take part in leukocyte and platelet activation at the site of vascular injury (Gear & Camerini, 2003).

1.3.3.2 Dense granules

Dense granules are electron-dense organelles of around 20-30 nm in diameter observed in the platelet cytoplasm when viewed in cross section by electron microscopy (White, 1993). In contrast to alpha granules, every platelet contains only 3-8 dense granules per cell (White, 1993). Dense granules contain a high concentration of calcium, serotonin, adenosine diphosphate (ADP), adenosine triphosphate (ATP) and pyrophosphate (Ruiz*et al*., 2004; Prada *et al*., 1967; White, 1968b; Martin *et al*., 1974), as well as membrane glycoproteins such as Integrin $\alpha_{IIb}\beta_3$, GPIb-V-IX and P-selectin. Platelet dense granule secretion is important for platelet aggregation as the release of

autocrine signalling molecules such as ADP, ATP and serotonin are known to play a role in triggering platelet recruitment to the growing thrombus (Nesbitt *et al*., 2003) through thei;r respective receptors on the platelet surface (P_{2Y1}/P_{2Y12} receptors for ADP, P_{2X1} receptor for ATP and 5-HT_{2A} receptor for serotonin). In addition, release of serotonin may also play a key role in vasoconstriction of smooth muscle cells in the media of the damaged blood vessel helping reduce blood flow through the damaged blood vessel (Lesurtel *et al*., 2006; McNicol & Israels, 1999).

1.3.3.3 Lysosomes

Platelets also contain a small number of lysosomes. They originate from the endosomal membrane system (Huizing *et al*., 2008). Upon platelet activation, lysosomal secretion occurs at a slower rate and requires stronger agonist stimulation than the α- and dense granules (Kaushansky *et al*., 2010). Lysosomes contains a number of different hydrolases such as as β-glucuronidase, β-galactosidase, elastase, heparitinase, β-glycerophosphatase and collagenase which are released upon platelet activation (Marcus *et al*., 1966, Bentfeld-Barker & Bainton, 1982). Lysosomal secretion at the site of vascular damage elicits release of elastase and collagenase at the site of thrombus formation – potentially playing a role in remodeling of the extracellular matrix of the damaged vessel (Zhang *et al*., 2001). Heparitinase release cleaves endothelial cell heparin and the resultant soluble heparin has been shown to function as an inhibitor of smooth muscle cell growth (Castellot *et al*., 1982).

1.4. Megakaryocytes as a model system for studying the membrane complex

Given the small diameter of the platelet and the nanometer scale of the open canalicular system, live cell imaging of the pericellular Ca^{2+} signals is difficult to localise to subregions of the platelet. In addition, it is not possible to genetically manipulate the anucleate platelet. Megakaryocytes are the parent cell of the platelet, and as such much larger than the platelet (mature megakaryocytes range from 20-100 μm in diameter). Megakaryocytes eventually fragment into platelets through a coordinated series of developmental changes (Richardson *et al*., 2005).

Importantly, megakaryocytes possess an invaginated membrane system analogous to the OCS of the platelet, called the demarcation membrane system (Yamada, 1957; Behnke, 1968; Nakao *et al.*, 1968). The DMS extends inwardly through the megakaryocyte dividing it into small sections of cytoplasmic compartments which were previously thought to demarcate the location of future platelets (Breton-Gorius & Reyes, 1976; Paulus *et al.*, 1979; Tavassoli, 1980). Recent work has suggested that this system acts as a membrane reservoir needed to form the proplatelets (Yamada, 1957; Radley and Haller, 1982; Schulze *et al*., 2006). The DMS has been shown electrophysiologically to be continuous with the surface membrane of the megakaryocyte (Mahaut-Smith *et al*., 2003).

Previous studies have tracked the DMS using fluorescent membrane indicators (Mahaut-Smith *et al*., 2003), soluble extracellular fluid tracers (Mahaut-Smith *et al*., 2003), or through fluorescent labelling of either GPIb (Eckly *et al*., 2013) or PIP_2-binding proteins (Schulze *et al*., 2006). Recently, these techniques have been used to further study the origin of the DMS in the developing megakaryocyte. Tracking the formation of

the DMS has shown that its initial form, the pre-DMS, occurs early in the megakaryocyte development process and is found to extend from the cell surface into a perinuclear location between the lobules of the megakaryocyte nucleus (Eckly *et al*., 2013). From here the DMS develops in a more elaborate manner extending through the whole of the cytosol of the megakaryocyte. Most importantly, in later stages of megakaryocyte development, the DMS can be seen to form intimate connections with the endoplasmic reticulum (ER) – creating a structure similar to the platelet membrane complex (Eckly *et al*., 2013). This ER-DMS association has also been observed by other investigators (Breton-Gorius & Guichard, 1972) suggesting this nanojunction is a key feature of mature megakaryocytes.

The megakaryocyte therefore provides a potentially attractive model system as it possesses a proteome closely-related to that of the platelet, has a nanojunction similar to the membrane complex of platelets made up of the DMS and ER, and is open to genetic manipulation (e.g. Schulze *et al*., 2006). In addition, due to their larger size, using human megakaryocytes may help make live-cell imaging of microdomains of Ca^{2+} more feasible. Due to these favorable properties, megakaryocytes cultured from $CD34^{+}$ haematopoietic stem cells may present a model system in which we can follow the development, structure and function of the platelet membrane complex.

1.4.1 Principles of in vitro megakaryocyte culture

The ability of stem cells to produce many kinds of cells upon proliferation and differentiation promises a wide scope of development in treating many diseases as well as future improvement in transfusion medicine. Our knowledge about *in vitro* culturing of megakaryocytes has been driven by the aim of further producing platelets *in vitro* from these cells, to support the increasing demand for platelet transfusions in patients who are thrombocytopenic due to chemotherapy or haematopoietic stem cell transplantation (Kessinger *et al*., 1988). This clinical need has driven an improvement of the methods used to derive mature megakaryocytes and functional platelets from $CD34^+$ cells. A number of studies have shown the feasibility of effectively producing megakaryocytes and platelets *in vitro* from human stem cells from bone marrow, umbilical cord and peripheral blood through appropriate treatment with cytokines including thrombopoietin (Long *et al*., 1982; Gordon *et al*., 1990; Ogawa, 1993; Morita *et al*., 2011). In vitro production of platelets requires a consideration of the wide range of variables that can regulate megakaryocyte growth and development from hematopoietic stem cells (Reems *et al*., 2010).

The most studied aspects of *in vitro* culturing of megakaryocytes is the composition of the cocktail of cytokines used to trigger proliferation, differentiation and growth of megakaryocytes. Thrombopoietin is considered to be the key cytokine responsible for triggering megakaryocyte growth and differentiation (Gurney *et al*., 1994; Alexander *et al*., 1996; Kaushansky *et al*., 1995), in addition to its important role in the preservation of the hematopoietic stem cell population (Kaushansky, 1999; Drachman, 2000). Other cytokines including Interleukin-3 (IL-3; Qudenrijn *et al*., 2000; Dolzhanskiy *et al.,* 1997;

Schattner *et al.,* 1996), stem cell factor (SCF; Dolzhanskiy et al., 1997; Cortin *et al.,* 2005), IL-6 (Proulx *et al*., 2003; Dolzhanskiy *et al*., 1997), IL-9 (Cortin *et al*., 2005; Fujiki *et al.,* 2002) and IL-11 (De Brauyn *et al*., 2005; Matsunaga *et al.,* 2006) act in synergism with thrombopoietin in increasing the megakaryocytes number. Other cytokines specifically IL-3, Flt-3 Ligand (De Bruyn *et al*., 2005; Matsunaga *et al*., 2006; Feng *et al.,* 2005; Sigurjonsson *et al.,* 2004) and SCF (Sitnicka *et al*., 1996; Kobayashi *et al.,* 1996) act with Thrombopoietin to assist the immature progenitor cells reproduction although some studies consider IL-3 as an inhibitor of megakaryocyte growth (Dolzhanskiy *et al.,* 1997).

Another key variable is the type of media used to grow megakaryocytes - media containing serum were commonly used, however because serum may contain growth inhibitors (Luft *et al*., 1998), many companies have started to produce media with serum alternatives namely albumin, insulin and transferrin (Brunner *et al*., 2010; Bieback *et al.,* 2009). In addition, the physical and chemical conditions of the culture such as the partial pressure of oxygen (LaIuppa *et al*., 1998; Mostafa *et al.,* 2000; Mostafa *et al*., 2001), media pH (Yang *et al.,* 2002) and temperature (Proulx *et al.,* 2004; Pineault *et al*., 2008) need to be regulated to meet the optimal conditions for megakaryocyte maturation and differentiation. Lastly, continuous swapping of culture media to get rid of metabolic waste products is important to prevent accumulation of waste materials such as ammonia and lactic acid, which inhibit megakaryocyte growth and improve the availability of oxygen, glucose and glutamine levels (Reems *et al.,* 2010).

1.4.2 Stages of megakaryocyte development

To understand the success of any *in vitro* megakaryocyte cultures it is important to understand the normal stages of megakaryocyte development. The stages of megakaryocyte maturation and differentiation are distinguished by the cytoplasmic and nuclear changes that occur throughout the process of megakaryopoiesis and thrombopoiesis (Deutsch & Tomer, 2006).

Megkaryocytes are derived from $CD34^+$ haematopoietic stem cells found within the bone marrow of adults (Long *et al.,* 1982; Gordon *et al.,* 1990; Ogawa, 1993; Morita *et al.,* 2011). Haematopoietic stem cells with CD34 protein were first identified in 1984 and have given special importance in considering the hematopoiesis in bone marrow (Civin *et al.,* 1984). Nowadays evidence has shown that cells with CD34 protein can also occur in stromal, vascular and epithelial tissues (Sidney *et al*., 2014).

The first stage of megakaryocyte development starts with about 20% of all the haematopoietic cells committed for platelet production called megakaryoblasts. A human marrow megakaryoblast is up to 24 micrometer in spherical diameter, the nucleus is somewhat large and mildly serrated containing poorly differentiated chromatin and multiple nucleoli. Tiny Golgi complex, some of mitochondria and α-granules with plenty of free ribosomes can be noticed in a few basophilic cytoplasm (Kaushansky *et al.,* 2010).

The early stages of megakaryopoiesis are characterized by the expression of the integrin α_{IIb} gene (Tronik-Le Roux *et al.,* 1995) and the cell surface protein integrin $\alpha_{IIb}\beta_3$ becomes clear and active at these stages with a marked increase in the cytoplasmic

content of this integrin in its granular compartment (Bennett, 2005). In addition, the glycoprotein Ib-IX complex (Debili *et al*., 2001) and glycoprotein V (Hickey *et al.,* 1993) are also expressed.

Interestingly, the megakaryoblast starts to invaginate its plasma membrane which forms the demarcation membrane system (Breton & Reyes, 1976) which is thought to play a vital role in the process of platelet production later (Italiano & Shivdasani, 2003).

The megakaryoblast shows a highly-lobular nucleus with increased chromosomal number ranging from 8-128 times that of normal cells which is characteristic of megakaryocytes and is created by repeated DNA replication without nuclear or cytoplasmic division in a process called endomitosis which is completed by the end of stage 2 of megakaryopoiesis (Ebbe & Stohlman, 1965).

The second stage is found in 25% of the megakaryocytes in bone marrow. This stage is characterised by cytoplasmic expansion with less dense basophilic staining and plenty of organelles and platelet-specific α- granules which contain specific proteins such as fibrinogen and von Willebrand Factor (vWF; Henijnen *et al*., 1998; Handagama *et al.,* 1987) as well as mitochondria and dense granules. Cell size is up to 30 µm in diameter, the nucleus is multilobed and the demarcation membrane system becomes more extended and obvious with more prominent endomitosis of the nucleus (Kaushansky *et al.,* 2010).

In stages 3 and 4 of megakaryocyte maturation, the cytoplasm continues to expand and becomes acidophilic and cell size is up to 50 µm in diameter. These cells posses large numbers of ribosomes and a large multi-lobed, laterally-located, pyknotic nucleus. The

demarcation membrane system extends more and substitutes the endoplasmic reticulum and Golgi apparatus (Kaushansky *et al*., 2010).

Furthermore, the megakaryocyte commences the formation of proplatelets (**Fig 1.6**) by the formation of long and precise cytoplasmic protrusions which extend as pseudopodia and are formed by exterior movement of the internal membranes (Patel *et al*., 2005) and serve to transport the organelles and other constitutive substances needed for platelet formation from the megakaryocyte cell body to the branched distal ends which represent the sites of future platelet production (Kaushansky *et al.,* 2010).

Proplatelet formation persists till the cytoplasm is totally exhausted and converted into proplatelets linked to each other by cytoplasmic filaments (Italiano *et al*., 1999; Andrews *et al*., 1993). The nuclear material is converted into an eccentric body containing scarce cytoplasm and finally decomposes (Patel *et al.,* 2005). In the end, the proplatelet tips grow into masses which become the primary sites of platelet production and liberation (Patel *et al.,* 2005) and this happens when the proplatelet masses start to release mono proplatelets due to the retraction which separate the proplatelets from the cell body (Italiano *et al*., 1999). The released proplatelets are a series of platelet-sized bodies connected in the middle by a shaft which thought to tighten gradually and detach releasing the platelet like particles (Patel *et al.,* 2005).

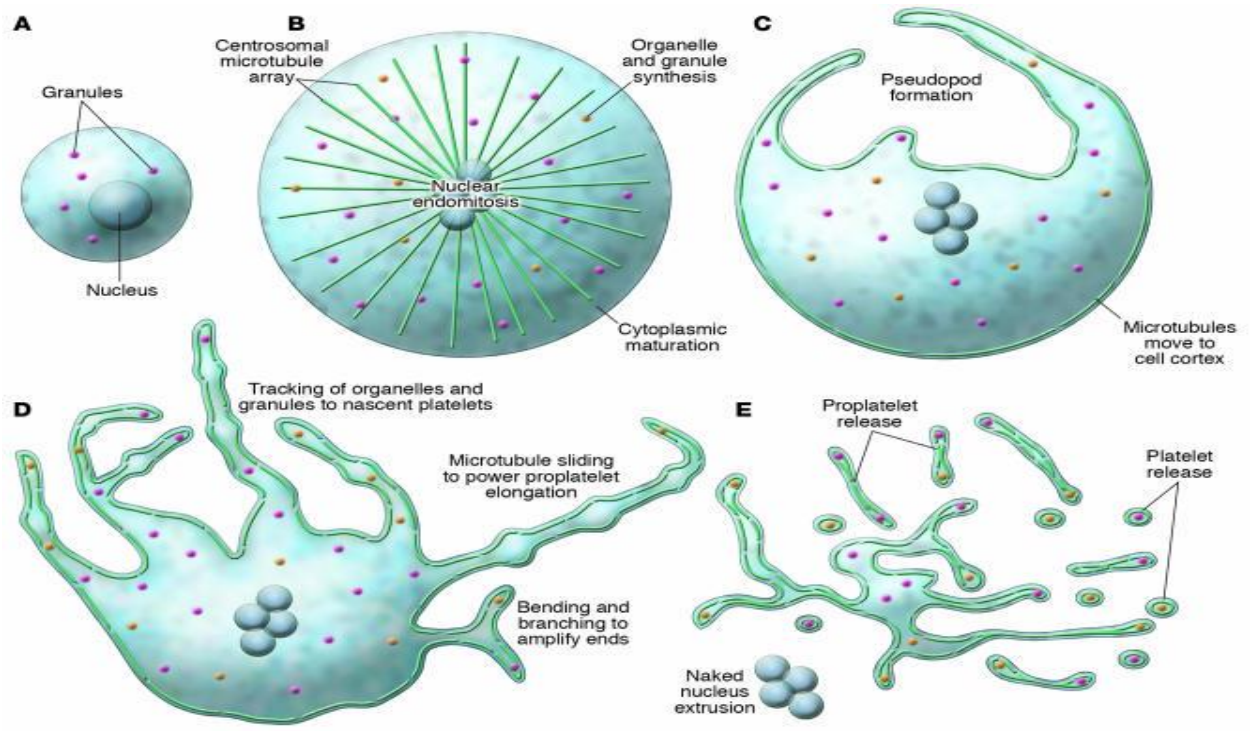

Figure 1.6: Platelet production from the mature megakaryocyte. (A and B) Immature megakaryocyte cells undergo nuclear endomitosis, cytoplasmic maturation, microtubule differentiation and production of organelles. (C) Microtubules arranged at the cell periphery and pseudopod formation signalling the production of proplatelets. (D) Microtubules slide and support the pseudopods which elongate, bend and branch and trap the organelles distally to the site of platelet production. (E) The cell is changed into a stack of proplatelets which split up into platelets (figure reproduced from Patel et al., 2005)

1.5. Platelet activation mechanisms

1.5.1 Platelet activation under blood flow requires platelet interaction with adhesive ligands of the subendothelial matrix

Platelets normally freely circulate in the blood in quiescent form. In the event of disruption of the endothelial lining (e.g. vascular injury or rupture of an atherosclerotic plaque) a chain of reactions immediately starts which ultimately leads to platelets triggering the clotting of the blood. The inert nature of resting platelets comes about due to the platelet fibrinogen receptor, Integrin $\alpha_{IIb}\beta_3$, being in an inactive confirmation (Bennett, 2005). Upon vascular damage platelets encounter a number of chemical stimuli from the damaged vessel wall which can trigger platelet activation (e.g. collagen, thrombin, and adenosine triphosphate), these initial stimuli are able to trigger platelets to activate their integrin $\alpha_{IIb}\beta_3$ (Jackson *et al*., 2003) – leading to the platelets ability to bind to one another, and therefore to start to aggregate.

Initial platelet tethering to the damaged vessel wall under conditions of arterial blood flow requires the binding of platelets to collagen via immobilised vWF. This interaction occurs via the GP Ib-IX-V receptor for vWF (Weiss *et al*., 1978) – however this initial binding and platelet activation is weak and cannot by itself support irreversible binding to the damaged vessel wall (Kulkarni *et al*.,2000). Further activation of platelets requires stronger activation to elicit stable aggregates.

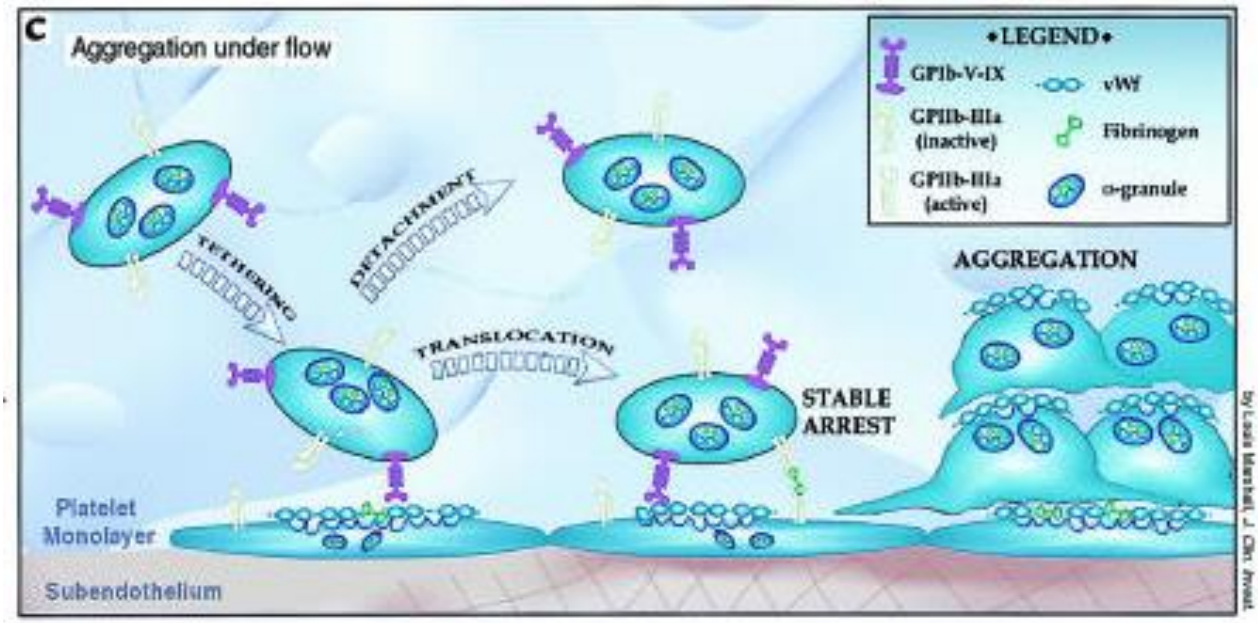

Figure 1.7: Primary haemostasis. A review of primary haemostasis showing the process of platelet aggregation which demonstrate the recruitment of nearby platelets activated by the exposed subendothelium at the site of damage, granule secretion and formation of first layer-platelet aggregation. The expression of vWF will help recruitment of more platelets by binding their GPIbα in a dynamic process between translocation and subtraction overwhelm by the interaction between surface $\alpha_{IIb}\beta 3$ receptor of unsettled platelets and stable platelets. This interaction is mediated by plasma vWF or fibrinogen towards stable thrombus formation. Modified from Kulkarni et al., (2000).

Previous work examining thrombus formation *in vivo* in the mesenteric artery of mice has indicated that there are two parallel stimuli that trigger platelet aggregation; platelet binding to subendothelial collagen, or activation through the local production of thrombin by the extrinsic coagulation cascade triggering platelet activation (Furie & Furie, 2008). The relative importance of these two pathways is uncertain and appears to depend on the experimental method used to induce vascular injury. For example, endothelial denudation elicited by treatment with ferric chloride triggered blood clotting principally by activating platelets via collagen exposure on the subendothelial matrix, whilst thrombus formation triggered by laser-induced injury to the vessel wall is principally dependent on thrombin production via activation of the extrinsic blood coagulation pathway (Furie &

Furie, 2008). Given both experimental stimuli are not representative of how a blood vessel is normally injured; it is likely that both of these activation pathways contribute to thrombus formation *in vivo*.

1.5.2 Platelet activation requires a rise in cytosolic Ca^{2+} concentration

Platelet agonists such as collagen and thrombin evoke platelet activation through eliciting a rise in cytosolic Ca^{2+} concentration ($[Ca^{2+}]_{cyt}$; Rink & Sage, 1990). This rise in $[Ca^{2+}]_{cyt}$ plays a central role in mediating blood clotting through its ability to control a range of different processes required for thrombus formation including adhesion, shape change, granule secretion, platelet cohesion, thromboxane and thrombin production and clot retraction (Born, 1972; Grette, 1962; Heptinstall, 1976; Heemskerk *et al*., 2013; Knight & Scrutton, 1984). Therefore understanding how calcium signals are generated will allow us to understand how platelets become activated, and so we might be able to identify novel strategies for preventing unwanted platelet aggregation as occurs in a variety of cardiovascular disorders including heart attack, stroke and deep vein thrombosis by preventing these Ca^{2+} signals.

1.5.3 Control of $[Ca^{2+}]_{cyt}$ in unstimulated platelets

In the undamaged vessel, the inactive platelet is kept quiescent by maintaining $[Ca^{2+}]_{cyt}$ at very low levels (≈ 50-100 nM). This is achieved through the parallel use of a series of primary active transporters of Ca^{2+} which remove Ca^{2+} from the platelet cytosol either by sequestration into intracellular Ca^{2+} stores (Sage *et al*., 2011) or through removal of

Ca^{2+} across the plasma membrane (Johansson & Haynes, 1988; Jones *et al*., 2010; Valant *et al*., 1992).

Platelets principally sequester Ca^{2+} into the dense tubular system using the Sarco/endoplasmic reticulum Ca^{2+}-ATPase isoform 2b (SERCA2b; Papp *et al*., 1991; Cavallini *et al*., 1995; Kovacs *et al*., 1997). In addition, platelets are also found to possess the SERCA3 isoform which appears to be related to an acidic Ca^{2+} store in platelets (Lopez *et al*., 2006; Ruiz *et al*., 2004). These distinct SERCA-dependent Ca^{2+} stores can be pharmacologically identified by their differential inhibition by low concentrations of thapsigargin, as a low concentration of thapsigargin can induce inhibition of SERCA 2b (Cavallini *et al*., 1995) whilst SERCA3 needs much higher thapsigargin concentrations to be inhibited (Wuytack *et al*., 1994; Bobe *et al*., 1994), and can also be inhibited specifically by 2,5-di –(t-butyl)-1,4-hydroquinone (TBHQ; Enyedi *et al*., 1992). Other studies have demonstrated that the two SERCA isoforms are differentially distributed between two Inositol 1,4,5-trisphosphate (IP_3)-dependent Ca^{2+} stores (Cavallini *et al*., 1995). This was further supported by immunolabelling studies which indicated different subcellular localizations of the two SERCA isoforms (Kovacs *et al*., 1997) and thus the release of Ca^{2+} from stores depends on the exposure to TBHQ or not and on the concentration of thapsigargin (Cavallini *et al*., 1995). Although currently not definitively characterized, the SERCA3-containing acidic stores likely represent the platelet lysosome and secretory granules (Lopez *et al.*, 2006; Ruiz *et al*., 2004; Sage *et a*l. 2011). In addition to SERCA3, recent work has provided initial evidence that the acidic Ca^{2+} stores also possess an additional secondary-active Ca^{2+}

transporter which utilizes the transmembrane pH gradient to also drive Ca^{2+} uptake into this store (Sage *et al*., 2011).

Resting platelets primarily remove Ca^{2+} across the plasma membrane utilizing a plasma membrane Ca^{2+} ATPase (PMCA; Johansson & Haynes, 1988; Jones *et al*., 2010). Human platelets principally express the PMCA4 isoform, although there is a small amount of PMCA1b isoform protein also observed in these cells (Martin *et al*., 2000). Interestingly, immunolabelling studies have found an assymetric distribution of PMCA in resting platelets, with much of the PMCA being found in the OCS in the vicinity of the DTS (Cutler *et al.*, 1978) – in line with its selective accumulation around the membrane complex.

In addition to the PMCA, platelets have also been shown to contain Na^{+}/Ca^{2+} exchanger (NCX) 3 isoform (Harper *et al*., 2010; Roberts *et al*., 2012). Although this transporter can remove Ca^{2+} from the cytosol, it has a much lower affinity for Ca^{2+} than the PMCA, but a much higher transport capacity – because of this the NCX system in platelets is thought to play a key role in rapidly removing Ca^{2+} from the cytosol upon platelet activation when $[Ca^{2+}]_{cyt}$ is raised (Valant *et al*., 1992; Sage *et al*., 2013).

1.5.4 Agonist-evoked rises in $[Ca^{2+}]_{cyt}$ occur via Ca^{2+} release and Ca^{2+} entry

Upon damage to the blood vessels, platelet agonists such as thrombin and collagen evoke platelet activation through triggering intracellular signalling cascades through the binding of these agonists to their respective receptors - with collagen activating platelet via the activation of glycoprotein VI and integrin $\alpha_2\beta_1$ (Jackson *et al*., 2003) and thrombin

triggering platelet activation via the cleavage of the protease-activated receptor (PAR) isoforms PAR1 and PAR4 (Vu *et al*., 1991; Kahn *et al*., 1998). Both of these receptors invoke platelet activation through triggering a rise in $[Ca^{2+}]_{cyt}$ through their activation of phospholipase C (Figure 8) which catalyses the breakdown of phosphatidylinositol 4,5-bisphosphate (PIP_2) to the second messengers, IP_3 and 1,2-diacylglycerol (DAG; Rittenhouse and Allen, 1982; Watson *et al*., 1985). In addition there is evidence that platelet activation with both thrombin and the GPVI-specific agonist, collagen-related peptide (CRP) leads to the production of another second messenger, nicotinic acid adenine dinucleotide phosphate (NAADP: Coxon *et al*., 2012; Lopez *et al*., 2006; Sage *et al*., 2011). The agonist-evoked IP_3 production elicits Ca^{2+} release from the DTS by triggering the opening of Ca^{2+}-permeable IP_3 receptors (Authi & Crawford, 1985; Brass & Joseph, 1985; Sage *et al*., 2011). In contrast, NAADP production appears to trigger Ca^{2+} release from the acidic Ca^{2+} stores (Coxon *et al*., 2012; Lopez *et al*., 2006; Sage *et al*., 2011), presumably through the two-pore channels, TPCN1/2 (Ruas *et al*., 2015) which have previously been found in the platelet proteome (Burkhart *et al*.,2012). These channels are expressed on the membranes of endosomes and lysosomes where they form receptors for nicotinic acid adenine dinucleotide phosphate (NAADP) (Zhu et al., 2010)

The Adenosine Triphosphate (ATP)-gated receptor-operated P_{2X1} channel (MacKenzie *et al.*, 1996; Mahaut-Smith *et al.,* 2000) is the simplest one as it elicits a small rise in $[Ca^{2+}]_{cyt}$. Recent studies have found that this channel most likely act as part of an autocrine signalling system activated when platelets secrete ATP from their dense granules, and which works to reinforce the activation of principal agonists such as

collagen and thrombin (Fung *et al*., 2007; Oury *et al*., 2001). This pathway appears to be particularly important in mediating rapid platelet activation under conditions of high shear stress (Hechler *et al*., 2003).

In addition to Ca^{2+} release from intracellular stores, platelets are able to elicit Ca^{2+} entry through the plasma membrane through a number of Ca^{2+}-permeable ion channels (**Fig. 1.8**).

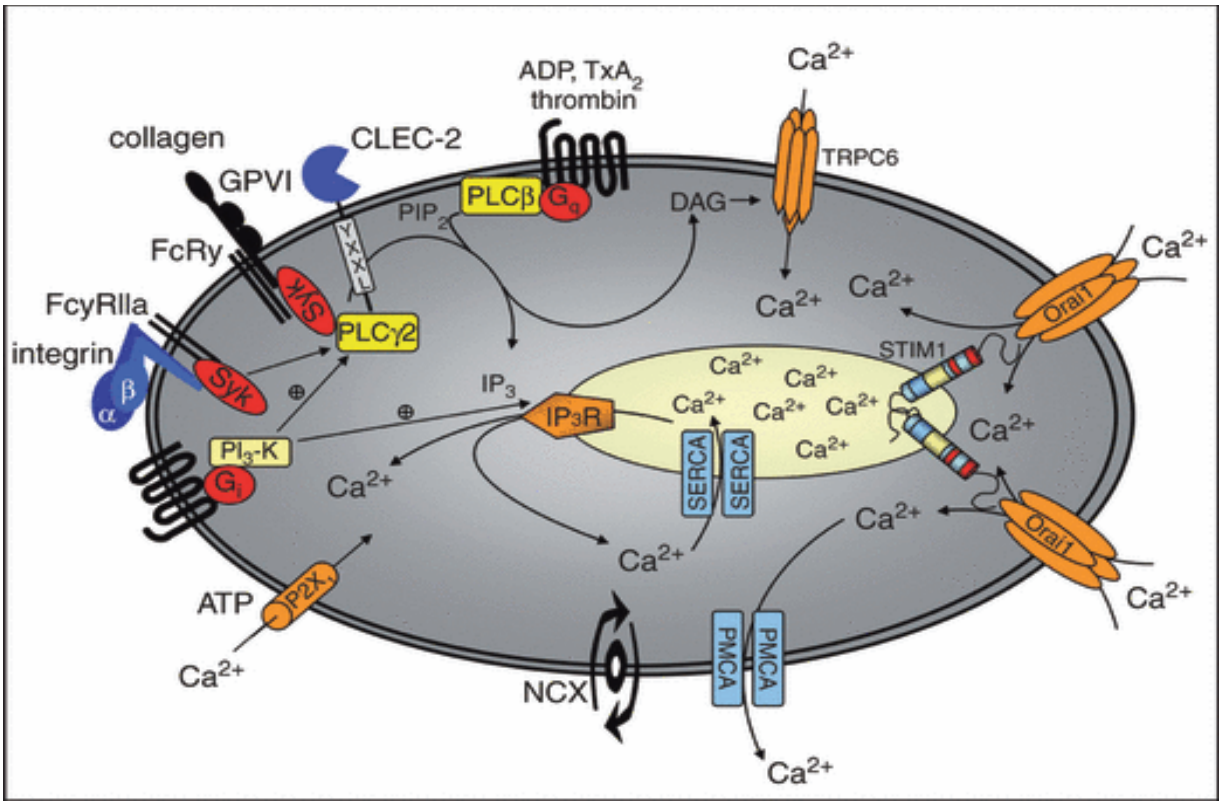

Figure 1.8: The major molecular pathways for platelet Ca^{2+} signalling. Activation of platelets by agonists leads to the production of IP_3 and DAG. The IP_3 releases the store Ca^{2+} and STIM1 stimulates Orai1 channels for Ca^{2+} influx (SOCE) while DAG induces non-SOCE through TRPC6 for Ca^{2+} influx. Secondary Ca^{2+} entry occurs by receptor operated Ca^{2+} channel, Na^{+}/Ca^{2+} exchanger and P_{2X1}. In turn Ca^{2+}removal occurs through SERCAs into the store and to the cell exterior through the plasma membrane Ca^{2+} ATPase (PMCAs; figure reproduced from Varga-Szabo et al., (2009)).

Perhaps the most important Ca^{2+} entry pathway is store-operated Ca^{2+} entry (SOCE). In this mechanism, Ca^{2+} entry is elicited through a store-operated channel when Ca^{2+} levels fall in the intracellular Ca^{2+} stores. Recent work has identified Orai1 as a principal component of the store-operated channel (Braun *et al*., 2009; Bergmaier *et al*., 2009). Although an Orai1 homomultimer may comprise the store-operated channel, previous work had suggested that this channel may also contain channels such as TRPC1 which may modulate the Ca^{2+} signal elicited through this channel (Rosado *et al*., 2002; Brownlow & Sage, 2005). However in contrast to Orai1-deficient mice, TRPC1 knockout mice show no obvious deficit in their Ca^{2+}signalling – therefore arguing against this channel forming a significant component of the platelet store-operated channel in mice (Vargas-Szabo *et al*., 2009).

To be activated by store-depletion the store-operated channel requires a signal to be sent from the DTS to the plasma-membrane-localised Orai1-containing channel. Recent work has identified that the DTS-localised STIM1 protein is able to sense changes in the Ca^{2+} concentration within the intracellular Ca^{2+} stores in both human and mouse platelets (Vargas-Szabo *et al., 2008;* Misceo *et al*., 2014; Nakamura *et al*., 2013; Markello *et al*., 2015), and communicate this to the Orai1-containing channel through conformational coupling between the two proteins. Interestingly, both Orai1- and STIM1-knockout mice showed no obvious bleeding diathesis, but did demonstrate reduced platelet aggregate formation under flow (Braun *et al*., 2009; Vargas-Szabo *et al*., 2008) – suggesting a key role for this channel in mediating thrombus formation.

Platelets are also known to contain DAG-activated second messenger-operated channels such as TRPC3 and TRPC6 (Hassock *et al*., 2002; Harper *et al*., 2013; Estacion *et al*., 2006; Onohara *et al*., 2006). Studies of TRPC6 knockout mice have shown that these cells are unable to elicit DAG-mediated Ca^{2+} entry, yet Ca^{2+} entry through the store-operated channel appears unaffected (Ramanathan *et al*., 2012). Interestingly the store-operated entry appears to be sufficient enough to maintain *in vitro* and in *vivo* platelet activation suggesting a minimal role of TRPC6 in the initial activation of murine platelets (Ramanathan *et al*., 2012). However, more recent work by Harper *et al*., (2013), has demonstrated a role for the DAG-activated TRPC3 and TRPC6 isoforms in eliciting phosphatidylserine exposure in agonist-evoked platelets – suggesting that Ca^{2+} entry through these channels principally affects platelet-mediated activation of the coagulation cascade, but not primary haemostatic reactions.

Lastly, previous work has suggested that the Na^{+}/Ca^{2+} exchanger may also act as a Ca^{2+} entry mechanism by acting in reverse mode to bring Ca^{2+} into the platelet when cytosolic Na^{+} levels are raised (Roberts *et al*., 2012; Harper *et al*., 2013) – however the relative importance of this over the traditional forward mode exchange of this transporter is currently unclear (Harper *et al*., 2009; Sage *et al*., 2013). Current work suggests that the relative importance of reverse mode and forward mode exchange may be different for collagen and thrombin - with reverse mode being elicited by collagen activation of platelets (Roberts *et al*., 2012), whilst in thrombin-stimulated platelet forward mode exchange likely dominates (Sage *et al.*2013).

1.5.5 Maintained Ca^{2+} rises underlies changes in platelet phenotype

A rise in the $[Ca^{2+}]_{cyt}$ is a crucial event in platelet activation triggered by agonists exposed at the site of any vascular damage. This cytosolic Ca^{2+} elevation drives a variety of signalling processes that end with platelet aggregation leading to thrombus formation at the site of vascular damage (Rink and Sage, 1990). Therefore, knowing how the platelets initiate and regulate their Ca^{2+} signalling processes could help us to produce new anticoagulant drugs that act by interrupting these signals.

Ca^{2+} signals in all cells have two crucial variables which may underlie their ability to regulate biological events (Berridge *et al*., 2000); the amplitude of the change in Ca^{2+} away from resting $[Ca^{2+}]_{cyt}$ and the duration of Ca^{2+} rises. A number of previous platelet studies have demonstrated that extending the duration of the platelet Ca^{2+} signal is important in mediating a range of transitions in the platelet response (Heemskerk *et al*., 2013). Mazzucato *et al.* (2002) found that when Ca^{2+} signals were monitored in platelets perfused over vWF-coated coverslips, different Ca^{2+} signalling patterns could be observed with different functional effects. Transient Ca^{2+} signals caused by Ca^{2+} release from the DTS triggered transient platelet adhesion, with platelets detaching after the Ca^{2+} signal had declined towards resting levels. In contrast, when platelets were observed to have maintained Ca^{2+} signals due to autocrine ADP signalling leading to Ca^{2+} entry across the plasma membrane, there was irreversible adhesion and aggregate formation. Similar results were found *in vivo* studies of thrombus formation in rabbits by Van Gestel *et al*., (2002) – who demonstrated that platelets binding to a forming thrombus that maintained their Ca^{2+} signals formed part of the thrombus, whilst platelets in which the Ca^{2+} signals started to drop off were found to embolise. These

results therefore suggest that maintained and synchronous Ca^{2+} signalling is crucial for thrombus formation and growth (Nesbitt *et al*., 2003).

A transition in activated platelet function is also known to be important in facilitating secondary haemostatic reactions leading to the local activation of the clotting cascade, thrombin activation and fibrin formation to help stabilize the primary platelet aggregate at the site of vascular injury – as clotting factors require the expression of anionic phospholipids to recruit them to the platelet surface. Interestingly, studies have also shown that platelets that were found to have prolonged Ca^{2+} increases were also found to facilitate the transition from a proaggregatory, fibrinogen-binding phenotype into a procoagulant, phosphatidylserine platelet phenotype (Kulkarni & Jackson, 2004; Jackson & Schoenwalder, 2010).

As can be seen from the above discussion, prolonged Ca^{2+} signalling plays a role in determining the rate and extent of both primary and secondary haemostatic systems and thus targeting Ca^{2+} signalling systems to block prolonged Ca^{2+} signalling may be useful for limiting the extent of unwanted platelet aggregation in heart attacks and strokes. Previous studies of agonist-evoked Ca^{2+} signalling in patients with a delta storage pool bleeding disorder has shown that agonist-stimulated release of autocoids from dense granules is required to prolong agonist-evoked Ca^{2+} signals (Lages & Weiss, 1999). Thus study goes on to show that secondary stimulation of the platelet helps to maintain agonist-evoked Ca^{2+} signals by further opening Ca^{2+}-permeable ion channels in the platelet plasma membrane. This work suggests that dense granule secretion is critical to the production of prolonged Ca^{2+} signals and thus could be the underlying cause of the failure to effectively clot in these patients.

1.5.6 Pericellular Ca^{2+} signalling helps maintain agonist-evoked cytosolic Ca^{2+} signals in human platelets.

Studies in our lab have demonstrated a role for normal NCX function in regulating the rate and extent of dense granule secretion in platelets stimulated in a number of different ways (Harper *et al*., 2009; Harper *et al*., 2010; Sage *et al*., 2013). More recently, our lab has provided evidence that this appears to be principally related to this transporter specifically transporting Ca^{2+} into the OCS, where it can accumulate and recycle back into the platelet through Ca^{2+}-permeable ion channels, facilitating Ca^{2+}-regulated dense granule secretion (Sage *et al*., 2013 Knight & Scrutton, 1984). Preventing the pericellular Ca^{2+} rise through preventing Ca^{2+} efflux from the platelet, buffering the Ca^{2+} accumulation within the pericellular region or blocking Ca^{2+} re-entry through the plasma membrane inhibited thrombin-evoked Ca^{2+} increases as well as reducing dense granule secretion (Sage *et al*., 2013).

Analysis of these pericellular Ca^{2+} rises found that these appeared to originate from a specific subdomain of the platelet. Considering the known ultrastructure of the platelet and the location of this Ca^{2+} rise in the pericellular region, this work suggested that the membrane complex might provide a suitable structure for creation of this initial pericellular Ca^{2+} accumulation (Sage *et al*., 2013). Further mathematical analysis of the measured Ca^{2+} fluxes into and out of the platelets further supported the need for the membrane complex in mediating the pericellular Ca^{2+} hotspot (Sage *et al*., 2013). These data therefore suggested that drugs which disrupt this subcellular structure in platelet might provide a novel mechanism by which to dampen normal platelet function in patients at risk of heart attacks and strokes. This idea is also supported by previous

reports about patients with bleeding disorders related to defective platelet membrane structure (Canizares *et al*., 1990; Green *et al*., 1981; Meiamed *et al*., 1984; Parker *et al.,* 1993), including one family where a hereditary abnormality of the membrane complex structure was found to be associated with a defect in thrombin-induced Ca^{2+} signalling (Parker *et al.,* 1993).

1.5.7 Nicergoline prevents pericellular Ca^{2+} recycling in human platelets

Previous studies have shown that the known anti-thrombotic drug, nicergoline, has different functions at two different concentrations; at low concentration it has a blocking effect on the α-adrenoreceptors, while much higher concentrations of this drug are needed to inhibit *in vivo* platelet functions such as platelet activation, aggregation and secretion (Lanza *et al.,* 1986; Le Menn *et al*., 1979). These studies suggested that the anti-platelet effect was mediated by nicergoline's ability to disrupt the cortical microtubule ring and thus trigger a redistribution of both the dense tubular system and open canalicular systems (Le Menn *et al*., 1979). Through this effect, it is possible that nicergoline disrupts the membrane complex (MC). This is consistent with previous work that had shown that the cortical microtubules interact closely with the DTS. (Behnke, 1967; White, 1972). Therefore the cortical microtubule bundle may provide a method to anchor this structure in specific areas of the platelet including at the MC.

Previous work had identified that the membrane complex might be the site of creation of the pericellular Ca^{2+} accumulation (Sage *et al*., 2013). Therefore we hypothesised that nicergoline might interrupt pericellular Ca^{2+} recycling and this might be the basis for its

ability to block the normal haemostatic functions of platelets (Lanza *et al*., 1986; Le Menn *et al.*, 1979; Walford et al., 2016). In this paper we confirmed that nicergoline can disrupt the structure of the cortical microtubule bundle as well as ultrastructure localization of the DTS, as observed via fluorescence microscopic observation using either a fluorescent taxol derivative or an antibody directed to ER-resident KDEL proteins respectively. When various aspects of platelet Ca^{2+} signaling were observed in the absence of extracellular Ca^{2+}, nicergoline could be observed to significantly reduce thrombin-evoked Ca^{2+} signals caused by an inhibition of pericellular Ca^{2+} recycling (Figure 9; Walford *et al*., 2016). These effects could however be reversed by preventing the reorganization of the cortical microtubule bundle by prior treatment with the microtubule-stabilising agen, taxol, prior to nicergoline treatment. These data therefore suggest that nicergoline elicits its effect on pericellullar Ca^{2+} recycling by triggering a microtubule-dependent relocation of the DTS away from the OCS. These results are consistent with the hypothesis that the MC is a critical structure in regulating and maintaining agonist-evoked cytosolic Ca^{2+} signals.

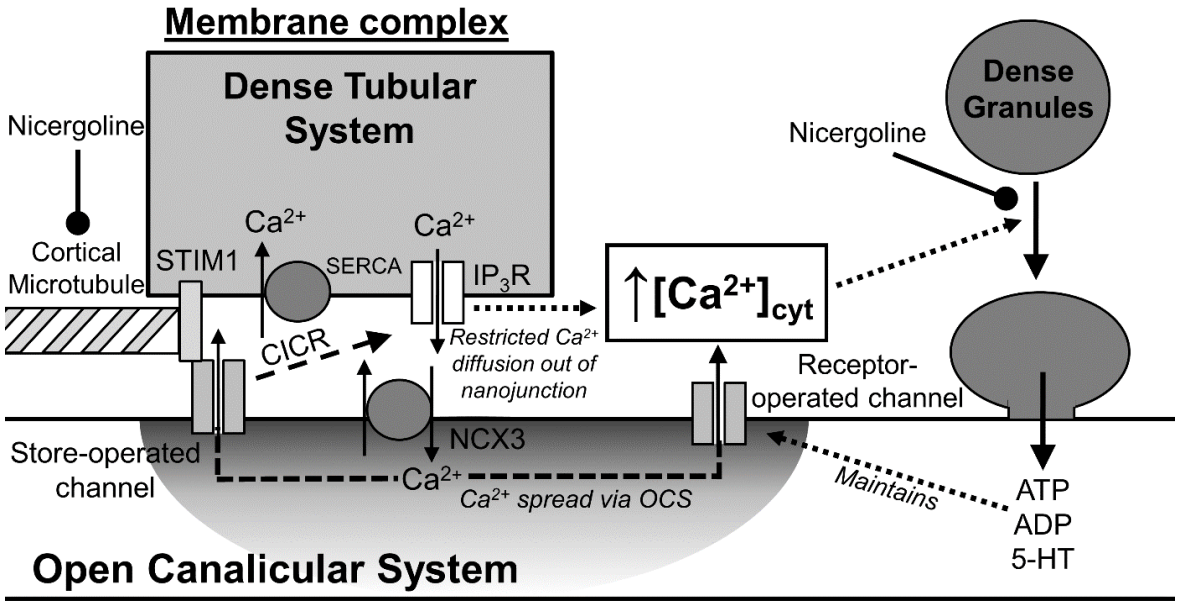

Figure 1.9: Pericellular Ca^{2+} recycling and the mechanism of action of nicergoline in human platelets. The interaction of the two membranes of the membrane complex support the primary Ca^{2+} signalling during platelet activation by helping to couple Ca^{2+} release from the IP_3 receptor to Ca^{2+} efflux through the NCX. This creates an accumulation of Ca^{2+} in the lumen of the OCS – such that it can create a concentration gradient driving Ca^{2+} back in the cytosol through the various Ca^{2+}-permeable ion channels in the plasma membrane. This in turns potentiates Ca^{2+} signalling by potentiating Ca^{2+} release and triggering secretion of autocrine signalling molecules from the dense granules. Addition of Nicergoline distorts the microtubule network which holds the DTS in intimate contact with OCS, leading to disruption of the close contact of the membranes at the MC, and thus preventing pericellular Ca^{2+} recycling, thus impairing the creation of the cytosolic Ca^{2+} signal (Figure adapted from Walford *et al*., 2016).

However this ability to reverse the effect of nicergoline on thrombin-evoked Ca^{2+} signals could not be observed when cells were stimulated with this agonist in the presence of extracellular Ca^{2+}. This discrepancy appears to be related to additional off-target effects of nicergoline on dense granule secretion when Ca^{2+} was present in the extracellular fluid, as nicergoline-induced inhibition of dense-granule secretion was only found to be partially reversed by taxol treatment (Walford *et al*., 2016). However our previous studies haven't identified how nicergoline treatment is able to disrupt the cortical microtubules, leading to redistribution of the DTS and OCS. Previously we hypothesized

that nicergoline might work through either altering the activity of molecular motors associated with microtubule motility or via altering the post-translational modification of tubulin (Walford *et al*., 2016).

In the next section we will review the current understanding of how each of these factors alters platelet function.

1.5.8 Post-translational modification of platelet microtubules

The function of microtubules is controlled by a variety of post-translational modifications (PTMs) such as (poly)glutamylation (Eddé et al., 1990; Alexander et al., 1991; Redeker et al., 1992), detyrosination (Arce et al.,1975; Hallak et al., 1977), acetylation (L'Hernault and Rosenbaum, 1985; Chu et al., 2011) and (poly)glycylation (Redeker et al., 1994). Tubulin subunits within microtubules often show a number of these known PTMs suggesting that they could play a role in controlling the functions of these microtubules (Szyk et al., 2014). The PTMs of tubulin subunits have been shown to regulate the microtubule function through an interaction with microtubule-stabilizing or destabilizing proteins helping to alter the rate of microtubule cycling (Chakraborti et al., 2016). Furthermore these modifications are known to alter the interaction of the microtubules with molecular motor proteins such as kinesin and dynein, thus facilitating their ability to act as points for cellular transport and force generation (Chakraborti et al., 2016). Of the different post-translational modification of microtubules, (de)tyrosination and acetylation are the best studied in human platelets.

Microtubules can be reversibly acetylated by the action of the N-acetyltransferases such as ARD1-NAT1 and the elongator complex, and deacetylated by both the SIRT2 and HDAC6 enzymes (Hubbert et al., 2002; Janke & Kneussel, 2010). Acetylation is found on stable microtubules which do not undergo the cycles of microtubule polymerisation and collapse. However acetylation is a consequence of microtubule stabilisation and not the cause of this phenomena (Palazzo *et al*., 2003). However acetylation is associated with modulating interaction of microtubules with motor proteins such as kinesin and dyneins (Reed *et* al., 2006; Cai *et al.,* 2009).

Data has shown that the microtubules that make up the marginal band consist of stable and highly polymerized, acetylated and tyrosinated α-tubulin subunits – suggesting the presence of both older, static microtubules as well as newer, more dynamic structures (Patel-Hett *et al*., 2008). Upon platelet activation, the marginal band of microtubules is subjected to a contraction force towards the centre which is associated with microtubule deacetylation by HDAC6 (Sadoul *et al*., 2012). Further studies with HDAC inhibitors have shown that acetylation of microtubules in human platelets can regulate both the resting structure of the cortical microtubule bundles, as well as the collagen-mediated signalling events which can lead to its reorganisation (Aslan *et al*., 2013). These studies therefore suggest that acetylation of the microtubules could impact significantly on platelet function.

Detyrosination is the most well-known tubulin modification achieved by removing the tyrosine from the C-terminal region by a carboxypeptidase of unknown origin (Hallak *et al*., 1977). Tyrosinated tubulin molecules are known to be used by newly polymerizing microtubules, and this tyrosination is used as a marker of newly formed microtubules

(Janke & Bullinski, 2011). Similarly detyrosination of tubulin is responsible for stabilization of the microtubules (Schulze *et al*., 1987) as these microtubules are kept polymerized without collapse (Janke & Kneussel, 2010). Previous studies in human platelets have demonstrated that tyrosinated tubulin molecules are generally found in the cortical microtubule bundle, whereas detyrosinated microtubules are found in the coiling sections of the microtubules which are responsible for spheration of platelets upon agonist-activation (Diagouraga *et al*., 2014).

These data therefore suggest the possibility that nicergoline-induced alterations in the PTM of microtubules could be the causes of the observed change in the structure of the cortical microtubule bundle.

1.5.9 Molecular motors in human platelets

In addition to PTMs of microtubules altering their structure, molecular motors such as kinesin, dyneins and myosin may play a role in generating active forces to move attached cargos (Akhmanova & Hammer, 2010; Reed *et al*., 2006; Dompierre *et al*., 2007) or to deform or remodel the cell (Merdes *et al*., 1996; Piperno *et al*., 1987; Schatten *et al*., 1988). A review of the platelet proteome has identified that each of these molecular motors are found in human platelets (Sadoul *et al*., 2012), however there are variable amounts of data available regarding their role in regulating normal platelet function.

Myosin is a large ATPase molecule that can hydrolyse ATP releasing energy from the high-energy phosphate bond to generate a contractile force that can pull actin over the

myosin molecule generating contractile forces. The force generated by the myosin motor has been demonstrated to induce platelet shape change, internal contraction and clot retraction (Johnson *et al*., 2007, Daniel *et al*., 1984; Cohen *et al*., 1982; Feghhi *et al*., 2016). Upon platelet activation, constriction of the cortical cytoskeleton results in the centralization of platelet secretory granules by this shrinking ring of microtubules and actin. This results in the concentration of granules in the middle of the cell thus facilitating their exocytosis (White & Burris, 1984).

In support of this previous studies have demonstrated that myosin plays a role in promoting granule secretion (Painter & Ginsberg, 1984; Flaumenhaft, 2003).

Dynein acts as a microtubule-associated motor which can help to move attached cargo along these cytoskeletal elements in a minus-end directed manner (Karki & Holzbaur, 1999). In particular, dyneins have been shown to play a role in controlling endoplasmic reticulum positioning and growth within cells (Wózniak *et al*., 2009), and thus may play a role in controlling the distribution of the DTS within the platelet. Recent work has demonstrated that dyneins play a role in maintaining the structure of the cortical microtubule ring by counteracting the force exerted by the plus-end directed kinesin motors (Diagouraga *et al*., 2014). Upon platelet activation, the antagonistic action of the microtubule motors is disrupted with kinesin activity reduced and dynein function upregulated leading to elongation of the microtubule bundle (Diagouraga *et al*., 2014).

Previous studies has defined that kinesins function as molecular motor proteins that use ATP hydrolysis to move anchored cargo generally towards the plus ends of the microtubules (Wells *et al*., 1999). This movement facilitates the position and

transportation of organelles and secretory granules inside the cell (Marx *et al*., 2009). Previous work in platelets have demonstrated a role for kinesins in preventing dynein-induced coiling of the cortical microtubules, with pre-treatment with the kinesin-inhibitor, aurintricarboxylic acid (ATA; Hopkins *et al*., 2010), inducing spontaneous coiling of the cortical microtubules (Diagouraga *et al*, 2014). Interestingly previous studies have also shown that ATA is known to possess anti-thrombotic capacities in *in vivo* models of thrombus formation (Phillips *et al*., 1988; Owens & Holme, 1996; Azzam *et al*. 1996, Takiguichi *et al*., 1996).

1.6 Aims and objectives of the project

Our hypothesis is that nicergoline works by either altering the efficiency of the molecular motors associated with microtubule motility (such as myosin, kinesin and dynein), or via its ability to alter post translational modifications of tubulin such as changing the acetylation or tyrosination state of microtubules. In this project we will examine how inhibition of histone deacetylases, myosin, kinesin and dynein affects agonist-evoked Ca^{2+} signals as well as the change in function of human platelets to examine whether these replicate the effects of nicergoline, or whether treatment concurrently with nicergoline could reverse the effect of this drug. Through this approach, we aim to identify the molecular mechanism by which nicergoline inhibits the cortical microtubule structure, DTS distribution and platelet Ca^{2+} signalling.

In addition, we hypothesized that nicergoline will inhibit Ca^{2+} signalling in $CD34^{+}$-derived human megakaryocytes in a similar manner to that found in human platelets. We

therefore aimed to assess the effect of nicergoline on thrombin-evoked Ca^{2+} signalling in these cells and evaluate their similarity to that found in human platelets. If verified, it was hoped that $CD34^{+}$-derived human megakaryocytes may be used as a model system in which to identify the molecular target of nicergoline in human platelets in the future.

2. Materials and Methods

2.1 Materials

Fura-2/AM was from TEFlabs Inc. (Austin,TX). Thrombin was from Merck Chemicals (Nottingham, U.K.). Apyrase, adenosine triphosphate, aurin tricarboxcylic acid, DNAse I, 5-5'-Dimethyl-BAPTA/AM, blebbistatin, trichostatin A, poly-L-lysine solution, Hoechst 33342 and the Luciferin-luciferase ATP assay kit were from Sigma Aldrich (Gillingham, UK). StemSpan™ SFEM-II media and StemSpan™ CC100 cytokine cocktail were from Stemcell technologies (Cambridge, UK). Recombinant human thrombopoietin (TPO), Interleukin 6 (IL-6), Interleukin 9 (IL-9) and Stem Cell Factor (SCF) were obtained from PeproTech EC Ltd. (London, UK). Nunc™ 8-well Lab-Tek™ II chambered coverglass were from Fisher Scientific UK (Loughborough, UK). Fluo-5N/AM, Fluo-4 pentapotassium salt, Tubulin Tracker and Rhod-5N tripotassium salt were from Life Technologies Ltd (Paisley, UK). Human $CD34^{+}$ cells from bone marrow were obtained from Lonza (Blackley, UK). Fetal calf serum was from Labtech international Ltd. (Lichfield, UK). Nicergoline and ciliobrevin A were from Tocris Bioscience (Bristol, UK).

Phalloidin iFluor555 and anti-KDEL antibody were from Abcam (Cambridge, UK). All other reagents were of analytical grade.

2.2 Methods for human platelet experiments

2.2.1 Platelet preparation

All experiments were approved by Keele University Research Ethics Committee, and were conducted in accordance with the Declaration of Helsinki. Blood was taken with informed, written consent from healthy, drug-free volunteers by venepuncture from the antecubital fossa. 5 mL whole blood was mixed with 1 mL acid citrate dextrose (ACD) anticoagulant (85 mM sodium citrate, 78 mM citric acid, and 111 mM D-glucose) and centrifuged for 8 min at 700 g. The platelet-rich plasma (PRP) was then collected and treated with 100 µM aspirin and 0.1 U/mL apyrase.

2.2.2 Monitoring platelet cytosolic Ca^{2+} concentration ($[Ca^{2+}]_{cyt}$)

PRP was incubated with 2.5 µM Fura-2/AM for 45 mins at 37°C. Platelets were then collected by centrifugation at 350 g for 20 min. The cells were then resuspended in Hepes-buffered saline [HBS; 145 mM NaCl, 10 mM Hepes (*N*-2-hydroxyethylpiperazine-*N*-2-ethanesulphonic acid), 10 mM D-glucose, 5 mM KCl, 1 mM $MgSO_4$, pH 7,45], which was supplemented daily by addition of 0.1% [w/v] bovine serum albumin, 200 µM $CaCl_2$, 0.1 U/mL apyrase and 10 mM glucose (supplemented HBS). Fluorescence readings were recorded using a Cairn Research Spectrophotometer (Cairn Research, Faversham, U.K.) from 1.2 mL aliquots of washed human platelet suspensions that

were magnetically stirred and held at 37°C. Fluorescence was recorded when cells were excited with 340 nm and 380 nm light, and emission wavelengths were collected between 470-550 nm. Readings were routinely corrected for autofluorescence by subtraction of 340 and 380 nm values recorded from a cuvette containing HBS alone. Calibration of fluorescence readings was performed by determing the 340 and 380 nm values obtained from platelets samples from both drug- and DMSO-containing platelet samples in which the dye had been released from the cell by lysis by addition of a final concentration of 0.02% [v/v] Triton X-100. Ca^{2+} was then raised to saturating levels by addition of 3 mM $CaCl_2$. Ca^{2+} was then removed from the extracellular medium by sequential addition of 15 mM EGTA and 30 mM Tris until there was no further decrement in the 340 nm values – indicating effective buffering of all extracellular Ca^{2+}. The corrected 340/380 nm fluorescence ratio of all experimental runs was then calculated and calibrated into $[Ca^{2+}]_{cyt}$ and using the method of Grynkiewicz *et al*., (1985).

2.2.3 Quantification of agonist-induced cytosolic Ca^{2+} rises

Quantitative changes of thrombin-evoked intracellular Ca^{2+} concentration were calculated by integrating the difference in fluorescence readings obtained from basal and readings of 3.5 min duration after thrombin stimulation.

2.2.4 Monitoring agonist-evoked rises in platelet extracellular Ca^{2+} concentration ($[Ca^{2+}]_{ext}$)

This was conducted in accordance with our previously published methodology (Sage *et al*., 2013). PRP obtained from fresh human blood was centrifuged at 350*g* for 20 minutes and the platelet pellet obtained was then resuspended in supplemented HBS to produce a cell density of $2x10^8$ cells/mL. Samples of 1.2 mL were used at 37°C under continuous magnetic stirring to monitor the $[Ca^{2+}]_{ext}$ after the addition of 2.5 µM Fluo-4 K^+ salt immediately prior to the start of experiment. A Cairn Research Spectrophotometer was used to record fluorescence at 480 nm excitation wavelength and 500-550 nm emission wavelengths. Thrombin-evoked rises in $[Ca^{2+}]_{ext}$ were then quantified by the integration of the readings of fluorescence changes from basal with respect to time for 3.5 minutes after the addition of thrombin.

2.2.5 Monitoring platelet intracellular store Ca^{2+} concentration ($[Ca^{2+}]_{st}$)

This was conducted in accordance with our previously published methodology (Sage *et* al., 2011). PRP was mixed with 500 nM Fluo-5N/AM at and incubated for 2 hours at 37°C. Platelets were then extracted from plasma by centrifugation at 350 *g* for 20 minutes and resuspended in supplemented HBS to a density of $2x10^8$ cells/mL.

1.2 mL of platelet suspension was used at 37°C under continuous magnetic stirring to study the changes in $[Ca^{2+}]_{st}$. Changes in Fluo-5N fluorescence were recorded at 485 nm excitation and 515 nm emission wavelengths using a Cairn Research Spectrophotometer. Readings were then corrected for autofluorescence recorded by

measuring fluorescence in a sample of HBS containing DMSO or the drug of interest alone. Agonist evoked changes in $[Ca^{2+}]_{st}$ were quantified by the integration of the changes in fluorescence signal records from basal with respect to time for 3.5 mins after agonist addition.

2.2.6 Monitoring platelet shape change by light transmission aggregometry

Washed human platelet suspensions were prepared by centrifuging PRP at 350 g for 20 minutes. Platelets were then resuspended in supplemented HBS to a density of $2x10^8$ cells/mL. Samples were then pre-incubated with the drug to be tested at 37°C under continuous magnetic stirring. 1 mM EGTA was added immediately prior to the experiment. 450 µL of washed platelet suspension was added to the cuvette, and diluted with 50 µL of supplemented HBS containing EGTA and the same concentration of drug or DMSO to ensure light transmission changes stayed within the range of the instrument. Cells were held at 37°C under continuous magnetic stirring in a dual channel Chrono-Log light transmission aggregometer (Labmedics, Oxfordshire, UK). Changes in light transmission were calibrated by comparison against an aggregometry cuvette containing supplemented HBS alone.

2.2.7 Monitoring platelet aggregation by light transmission aggregometry

Washed human platelet suspensions were prepared by centrifuging PRP at 350 g for 20 minutes. Platelets were then resuspended in supplemented HBS to a density of $2x10^8$ cells/mL. Samples were then pre-incubated with the drug to be tested at 37°C under

continuous magnetic stirring. The extracellular Ca^{2+} concentration was then raised to 1 mM immediately prior to the experiments. 500 µL of drug-treated washed platelet suspension was added to the cuvette. Cells were held at 37°C under continuous magnetic stirring in a dual channel Chrono-Log light transmission aggregometer (Labmedics, Oxfordshire, UK). Changes in light transmission were calibrated to % maximum aggregation by comparison against an aggregometry cuvette containing supplemented HBS alone.

2.2.8 Monitoring platelet dense granule secretion

Washed human platelets suspensions were prepared by centrifuging PRP at 350 g for 20 minutes. Platelets were then resuspended in supplemented HBS to a density of $2x10^8$ cells/mL. Washed platelets were then incubated at 37°C under continuous stirring with either 30 µM aurin tricarboxylic acid or an equivalent volume of DMSO for 10 minutes at 37°C under continuous magnetic stirring. EGTA was added to cells at 1mM final concentration prior to the start of experiment. 100 µL of each treated platelet sample was then transferred to a 96-well microtiter plate and 10 % [v/v] Luciferin luciferase assay mix was added immediately before running the experiment. Luminescence readings were measured in a BioTek Synergy 2 microplate reader. The microplates were held at 37°C and luminescence readings were made prior to thrombin addition (L_0) and immediately after addition of 0.5 U/mL thrombin (L). All samples were normalized to a maximum ATP reading obtained by recording luminescence after the addition of 10µM ATP to each well at the end of each run (L_{max}).

The percentage of maximum luminescence was obtained using the following formula:

$$\%\ Maximum\ luminescence = 100\ \times \left(\frac{L\ - L_0}{L_{max} - L_0}\right)$$

2.2.9 Measurement of fixed platelet F-actin content

Washed human platelet suspensions were prepared by centrifuging PRP at 350 g for 20 minutes. Platelets were then resuspended in supplemented HBS to a density of $2x10^8$ cells/mL. 1.5 mL samples were incubated with a final concentration of either 30 µM aurin tricarboxylic acid (ATA) or an equivalent volume of DMSO for 10 minutes at 37°C under continuous magnetic stirring. EGTA was then added at a final concentration of 1mM. 0.5 mL of the resting platelet sample was then fixed by addition of 3% [w/v] formaldehyde. The remaining 1 mL sample was stimulated with 0.5 U/mL thrombin for 1 minute at 37°C under stirring. After this another 0.5 mL sample was fixed by the addition of 3% [w/v] formaldehyde. Cells were stored at 4°C until the day of experiment. Fixed samples were treated in line with previously published studies (Rosado *et al*., 2000). Fixed platelet samples were centrifuged for 1 minute at 8700 g, the supernatant removed and the fixed platelet pellet was resuspended in PBS containing 1 mg/mL bovine serum albumin (BSA) and 0.1% Triton X-100 to permeabilise the platelet plasma membrane, and incubated for 10 minutes at room temperature. The platelet suspension was then centrifuged again for 1 minute at 8700 g and the pellet resuspended in PBS containing 1 mg/mL BSA and 1 µM iFluor555-phalloidin and incubated in the dark at room temperature for 30 minutes. Cells were finally recollected by centrifugation for 1 minute at 8700 g, and resuspended in PBS containing 1mg/mL BSA. Aliquots of 100 µL

of each sample were loaded into 96-well microtiter plate in triplicate. Cells were examined for F-actin content in both the resting and thrombin-stimulated state using a BioTek Synergy 2 microplate reader and fluorescence was recorded at 540 nm excitation wavelength and 590 nm emission wavelength. Thrombin-evoked changes in F-actin content were calculated by subtracting the fluorescence measurement taken from the resting sample from that obtained from the thrombin-stimulated sample. The mean of the triplicate of each sample was then calculated and used as 1 independent sample (n).

2.2.10 Single cell imaging of agonist evoked $[Ca^{2+}]_{ext}$ changes in live human platelets

Experiments were performed with our previously published protocol (Sage *et al*., 2011). Washed human platelet suspensions were prepared by centrifuging PRP at 350 g for 20 minutes. Platelets were then resuspended in supplemented HBS to a cell density of $2x10^8$ cells/mL. Washed platelet samples were then preincubated with either 30 µM ATA or an equivalent volume of DMSO for 10 minutes at 37°C under continuous magnetic stirring. Samples were treated with 1 mM EGTA. Cell suspensions were then loaded onto poly-L-lysine-coated chambered coverslides and allowed to settle for 5 minutes prior to imaging. 10 µM Fluo-4 salt was then added and mixed gently immediately prior to the experiment. Cells were imaged before and for 5 minutes after addition of 0.5 U/mL thrombin using Fluoview FV1200s laser-scanning confocal microscope (Olympus, UK) with a PLAPON 60x oil immersion objective. Cells were excited with 473 nm light and emission was collected at 490-520 nm.

2.3 Methods for human megakaryocyte cell experiments

2.3.1 In vitro culture of CD34$^+$ cells into human megakaryocytes

Human CD34$^+$ cells were obtained from Lonza (Slough, UK). Upon arrival, CD34$^+$ cells were cultured in SFEM-II media containing StemSpan™ CC100 cytokine cocktail SFEM-II expansion medium for 7 days at 37°C in 5% CO_2 and 20% O_2 as per the manufacturer's instructions. Cells were then aliquoted and frozen in liquid nitrogen. CD34$^+$ cell aliquots were revived as per the manufacturers instruction and resuspended into SFEM-II media supplemented with 30 ng/mL TPO, 7.5 ng/mL IL-6, 13.5 ng/mL IL-9 and 1 ng/mL SCF, according to the method of Pineault *et al*., (2013). Cells were plated at between 2-5 x 10^5 cells/mL into the central wells of a 24-well tissue culture plate and incubated at 37℃ in a humidified atmosphere containing 5% CO_2 and 20% O_2 for up to 14 days.

2.3.2 Assessment of megakaryocyte development from CD34$^+$ cells

Cells were examined by light microscopy (Days 2,7 and 11) throughout the culture to track changes in cell proliferation and colony formation. Cell viability was checked on day 7-9 of the culture using trypan blue.

Megakaryocyte cellular structure was also examined by fluorescent microscopy on days 2 and 7 of the megakaryocyte culture. On the day of preparation, Cells were incubated with 1 µM Fluo-5N/AM for 2 hours and 5 µg/mL Hoechst 33342 for 1 hour at 37°C under 5% CO_2 and 20% O_2. Cells were then collected by centrifugation at 228 x g for 10 minutes. The supernatant was discarded and the cell pellet was then resuspended into

supplemented HBS containing 0.1% [w/v] bovine serum albumin, 200 µM $CaCl_2$, 0.1 U/mL apyrase and 10 mM glucose to a final density of $1x10^5$ cells/mL. Poly-L-lysine-coated Nunc chambered coverglass was washed with supplemented HBS before cell addition. 200 µL of the cell suspension was then added to the well and cells were allowed to settle for 30 minutes at room temperature. Immediately prior to imaging, 10 µM Rhod-5N tripotassium salt was added to the suspension. Cellular fluorescence was then examined using a Fluoview FV1200 laser-scanning confocal microscope (Olympus, UK) with a PLAPON 60x oil immersion objective. Cells were excited with 405 nm (Hoechst 33342), 473 nm (Fluo-5N) and 543 nm (Rhod-5N) light and emission was collected at 460-490 nm, 490-520 nm and 590-620nm respectively.

2.3.3 Single cell examination of cell-surface markers of megakaryocyte development in CD34$^+$ cell culture

Megakaryocyte cultures were fixed on day 2 or day 7-9 by addition of 3% [w/v] formaldehyde and stored at 4°C until use. Megakaryocyte samples were centrifuged at 6000 x g for 1 minute, and the pellet resuspended into 100 uL of PBS containing 1 mg/mL BSA and a 1:100 dilution of APC-labelled CD41a antibodies and FITC-labelled CD42b antibodies and incubated at room temperature for 30 min. Cells were recollected by centrifugation and finally resuspended in PBS containing 1 mg/mL BSA. Cells were loaded onto Poly-L-lysine Nunc Chambered coverslips and imaged using a Fluoview FV1200 laser-scanning confocal microscope (Olympus, UK) with a PLAPON 60x oil immersion objective. Cells were excited with 473 nm (FITC) and 543 nm (APC) light and emission was collected at 490-520 nm and 590-620 nm respectively.

2.3.4 Single cell imaging of thrombin-evoked intracellular Ca^{2+} and extracellular Ca^{2+} signalling in nicergoline treated $CD34^{+}$-derived megakaryocytes

A 1 mL sample of $CD34^{+}$-derived cells on day 9 of the culture was incubated with 5 µM Fluo-2/AM and 5 µg/mL Hoechst 33342 dyes. After 1 hour incubation at 37ºC, 0.1 U/mL apyrase was added to the sample and sample centrifuged at 8400 g for 1 minute. Supernatant was removed and pellet resuspended with 250 µL of supplemented HBS. 5 µM Rhod-5N dye and 1 mM $CaCl_2$ were then added. Cells were loaded onto a poly-L-lysine coated chambered coverslide after washing with 200 µl HBS and left for 30 minutes at room temperature to attach. 100 µM Nicergoline or an equivalent volume of DMSO was added to samples and they were incubated for 5 minutes at room temperature. Cells were imaged using a Fluoview FV1200 laser-scanning confocal microscope (Olympus, UK) with a PLAPON 60x oil immersion objective. Cells were excited with 405 nm (Hoechst 33342), 473 nm (Fluo-2) and 543 nm (Rhod-5N) light and emission was collected at 460-490 nm, 490-520 nm and 590-620nm, respectively.

2.3.5 Single cell imaging of the effect of nicergoline on intracellular Ca^{2+} stores in $CD34^{+}$-derived cultured human megakaryocytes

A 1 mL cell sample was taken on day 7 of megakaryocyte culture. $CD34^{+}$-derived cells were then incubated with 5 µg/mL Hoechst 33342 and 1 µM Fluo-5N dyes and the sample was incubated for two hours at 37°C under 5% CO_2 and 20% O_2. After incubation, 200 µl of sample was loaded onto poly-L-lysine-coated chambered coverslides after washing the slide with 200 µl HBS and left for 20 minute at room temperature to allow the cells to attach. The cell sample was mixed with 200 µl of

supplemented HBS containing 1 mM $CaCl_2$ and 5 µM Rhod-5N salt. Cells were then imaged before and after treatment with 100 µM Nicergoline. Imaging was done using a Fluoview FV1200 laser-scanning confocal microscope (Olympus, UK) with a PLAPON 60x oil immersion objective. Cells were excited with 405 nm (Hoechst 33342), 473 nm (Fluo-5N) and 543 nm (Rhod-5N) light and emission was collected at 460-490 nm, 490-520 nm and 590-620nm respectively.

2.3.6 Microplate reader based measurements of agonist-evoked Ca^{2+} signals in nicergoline treated $CD34^{+}$-derived cultured human megakaryocytes

On day 7-9 of the culture cells were incubatd with 2.5 µM Fura-2/AM for 45 minute at 37°C. Cells were then spun at 228 g for 10 minutes, and resuspended in supplemented HBS to a final cell density of $5x10^4$ cells/mL. Cells were treated with either 100 µM nicergoline or an equivalent volume of its vehicle, DMSO, and incubated at 37°C under continuous magnetic stirring for 10 minutes. Cells were then transferred into a 96-well microplate. Extracellular Ca^{2+} was then either raised to 1 mM or chelated by addition of 1 mM EGTA. Cells were stimulated with 0.5 U/mL thrombin and fluorescence was recorded using a BioTek Synergy 2 microplate reader using a 360 nm excitation wavelength filter and collected using a 440 nm emission filter. The recorded value of basal fluorescence was recorded before thrombin addition and a maximal fluorescence value was obtained after treatment of each sample with 10% Triton at the end of each run. Changes in $[Ca^{2+}]_{cyt}$ was quantified by the integration of the change in fluorescence records from basal with respect to time for 5 minutes after thrombin addition.

2.4 Statistical analysis

Values obtained are referred to as the mean ± standard error of the mean of the number of independent observations (*n)* indicated. Student's paired *t*-test was used in experiments in which two samples were directly compared. When three or more samples were compared a one-way ANOVA Test was initially used before a *post hoc* Tukey Test was used to determine statistical significance.

3. Results

Previous work in our lab has shown that nicergoline inhibits agonist-evoked platelet Ca^{2+} signalling and dense granule secretion due to disruption of the cortical microtubule bundle. This effect is likely due to the disruption of the membrane complex due to the dissociation of the DTS from the OCS (Walford *et* al., 2016). This uncoupling of the intracellular Ca^{2+} stores from the OCS therefore reduces the efficiency of Ca^{2+} released from the intracellular stores being removed into the pericellular space enclosed within the OCS. This reduces the pericellular Ca^{2+} accumulation and prevents the creation of a concentration gradient to allow the Ca^{2+} to recycle back into the platelet which would otherwise maintain the agonist-evoked rises in the cytosolic Ca^{2+} concentration at higher levels.

Therefore in this project we aim to understand how nicergoline elicits a reorganisation of the microtubule network and its effect on agonist evoked platelet Ca^{2+} signalling.

3.1 Investigating the effect of trichostatin A, an inhibitor of microtubule deacetylation, on agonist-evoked human platelet function

Tubulin is subject to a wide range of different post-translational modifications which can significantly alter its structure and function within cells (Song & Brady, 2015). Recent studies have shown that the cortical microtubule bundle of resting platelets is highly acetylated, and this is removed by the histone deacetylase (HDAC), HDAC6, upon platelet activation (Sadoul *et al*., 2012). Furthermore, these authors found that trichostatin A, a selective class I and II mammalian HDAC Inhibitor (Vanhaecke *et al*.,

2004) was capable of inhibiting tubulin deacetylation during platelet stimulation (Sadoul *et al*., 2012). Treatment with this histone deacetylase inhibitor can alter the structure of the cortical microtubule ring in resting platelets, suggesting the potential for it to have a similar effect to nicergoline (Aslan *et al*., 2013). In addition, HDAC inhibitors were found to alter downstream signalling pathways and the kinetics of the spreading response of activated platelets (Aslan *et al*., 2013). These data suggest that alterations in the function of these enzymes could play a role in controlling the cellular architecture of platelets. Due to this potential effect of HDAC inhibitors on cortical microtubule structure, experiments were performed to examine whether treatment of platelets with the HDAC inhibitor, trichostatin A (TSA) can either mimic or modulate the inhibitory effect of nicergoline on platelet Ca^{2+} signals and other platelet functional responses.

Our previous studies demonstrated that the effect of nicergoline on detaching the DTS from the OCS in a microtubule-dependent manner could be observed specifically in the absence of extracellular Ca^{2+} (Walford *et al*., 2016). However in the presence of extracellular Ca^{2+}, additional effects of nicergoline could be observed on blocking dense granule secretion through a microtubule-independent effect (Walford *et al*., 2016). Therefore to allow us to isolate the microtubule-dependent effect of nicergoline we first investigated the effect of TSA on Ca^{2+} signals elicited in the absence of extracellular Ca^{2+}.

3.1.1 Trichostatin A elicited no significant effect on thrombin-evoked cytosolic Ca^{2+} signalling elicited in the absence of extracellular Ca^{2+} in human platelets

Fura-2-loaded human platelets were pretreated with either 10 µM TSA, or an equivalent volume of its vehicle (DMSO) for 30 minutes, and then further treated with either 100 µM nicergoline or an equivalent volume of DMSO for a further 10 minutes at 37°C under continuous magnetic stirring. Experiments were performed with this sequential drug treatment regime to examine whether prior inhibition of HDAC could prevent or mimic the effects of nicergoline on thrombin-evoked platelet responses. Pretreatment of control cells with TSA had no significant effect on thrombin-evoked rises in cytosolic Ca^{2+} concentration ($[Ca^{2+}]_{cyt}$; 104.9 ± 5.0% of control; n = 6, $P > 0.05$, **Fig 3.1**). Attempts to characterize the effect of TSA on the actions of nicergoline failed due to a failure of the positive control experiments. This appeared to be due to an effect of this batch of nicergoline not becoming fully solubilized by the magnetic stirring during the preincubation period, leading to artifacts in the Fura-2 traces that were not observed during the initial study (*Data not shown*; Walford *et al*., 2016).

3.1.2 Trichostatin A cannot reverse the effect of nicergoline on thrombin-evoked Ca^{2+} removal into the extracellular fluid in human platelets

To confirm these initial findings further experiments were conducted to examine whether TSA could mimic, or modulate, the effects of nicergoline on thrombin-evoked Ca^{2+} removal from platelets stimulated in the absence of extracellular Ca^{2+}. Washed human platelets were sequentially treated with 10 µM TSA (or DMSO) for 30 minutes, and 100 µM nicergoline (or DMSO) for further 10 minutes at 37°C under continuous magnetic

stirring. Pretreatment with just TSA had no significant effect on thrombin-evoked rises in $[Ca^{2+}]_{ext}$ compared to double DMSO-treated cells (89.9 ± 6.9% of double DMSO-

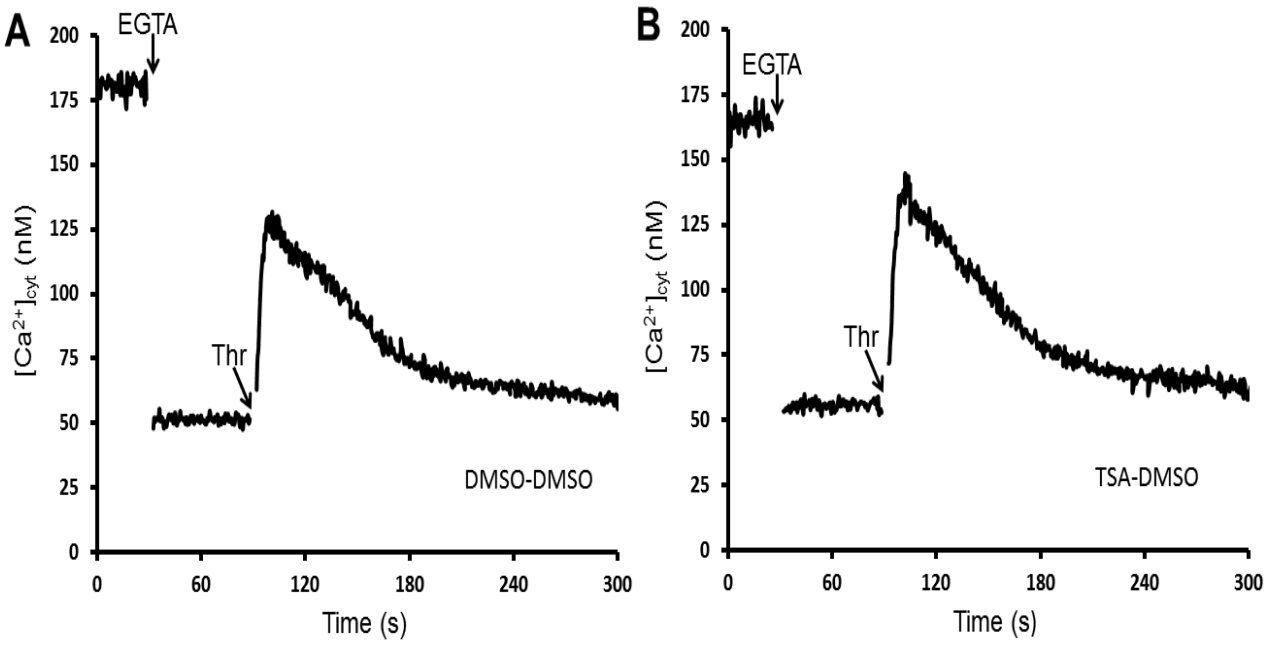

Fig. 3.1 Trichostatin A elicited no significant effect on thrombin-evoked cytosolic Ca^{2+} signalling elicited in the absence of extracellular Ca^{2+} in human platelets. Fura-2-loaded human platelets were pretreated with either 10 µM TSA (B) or an equivalent volume of its vehicle, DMSO (A) for 30 minutes at 37°C under continuous magnetic stirring. Extracellular Ca^{2+} was chelated with 1 mM EGTA at the beginning of the experiment followed 1 minute later by the addition of 0.5 U/mL thrombin.

treated cells, n = 6, $P > 0.05$; **Fig. 3.2C**). In contrast, nicergoline treatment significantly reduced thrombin-evoked rises in $[Ca^{2+}]_{ext}$ to 52.3 ± 2.4 % of double DMSO-treated cells (n = 6, $P < 0.05$, **Fig. 3.2B**), which was consistent with our previous findings (Walford *et al*., 2016). When platelets were pre-treated with TSA followed by nicergoline, there was still a significant inhibition compared to double DMSO-treated cells (62.9 ± 7.7 %; $P < 0.05$; **Fig. 3.2D**) as well as compared to cells treated with TSA alone ($P < 0.05$).

3.1.3 TSA has no effect on thrombin-evoked shape change in control-or nicergoline-treated platelets.

Further experiments looked to confirm whether these effects on thrombin-evoked Ca^{2+} signalling correlated with changes in platelet functionality. Experiments examined the effect of sequential treatment with either TSA or nicergoline alone, or with both compounds on platelet shape change and aggregation. As can be seen in **Fig. 3.3**, nicergoline treatment alone significantly inhibited both the maximum shape change observed (2.5 ± 0.5% of maximum light transmittance; $n = 10$; $P < 0.05$) and the time to peak of that shape change (25.9 ± 9.0 s; $P < 0.05$) when compared to cells treated with DMSO at both addition points (12.1 ± 1.2% and 12.6 ± 2.5 s respectively; $n = 10$). In contrast pre-treatment with TSA alone had no significant effect on the shape change response when compared to DMSO-treated control cells (10.8 ± 2.2% and 11.9 ± 1.9 s respectively; $n = 10$). The inhibitory effect of nicergoline treatment was not significantly modified by prior treatment with TSA as cells treated with both compounds demonstrated both a similar inhibition of the maximum shape change response (2.7 ± 0.5% of maximum transmittance; n = 10) and the time-to-peak of this responses (29.6 ± 10.2 s) when compared to nicergoline-treated cells ($P > 0.05$). Statistical analysis demonstrated that these TSA and nicergoline-pretreated cells still demonstrated a significantly inhibited response when compared to both untreated control cells and cells treated with TSA alone (both $P < 0.05$).

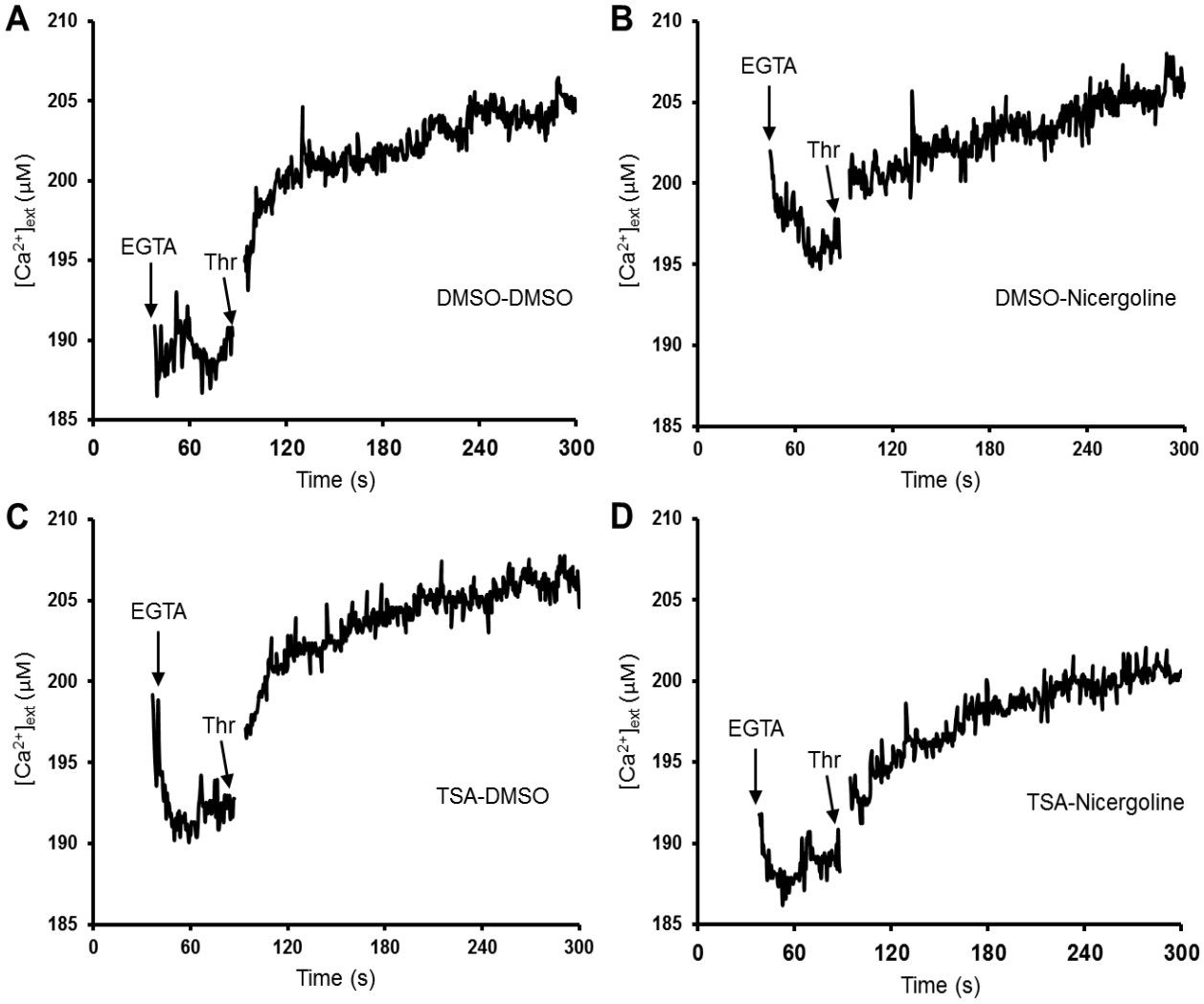

Fig. 3.2: Trichostatin A cannot reverse the effect of nicergoline on thrombin-evoked Ca^{2+} signalling in human platelets. Fura-2-loaded human platelets were resuspended in supplemented HBS. Cells were initially pre-treated with either 10 µM TSA or an equal volume of DMSO for 30 minutes at 37°C. This was then followed by an additional 10 minutes incubation with either 100 µM nicergoline or an equal volume of DMSO under the same conditions. 2.5 µM Fluo-4 salt was added immediately prior to the start of the experiment. Extracellular Ca^{2+} was chelated with 1 mM EGTA at the beginning of the experiment followed 1 minute later by the addition of 0.5 U/mL thrombin.

3.1.4 Trichostatin A has no effect on thrombin-evoked platelet aggregation in control- and nicergoline-treated platelets.

Additional experiments examined the effect of these compounds on platelet aggregation. As shown in **Fig. 3.4**, control cells treated with DMSO at both additions had a rapid onset of aggregation response (latency = 38.4 ± 9.8 s after thrombin addition; n = 5) which lead to near maximal aggregation (82.0 ± 4.7%; n = 5). Pretreatment with TSA alone had no significant effect on the maximum extent of aggregation observed (81.2 ± 5.2%; n = 5, $P > 0.05$). The latency of the aggregation response was slightly faster in TSA-treated cells compared to control cells, consistent with previous findings that HDAC inhibition may facilitate a faster platelet response (Sadoul *et al*. 2012), although this did not reach significance in this study (31.4 ± 1.7 s; n = 5, $P > 0.05$). In contrast, nicergoline treatment alone significantly slowed the latency of the aggregation response in thrombin-stimulated platelets (104.6 ± 17.6 s; n = 5, $P < 0.05$), although it had no significant extent on the maximum extent of platelet aggregation (74.0 ± 5.1%; n = 5, $P > 0.05$). This effect of nicergoline on the latency of the aggregatory response was not significantly modified by prior treatment with TSA, as platelets treated with both compounds still had a significantly prolonged latency (99.4 ± 8.4 s; n = 5, $P < 0.05$ to both control cells and TSA-treated cells alone). These cells also had a similar aggregatory response to control cells (78.0 ± 6.1%; n = 5, $P > 0.05$ to all other treatments).

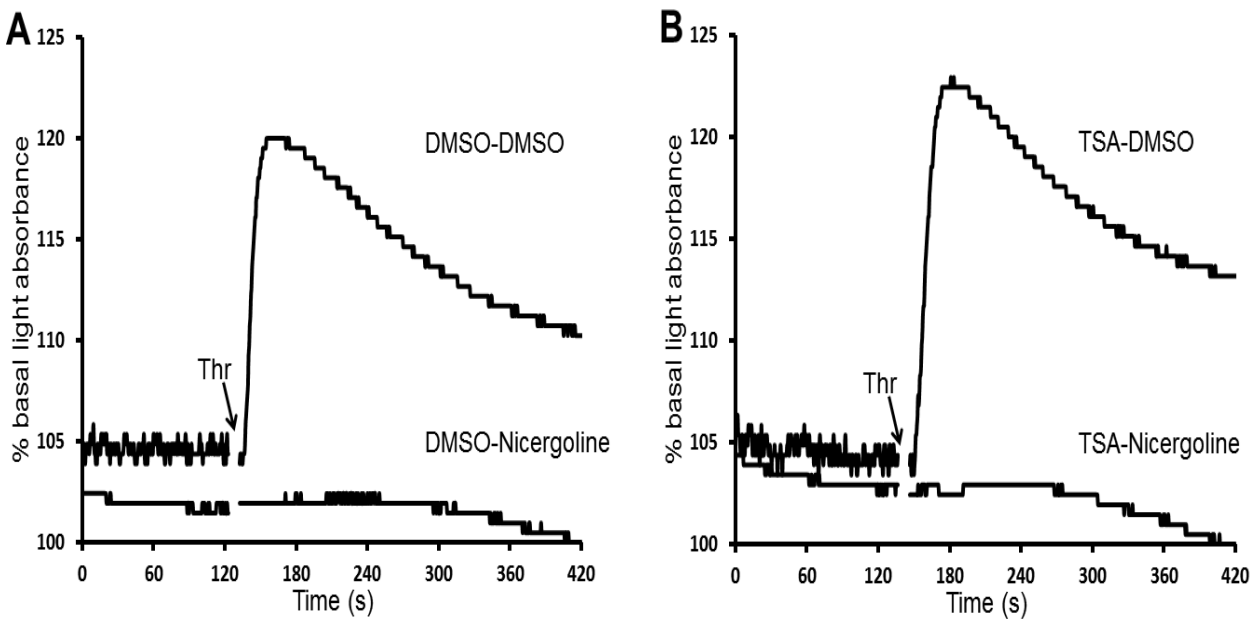

Fig. 3.3: TSA induced no effect on thrombin-evoked shape change in human platelets. Washed platelet samples were incubated at 37°C with either 10 µM TSA (B) or an equal volume of DMSO (A) for 30 minute at 37°C. This was then followed by a further 10 minute incubation under the same conditions with either 100 µM Nicergoline or an equal volume of DMSO (A,B). Extracellular Ca^{2+} was chelated by addition of 1mM EGTA just before the start of the experiment. Cells were then stimulated 2 minutes later with 0.5 U/mL thrombin.

These results suggested that prevention of HDAC-mediated microtubule deacetylation by pretreatment with TSA exerted no effect on platelet Ca^{2+} signalling and function, and was unable to reverse the inhibitory effect of nicergoline. These data therefore suggest that nicergoline does not exert its effect on human platelets through altering the acetylation state of the cortical microtubule bundle.

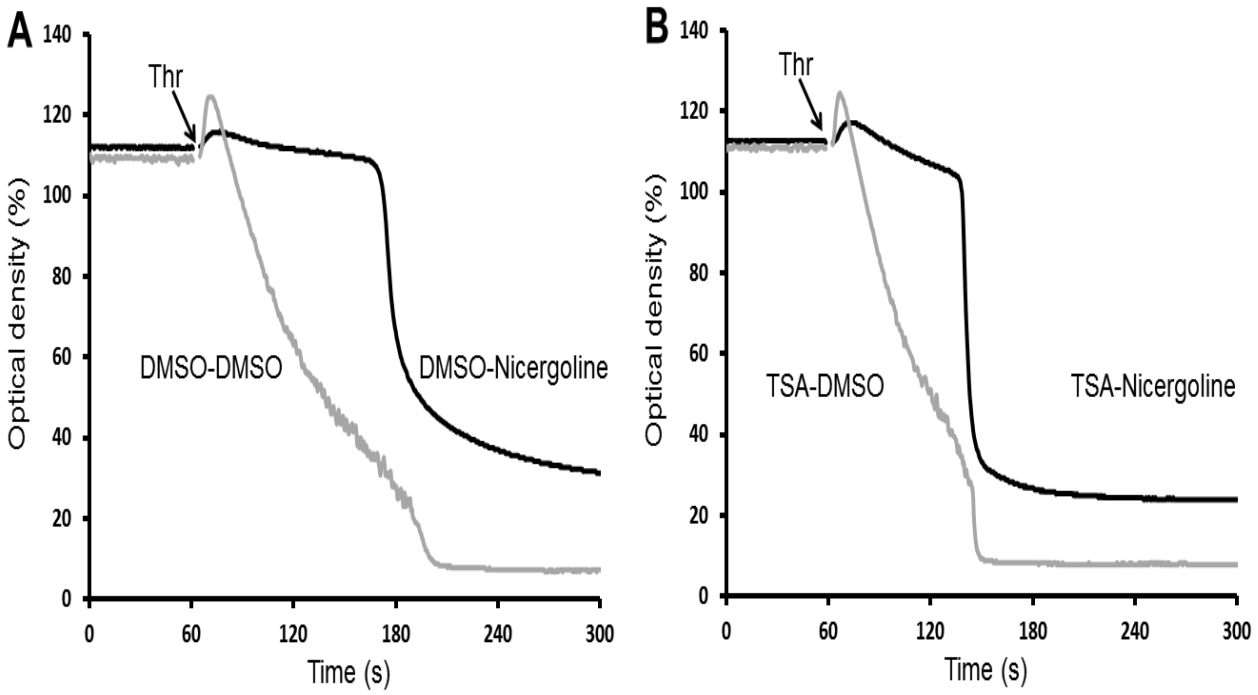

Fig 3.4: TSA has no effect on thrombin-evoked aggregation in control- and nicergoline-treated human platelets. Washed human platelets resuspended in supplemented HBS were incubated with either 10 µM TSA (B) or an equal volume of DMSO (A) for 30 minute followed by a further 10 minutes incubation with either 100 µM nicergoline or an equal volume of DMSO (A,B) at 37ºC. 1 M $CaCl_2$ was then added prior to the start of the experiment. Cells were then monitored and activated after 2 minutes with 0.5 U/mL thrombin.

3.2 Investigating the effect of blebbistatin, an inhibitor of the myosin motor protein, on thrombin-evoked human platelet function

Another mechanism by which nicergoline could alter the structure of the cortical microtubule bundle is through altering the activity of motor proteins which control the structure of the cortical cytoskeleton. The force generated by the myosin motor has been demonstrated to induce platelet shape change, internal contraction, granule secretion, and clot retraction (Johnson *et al*., 2007; Daniel *et al*., 1984; Cohen *et al*., 1982; White & Burris, 1984; Painter & Ginsberg, 1984; Flaumenhaft, 2003). If nicergoline alters the activation of myosin then this might explain the change in platelet structure and granule secretion observed upon nicergoline treatment (Walford *et al*., 2016). Experiments were therefore performed to examine whether the myosin inhibitor, blebbistatin, can mimic or modulate the effect of nicergoline on thrombin-evoked Ca^{2+} signalling.

Blebbistatin is a highly selective myosin II inhibitor. It possesses a powerful inhibitory effect due to its ability to bind with high affinity to the myosin-ADP-P_i complex, thereby blocking myosin activity through interfering with the phosphate release process preventing rigid actomyosin cross-linking (Kovacs *et al*., 2004). Previous studies have demonstrated that blebbistatin is able to block platelet shape change, clot retraction and internal contraction at doses between 10-100 μM (Johnson *et al*., 2007; Suzuki-Inoue *et al*., 2007).

3.2.1 Blebbistatin abolishes thrombin-evoked shape change in human platelets.

Myosin has previously been shown to be essential for agonist-evoked shape change in human platelets (Paul *et al*., 1999). To ensure that blebbistatin was functional, we examined the effect of 30 µM blebbistatin on thrombin-evoked shape change. As shown in **Fig. 3.5**, pretreatment with 30 µM blebbistatin for 2 minutes at 37°C completely abolished any thrombin-evoked shape change observed in all 6 experiments performed. In contrast a clear shape change averaging a light transmittance decrease of 9.4 ± 1.8% of maximum light transmittance was observed in control experiments (n = 6; $P < 0.05$).

3.2.2 High-dose blebbistatin inhibits thrombin-evoked rises in $[Ca^{2+}]_{cyt}$ elicited in the absence of extracellular Ca^{2+} in human platelets.

Fura-2-loaded human platelets were preincubated with either 10, 30 or 100 µM blebbistatin, or an equivalent volume of its vehicle DMSO for 10 minutes at 37°C under continuous magnetic stirring. Blebbistatin was found to be autofluorescent when excited with 340 and 380 nm light, consistent with previous observations (Várkuti *et al*., 2016). To correct for this, calibration and autofluorescence measurements were performed in the presence of each concentration of blebbistatin. However the autofluorescent artefacts arising from platelets treated with 100 µM blebbistatin were too large to generate reliable data regarding their effect on thrombin-evoked Ca^{2+} signals, therefore these data are not presented here. Thrombin-evoked Ca^{2+} signals elicited in the absence of extracellular Ca^{2+} were not significantly inhibited by pretreatment with 10 µM blebbistatin (89.3 ± 5.3% of control; n = 6, $P = 0.11$; **Fig. 3.6B**), however a significant

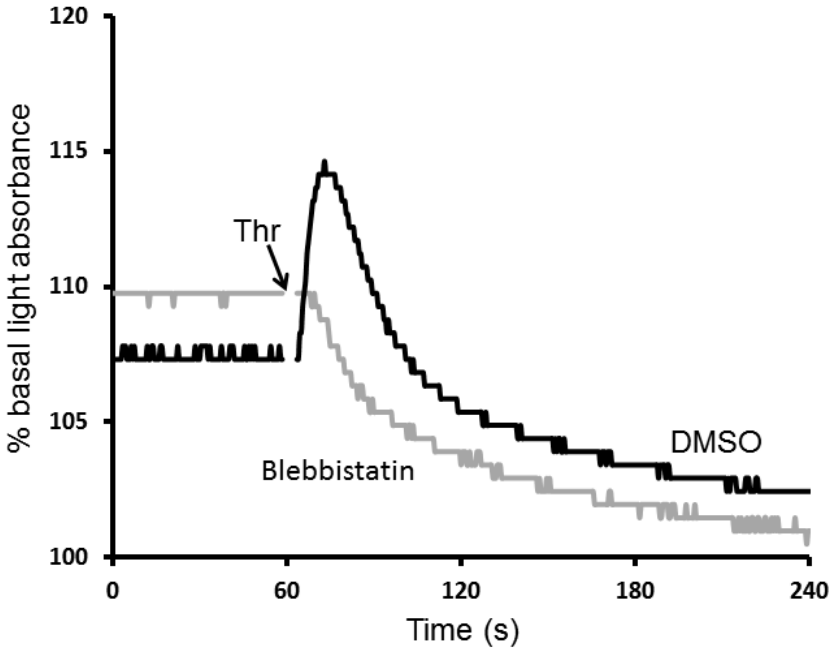

Fig. 3.5 Blebbistatin prevents thrombin-evoked human platelet shape change. Washed human platelets were resuspended in supplemented HBS, and incubated with either 30 µM blebbistatin or an equal volume of DMSO for 10 minutes at 37°C. 1 mM EGTA was then added immediately prior to the start of experiment. Two minutes later, shape change was initiated by addition of 0.5 U/mL thrombin.

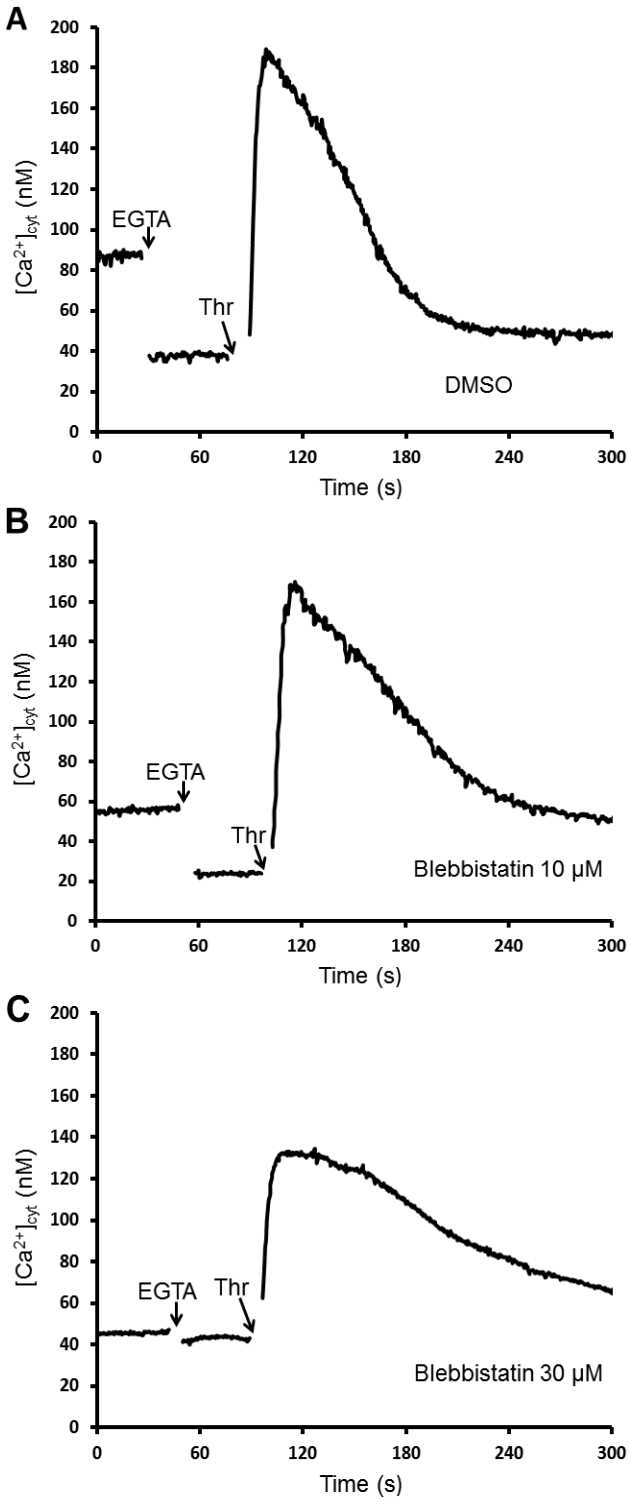

Fig. 3.6: Blebbistatin inhibits thrombin-evoked rises in $[Ca^{2+}]_{cyt}$ elicited in the absence of extracellular Ca^{2+} in human platelets. Fura-2-loaded human platelets were resuspended into supplemented HBS and were incubated with either 10 µM blebbistatin (B), 30 µM blebbistatin (C), or an equal volume of DMSO (A) for 10 minutes at 37℃. Extracellular Ca^{2+} was then chelated by addition of 1 mM EGTA and cells were then stimulated 1 minute later by addition of 0.5 U/mL thrombin.

inhibitory effect was observed in the presence of 30 μM blebbistatin (61.7 ± 10.1% of control; n = 6, $P < 0.05$; respectively; **Fig. 3.6C**). These data are consistent with the possibility that nicergoline inhibits platelet function through inhibition of myosin.

3.2.3 Nicergoline inhibits thrombin-evoked Ca^{2+} signalling in both the presence and absence of low-dose blebbistatin

To provide an initial assessment of whether nicergoline could elicit its effects on platelets through inhibiting myosin activity, experiments were performed to examine whether the inhibitory effect of blebbistatin was able to modulate the inhibitory effect of nicergoline when platelets were stimulated with thrombin in the absence of extracellular Ca^{2+}. If the effects of blebbistatin in combination with nicergoline was greater than the effect of either inhibitor alone on platelet Ca^{2+} signalling, it would suggest that these inhibitors are working through distinct effects on this signalling pathway. Therefore this would suggest that nicergoline is unlikely to be exerting its effect on platelet structure and function via an inhibitory effect on myosin. Initially Fura-2-loaded human platelets were pretreated with either 30 μM blebbistatin, or an equivalent volume of its vehicle (DMSO) for 10 minutes at 37°C under continuous magnetic stirring, and then further treated with either 100 μM nicergoline or an equivalent volume of DMSO for a further 10 minutes under the same conditions. However due to the relative insolubility of both nicergoline and blebbistatin, it was not possible to get reliable data from these experiments. Therefore these experiments were instead performed using 10 μM blebbistatin. Previous studies have shown that 10 μM blebbistatin is sufficient to

significantly block myosin-dependent platelet functions such as internal contraction (Johnson *et al*., 2007). Pretreatment with 10 µM blebbistatin had no significant effect on thrombin-evoked rises in $[Ca^{2+}]_{cyt}$ compared to double DMSO-treated cells (107.9 ± 3.6% of double DMSO-treated cells, n = 12, *P* = 0.06; **Fig 3.7C**). In contrast, nicergoline-pretreatment significantly reduced thrombin-evoked rises in $[Ca^{2+}]_{cyt}$ to 77.2 ± 3.0 % of double DMSO-treated cells (n = 12, *P* < 0.05, **Fig. 3.7B**), which was consistent with our previous findings (Walford *et al*., 2016).

When platelets were pre-treated with both blebbistatin and nicergoline, there was still an inhibitory effect compared to cells treated with blebbistatin alone (n =12; P < 0.05). However when compared to control cells treated with nicergoline alone, the addition of nicergoline to blebbistatin-treated cells could not be observed to have any additional significant inhibitory effect (91.1 ± 4.3 % of double DMSO-cells; P = 0.07, **Fig. 3.7D**). These results therefore suggested the possibility that myosin could be the target of nicergoline. However this is difficult to be unambiguously stated from these experiments as it was not possible to utilize concentrations of blebbistatin able to completely inhibit myosin activity due to issues of solubility and autofluorescence of this compound.

3.2.4 Blebbistatin is incompatible with Fluo-based Ca^{2+} indicators

Previously we have demonstrated that nicergoline inhibits thrombin-evoked Ca^{2+} removal into the extracellular fluid and release from intracellular stores (Walford *et al*., 2016). These experiments utilize Fluo-4 salts to measure Ca^{2+} removal into extracellular

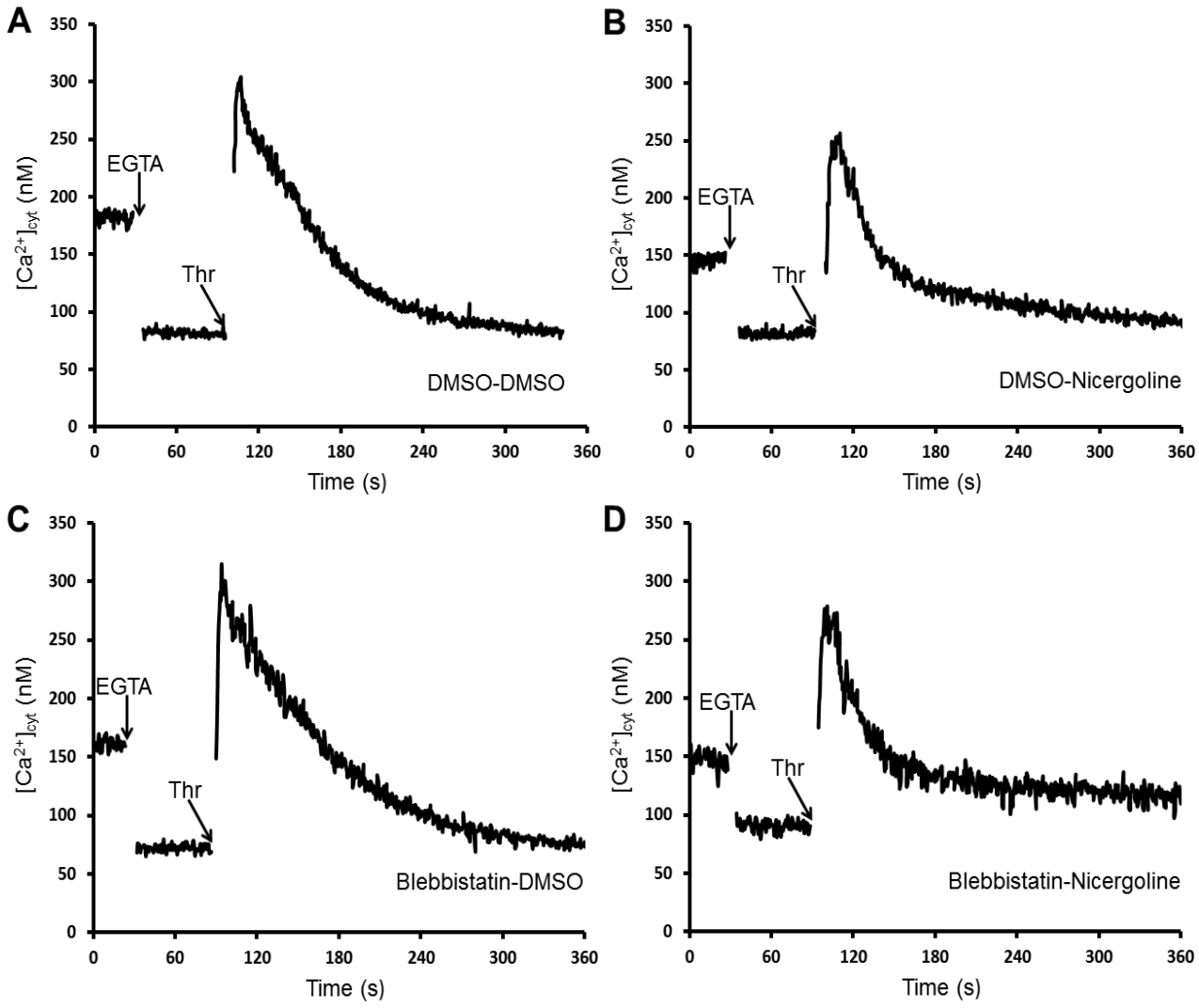

Fig. 3.7: Nicergoline is able to inhibit thrombin-evoked Ca^{2+} signalling in both the presence and absence of blebbistatin. Fura-2-loaded human platelet were resuspended in supplemented HBS and were incubated with either 10 µM blebbistatin (C,D) or an equal volume of DMSO (A,B) for 10 minutes at 37°C. Cells were then incubated for a further 10 minutes with either 100 µM nicergoline (B,D) or an equal volume of DMSO (A,C) at 37℃. 1 mM EGTA was then added 30 s after running the experiment. Cells were stimulated 1 minute later with 0.5 U/mL thrombin.

fluid, and Fluo-5N-loaded platelets to measure Ca^{2+} release from intracellular stores. As these two fluorescent indicators have distinct fluorescent properties to Fura-2, it was hoped that the autofluorescent properties of blebbistatin would have less interference at these wavelengths. Therefore experiments were performed to examine whether combined treatment with nicergoline and blebbistatin had cumulative effects to either treatment alone. However blebbistatin's autofluorescent properties were also found to overwhelm the fluorescence of both fluo fluorescent indicators therefore making these experiments infeasible.

3.2.5 Blebbistatin has no inhibitory effect on thrombin-evoked rises in $[Ca^{2+}]_{cyt}$ elicited in the presence of extracellular Ca^{2+}.

As nicergoline is also able to significantly inhibit thrombin-evoked Ca^{2+} signals elicited in the presence of extracellular Ca^{2+} (Walford *et al*., 2016), experiments were performed to examine if blebbistatin could replicate these effects. Pretreatment of Fura-2-loaded human platelets with blebbistatin at concentrations of either 10 μM or 30 μM had no significant effect on thrombin-evoked Ca^{2+} signals (90.2 ± 8.6% or 158.1 ± 59.1% of control, respectively (both n = 6, $P > 0.05$; **Fig. 3.8**). These data therefore indicate a significant difference between the pharmacological profile of blebbistatin and nicergoline, and suggests that myosin is not the target of nicergoline.

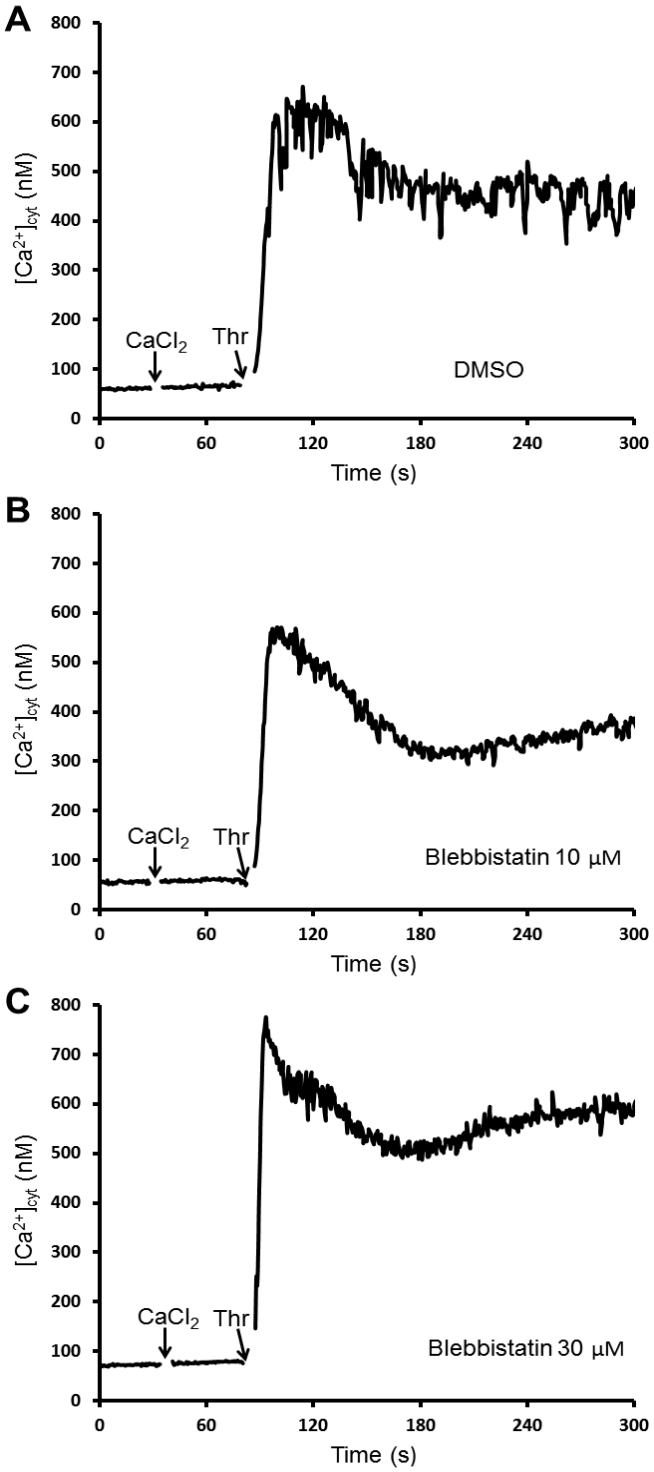

Fig. 3.8: Blebbistatin has no significant effect on thrombin-evoked rises in $[Ca^{2+}]_{cyt}$ elicited in the presence of extracellular Ca^{2+}. Fura-2-loaded human platelets were resuspended in supplemented HBS and incubated with either 10 μM blebbistatin (B), 30 μM blebbistatin (C), or an equal volume of DMSO (A) for 10 minutes at 37℃. Extracellular $CaCl_2$ was increased to 1 mM at the start of the experiment. 1 minute later, 0.5 U/mL thrombin was added to stimulate the cells.

3.2.6 Blebbistatin has no effect on thrombin-evoked platelet aggregation.

To confirm these findings, we examined the effect of blebbistatin on thrombin-evoked platelet aggregation elicited in the presence of extracellular Ca^{2+}. As shown in **Fig 3.9**, pretreatment of washed human platelets with 30 μM blebbistation had no significant effect on either the maximum extent (84.6 ± 6.0% for DMSO-treated cells and 70.2 ± 2.4% for blebbistain-treated cells; both n = 6; $P > 0.05$) or rate of platelet aggregation (99 ± 8 s for DMSO-treated cells and 103 ± 7 s for blebbistain-treated cells to reach maximum aggregation; both n = 6; $P > 0.05$). These results are distinct from nicergoline which significantly slows down the rate of platelet aggregation (see Section 3.1). Therefore these data suggest that myosin inhibition is not the primary mode of action of nicergoline.

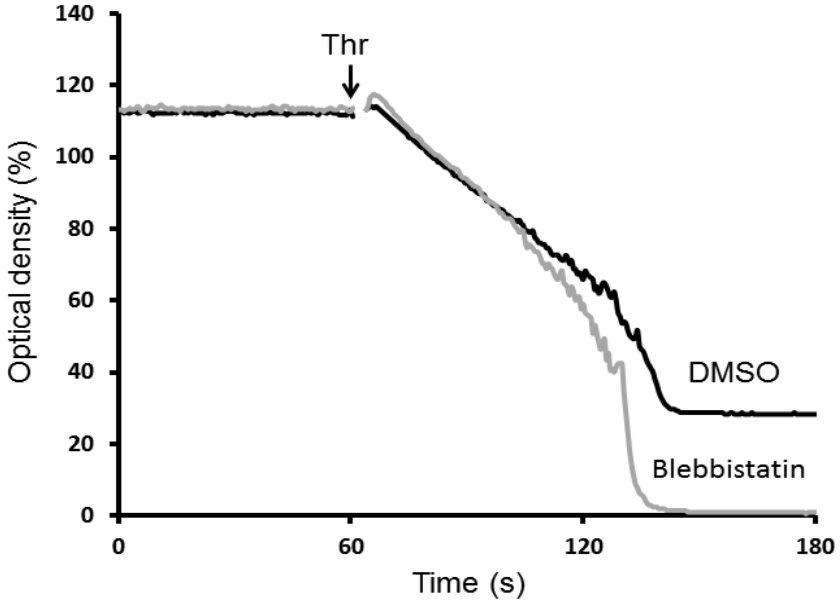

Fig. 3.9: Blebbistatin has no effect on thrombin-evoked human platelet aggregation. Washed platelets were resuspended in supplemented HBS and incubated with either 30 μM blebbistatin or an equivalent volume of DMSO at 37°C for 10 minutes. $CaCl_2$ was added to the cells prior the start of monitoring. Platelets were then stimulated with 0.5 U/mL thrombin.

3.3 Investigating the effect of the dynein inhibitor, ciliobrevin A, on thrombin-evoked human platelet function

Dynein is a molecular motor protein that plays a key role in regulating many cellular functions including organelle transport and movement of microtubules (Varma *et al*., 2008; Akhmanova & Hammer, 2010). Recent work has demonstrated that dyneins play a key role in maintaining the structure of the cortical microtubule ring by providing an antagonistic force to that of the kinesin motors (Diagouraga *et al*., 2014; also see Section 3.4). Therefore alterations in the activity of dynein might be able to alter the cortical microtubule structure by creating a net force for kinesin-mediated rearrangements. This could lead to the reorganization of the DTS bound to this structure, and thus alter platelet Ca^{2+} signalling (Walford *et al*., 2016). Ciliobrevin A has been previously demonstrated to be a specific reversible inhibitor of cytoplasmic dynein 1 and 2 activity which can prevent dynein-induced microtubule sliding (Firestone *et al*., 2012). Experiments were therefore performed to test whether ciliobrevin A treatment could mimic or modulate the action of nicergoline on platelet function.

3.3.1 Ciliobrevin A potentiates thrombin-evoked rises in $[Ca^{2+}]_{cyt}$ and thrombin-evoked reduction in $[Ca^{2+}]_{st}$ elicited in the absence of extracellular Ca^{2+}

Previous studies have demonstrated that ciliobrevin A inhibits dynein activity in a dose-dependent manner, with maximum inhibition observed at 100 µM without any significant alteration in kinesin activity (Firestone *et al*., 2012). Fura-2-loaded human platelets were preincubated with either 10, 50 or 100 µM ciliobrevin A, or an equivalent volume of its

vehicle DMSO for 30 minutes at 37°C under continuous magnetic stirring. The initial experiments showed that ciliobrevin A significantly quenched the Fura-2 fluorescence at the higher concentrations (50 µM and 100 µM). Although there was still a small residual quench of Fura-2 fluorescence at 10 µM ciliobrevin A, it was possible to overcome this effect by performing calibrations both in the presence and absence of this compound. When cells were pre-treated with 10 µM ciliobrevin A, thrombin-evoked Ca^{2+} signals elicited in the absence of extracellular Ca^{2+} were significantly potentiated to 120.6 ± 3.8% of those in cells treated with an equal volume of DMSO (n = 5, $P < 0.05$; respectively; **Fig. 3.10A,B**). These data suggested the possibility that dynein might negatively regulate Ca^{2+} signalling in human platelets and therefore if nicergoline was to artificially activate dynein this might be a potential method of action by which nicergoline has its effect on platelet Ca^{2+} signalling.

As it was not possible to make Fura-2-based $[Ca^{2+}]_{cyt}$ measurements at concentrations of ciliobrevin A that are able to induce maximal inhibition of dynein (Firestone *et al*., 2014), we instead attempted to make further measurements of thrombin-evoked Ca^{2+} signalling with the Fluo family of Ca^{2+} indicators as these have a distinct excitation and emission spectra from Fura-2. By doing this we hoped to overcome the quenching effects of ciliobrevin A at higher doses. Experiments using Fluo-5N-loaded platelets were performed to examine whether pretreatment with 100 µM ciliobrevin A affected thrombin-evoked Ca^{2+} release from intracellular Ca^{2+} stores, when cells were stimulated in the absence of extracellular Ca^{2+}. Our experiments found that 100 µM Ciliobrevin A introduced an autofluorescence to the experiment, however it was possible to correct for this effect by measuring this fluorescent rise by adding the same concentration to a

sample of the HBS in which the platelet sample was resuspended. By subtracting this autofluorescence we found that it was possible to nearly equalize the basal fluorescences (2.60 ± 1.88 arbitrary units for control cells and 2.65 ± 1.01 for ciliobrevin A-treated cells; n = 10; $P > 0.05$). However, there was a tendency for ciliobrevin A-treated cells to have a higher basal fluorescence than untreated cells, therefore to ensure this did not affect the results all fluorescence values were analysed both in their initial format as well as when normalized to the basal fluorescence recorded prior to thrombin stimulation (F/F_0). Pretreatment with 100 µM Ciliobrevin A for 30 minutes at 37ºC was found to significantly potentiate thrombin-evoked Ca^{2+} release from intracellular Ca^{2+} stores when platelets were stimulated in the absence of extracellular Ca^{2+}. This effect was observed when both the raw data traces (299.8 ± 35.4% of control; n = 10; $P < 0.05$; **Fig 3.10**) and the normalized traces (266.4 ± 39.7% of control; $P < 0.05$; **Fig 3.10C,D**) were analysed. These data suggest that the potentiation in thrombin-evoked cytosolic Ca^{2+} signals occurs due to an increased release of Ca^{2+} from the intracellular stores.

3.3.2 Pre-treatment with ciliobrevin A is unable to reverse the inhibitory effect of nicergoline on thrombin-evoked rises in $[Ca^{2+}]_{ext}$

To further confirm these experiments and to assess whether dynein activation might be the mechanism by which nicergoline can inhibit agonist-evoked Ca^{2+} signalling in human platelets, we examined the effect of treating platelets sequentially with either 100 µM ciliobrevin-A or an equal volume of its vehicle, DMSO, for 30 minutes at 37°C under

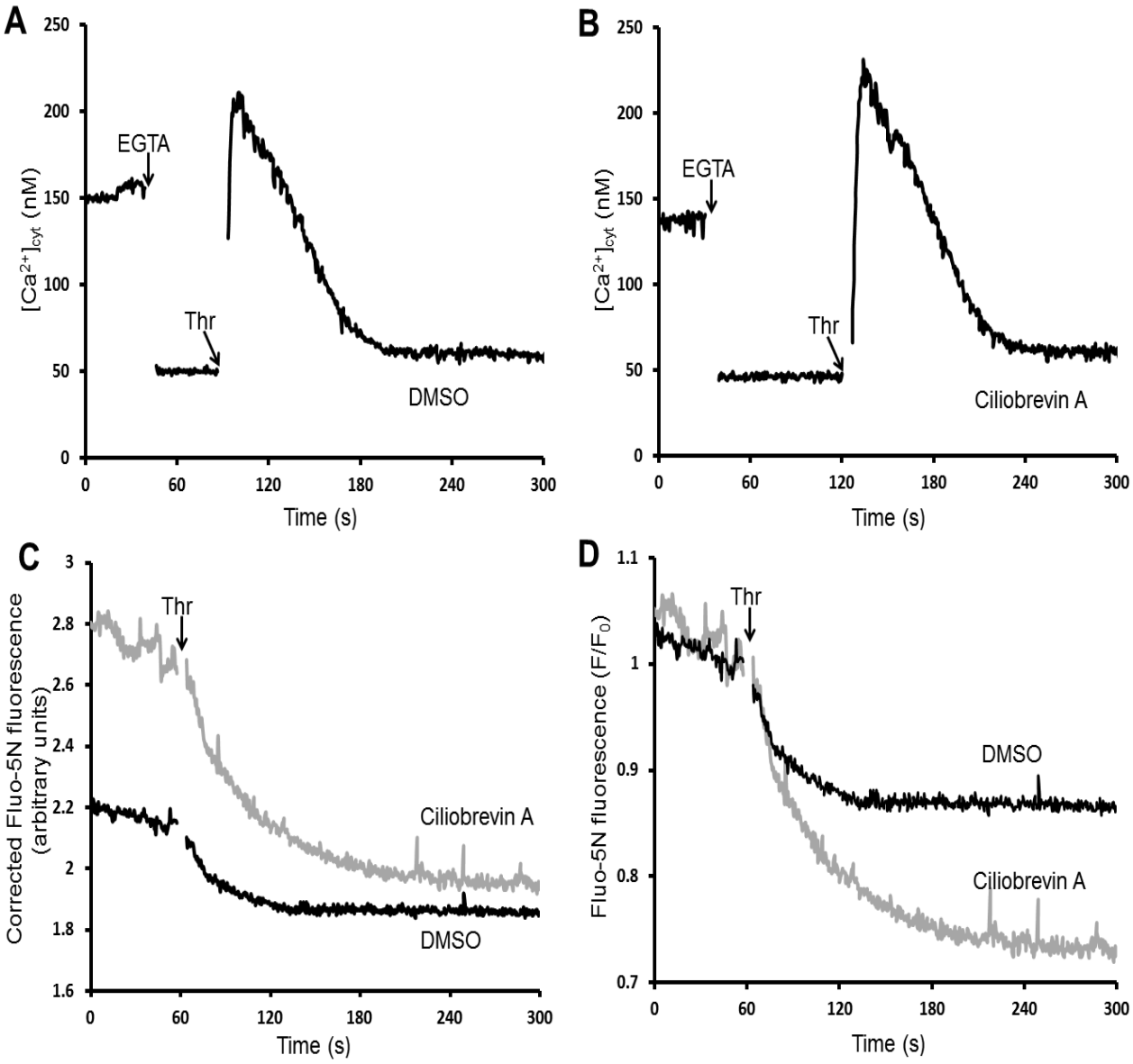

Fig. 3.10 Ciliobrevin A potentiates thrombin-evoked rises in $[Ca^{2+}]_{cyt}$ and thrombin-evoked reductions in $[Ca^{2+}]_{st}$ elicited in the absence of extracellular Ca^{2+}. Fura-2- (A,B) or Fluo-5N- (C,D) loaded human platelets; were resuspended in supplemented HBS and incubated with either 100 μM ciliobrevin A (B,C,D) or an equal volume of DMSO (A,C,D) for 30 minutes at 37℃. 1 mM EGTA was added at the start of the experiment to chelate extracellular Ca^{2+}. Cells were then stimulated 1 minute later by addition of 0.5 U/mL thrombin. (C) Fluo-5N fluorescence traces corrected for ciliobrevin autofluorescence. (D) shows the same traces as shown in (C) when the fluorescence values (F) are normalized to the basal fluorescence (F_0) prior to thrombin stimulation.

constant magnetic stirring, followed by a further 10 minute incubation under the same conditions with either 100 µM nicergoline or an equal volume of its vehicle, DMSO. Extracellular Ca^{2+} was then chelated with 1 mM EGTA and platelets stimulated by the addition of 0.5 U/mL thrombin.

To counter the autofluorescent effect of the ciliobrevin A, all data were calibrated for *total* extracellular Ca^{2+} concentration ($[Ca^{2+}]_{ext}$) using standard curves generated by adding known concentrations of Ca^{2+} to Fluo-4-containing HBS to which either nicergoline, ciliobrevin-A, both compounds or an equivalent volume of DMSO had been added. Prior to stimulation there was no significant difference in the mean $[Ca^{2+}]_{ext}$ measured in double DMSO-treated control cells (221.1 ± 4.7 µM), nicergoline-treated cells (212.8 ± 2.7 µM), ciliobrevin-treated cells (223.1 ± 11.6 µM), and cells treated with both inhibitors (224.3 ± 6.4 µM; all n = 6; $P > 0.05$ for all comparisons). The *free* $[Ca^{2+}]_{ext}$ is significantly smaller due to the presence of large concentrations of the Ca^{2+} chelator EGTA (e.g. the free $[Ca^{2+}]_{ext}$ for control cells can be calculated using the maxchelator software to be 17.7 nM which is significantly below the resting $[Ca^{2+}]_{cyt}$; Bers *et al*., 2010). These data therefore demonstrate that our calibration could overcome the presence of the autofluorescent ciliobrevin-A compound. In agreement with our previous studies, nicergoline pretreatment significantly inhibited the thrombin-rise in $[Ca^{2+}]_{ext}$ to 58.3 ± 2.3% of DMSO-treated control cells (n = 6; $P < 0.05$; Fig **3.11B**; Walford *et al*., 2016). In contrast, pretreatment with ciliobrevin-A significantly potentiated the thrombin-evoked rise in $[Ca^{2+}]_{ext}$ (154.0 ± 14.2% of DMSO-treated control cells; n = 6; $P < 0.05$; **Fig 3.11C**). However when cells were sequentially treated with both compounds, the inhibitory effect of nicergoline was further exacerbated, with the thrombin-evoked rise in

$[Ca^{2+}]_{ext}$ inhibited to 41.3 ± 4.5% of DMSO-treated control cells (n = 6; *P* < 0.05 compared to all other conditions; **Fig 3.11D**). These data therefore suggest that dynein activation is unlikely to be the mechanism of action by which nicergoline inhibits agonist-evoked Ca^{2+} signalling in human platelets.

3.3.3 Ciliobrevin A inhibits thrombin-evoked rises in $[Ca^{2+}]_{cyt}$ elicited in the presence of extracellular Ca^{2+}

To further assess the effect of ciliobrevin A on human platelet function, we also performed experiments to asesss the effect of ciliobrevin A on thrombin-evoked rises in $[Ca^{2+}]_{cyt}$ elicited in the presence of physiological extracellular Ca^{2+} conditions. As shown in **Fig 3.12**, pretreatment of Fura-2-loaded cells with 10 µM ciliobrevin A had a tendency to have a small inhibitory effect on thrombin-evoked rises in $[Ca^{2+}]_{cyt}$ elicited in the presence of extracellular Ca^{2+}. However this effect did not reach statistical significance (70.9 ± 12.7% of DMSO-treated control cells; n = 9; P = 0.07). These results are also inconsistent with nicergoline having its effect through altering dynein activity in human platelets. These results also suggest that as well as negatively regulating Ca^{2+} release from intracellular stores, dynein may have an additional effect on facilitating activation of a Ca^{2+} permeable channel on the platelet plasma membrane. Further studies will be required to further examine this possibility.

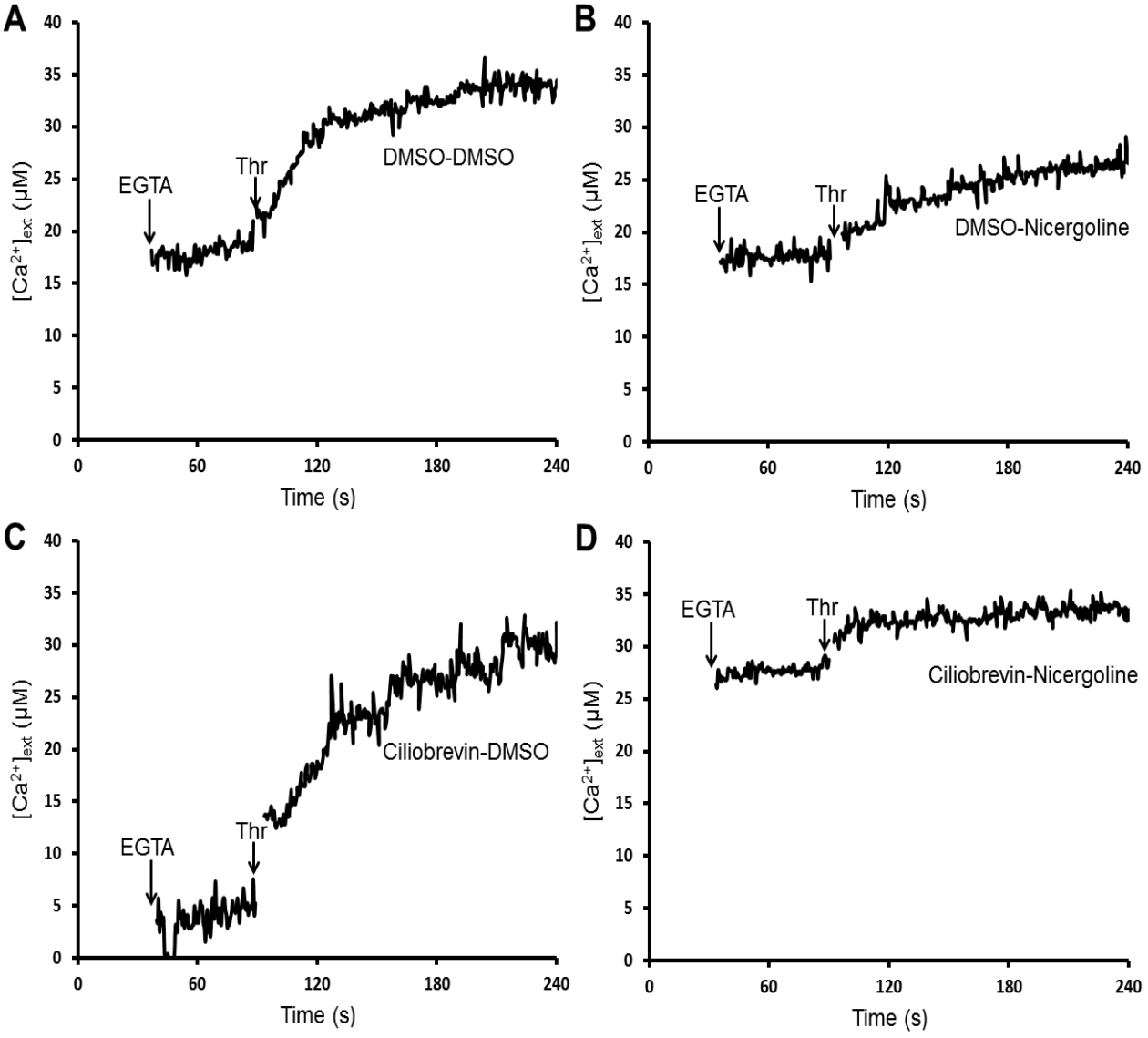

Fig. 3.11: Pre-treatment with ciliobrevin A is unable to reverse the inhibitory effect of nicergoline on thrombin-evoked rises in $[Ca^{2+}]_{ext}$. Washed human platelets were resuspended in supplemented HBS and incubated with either 100 µM ciliobrevin A (C,D) or an equivalent volume of its vehicle, DMSO (A,B) for 30 minutes at 37℃ under conditions of continuous magnetic stirring. Following this cells were preincubated under the same conditions for a further 10 minutes with either 100 µM nicergoline (B,D) or an equivalent volume of its vehicle, DMSO (A,C). 2.5 µM Fluo-4 salt was added to platelets just prior the start of monitoring the cells. 1 mM EGTA was added at the start of the experiment, and cells were stimulated 1 minute later with 0.5 U/mL thrombin.

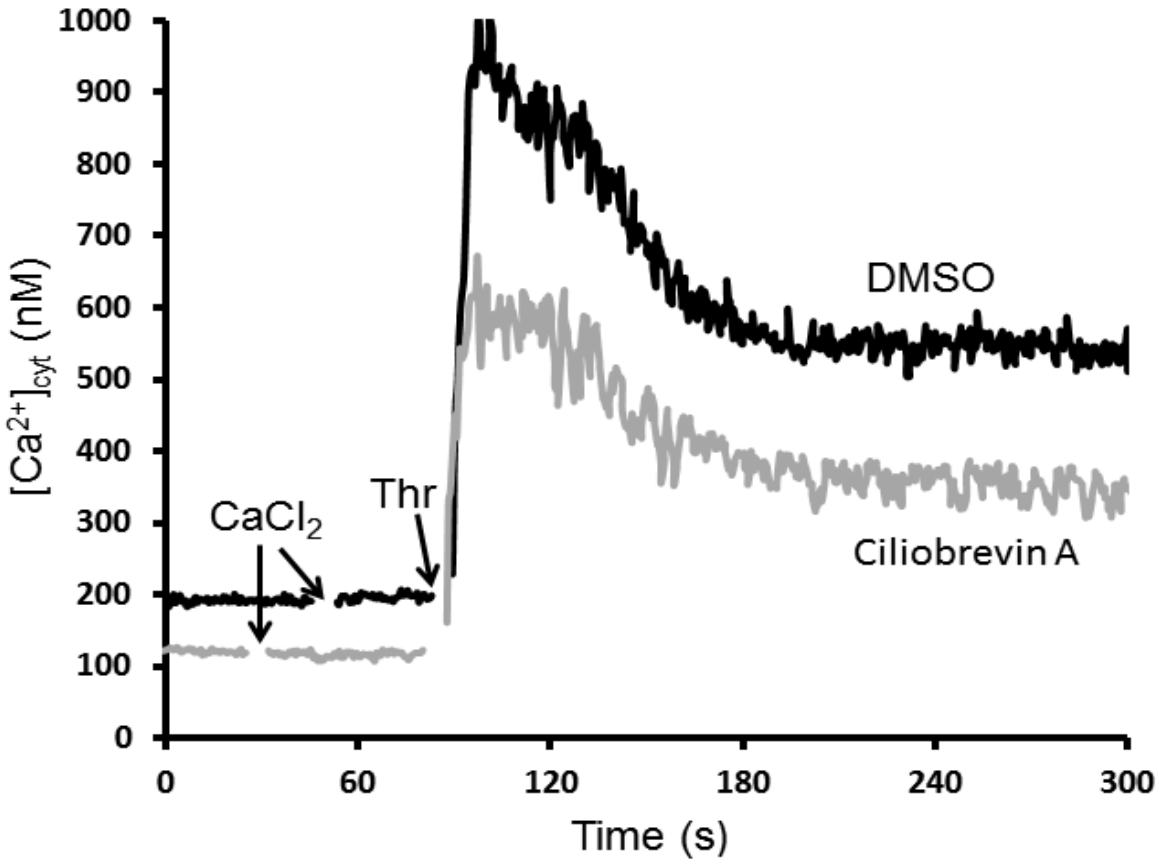

Fig. 3.12: Ciliobrevin-A inhibits thrombin-evoked rises in $[Ca^{2+}]_{cyt}$ elicited in the presence of extracellular Ca^{2+}. Fura-2 loaded human platelets were resuspended in supplemented HBS and incubated for 30 minutes with either 10 μM ciliobrevin A (B) or an equal volume of DMSO (A) at 37℃. Extracellular Ca^{2+} concentration was adjusted to 1 mM at the start of the experiment, and then cells were stimulated one minute later with 0.5 U/mL thrombin.

3.3.4 Ciliobrevin A has no significant effect on thrombin-evoked platelet aggregation

In line with the experiments done in the presence of extracellular Ca^{2+}, the inhibitory effect exerted by ciliobrevin A on cytosolic Ca^{2+} did not correlate with any effect on platelet aggregation as pretreatment with 100 µM ciliobrevin A had no effect on the rate or extent of platelet aggregation, with both maximum aggregation and time to reach maximum aggregation being similar between ciliobrevin-treated (77.8 ± 2.9% and 99.3 ± 2.1 s respectively) and control cells (78.6 ± 3.4% and 102.7 ± 4.7 s respectively; n = 6; both P > 0.05; **Fig. 3.13**) suggesting this inhibitory effect has limited impact on platelet functionality.

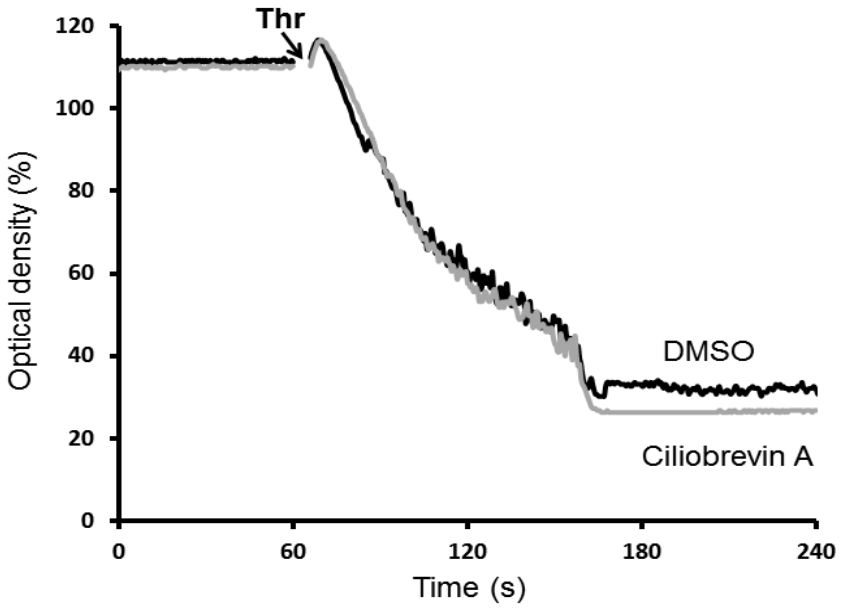

Fig. 3.13: Ciliobrevin A has no significant effect on thrombin-evoked human platelet aggregation. Washed human platelets resuspended in supplemented HBS were incubated with either 100 µM ciliobrevin A or an equal volume of its vehicle, DMSO for 30 minutes at 37°C. $CaCl_2$ was added to the cells prior the start of the experiment. Platelets were then stimulated with 0.5 U/mL thrombin to initiate aggregation.

3.4 Investigating the effect of an inhibitor of the motor protein kinesin on thrombin-evoked Ca^{2+} signalling in human platelets

Previous studies have defined that kinesins function as molecular motor proteins that play a role in determining the distribution of organelles and secretory granules inside the cell (Marx *et al*., 2009). Previous work on platelets has demonstrated a role for kinesins in maintaining the normal structure of the resting platelet through maintaining the normal structure of the cortical microtubule bundle. Treatment of resting platelets with the kinesin-inhibitor, aurintricarboxylic acid was shown to induce spontaneous coiling of the cortical microtubules (Diagouraga *et al*, 2014). As this coiling induces platelets to become spherical with a re-organised cortical microtubule bundle, we performed experiments to examine whether this kinesin inhibitor can mimic or modulate the inhibitory effects of nicergoline on platelet function.

3.4.1 ATA inhibits thrombin-evoked rises in $[Ca^{2+}]_{cyt}$ in human platelets stimulated in the presence of physiological levels of extracellular Ca^{2+}

Previous studies have demonstrated that ATA acts in a dose-dependent manner to inhibit platelet function with a maximum effect at 30 μM (Takiguchi *et al*., 1996). Fura-2-loaded human platelets were preincubated with 30 μM ATA, or an equivalent volume of its vehicle DMSO for 10 minutes at 37°C under continuous magnetic stirring. When platelets were stimulated with thrombin in the presence of physiological extracellular Ca^{2+} concentrations, thrombin-evoked rises in $[Ca^{2+}]_{cyt}$ were significantly inhibited to 14.2 ± 3.8% of control (n = 6, $P < 0.05$, **Fig. 3.14**).

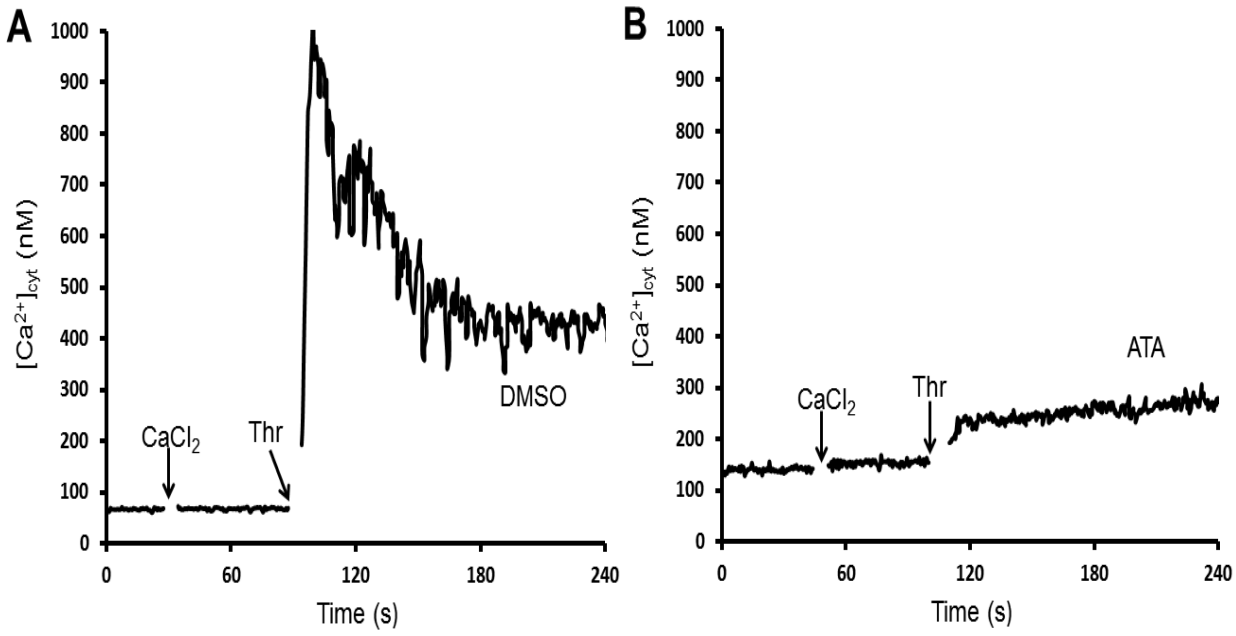

Fig 3.14: ATA inhibits the thrombin-evoked platelet rises in $[Ca^{2+}]_{cyt}$ elicited in the presence of extracellular Ca^{2+}. Fura-2-loaded human platelets were resuspended in supplemented HBS and incubated with either 30 µM ATA (B) or an equal volume of its vehicle, DMSO (A) for 10 minutes at 37ºC. Extracellular Ca^{2+} was raised to 1 mM and cells were then stimulated 1 minute later with 0.5 U/mL thrombin.

3.4.2 ATA inhibits thrombin-evoked platelet aggregation

To confirm these findings, additional experiments were performed to examine whether pretreatment with ATA could inhibit thrombin-evoked platelet aggregation. **Fig. 3.15** shows the effect of pretreatment of washed human platelets with either 30 µM ATA (or an equivalent volume of its vehicle, DMSO) for 10 minutes at 37°C under continuous magnetic stirring. ATA pretreatment significantly increased both the time to reach maximum aggregation (171.4 ± 3.0 s and 86.8 ± 8.7 s for ATA- and DMSO-treated cells respectively; n = 5; $P < 0.05$), as well as significantly inhibiting the maximum extent of platelet aggregation observed in thrombin-stimulated cells (56.0 ± 1.9% and 78.7 ± 2.3% of maximum for ATA- and DMSO-treated cells respectively; n = 5; $P < 0.05$). These data suggest the inhibitory effect of ATA on rises in $[Ca^{2+}]_{cyt}$ result in similar effects on platelet aggregation elicited under similar conditions.

3.4.3 ATA inhibits thrombin-evoked rises in $[Ca^{2+}]_{cyt}$ in human platelets stimulated in the absence of extracellular Ca^{2+}, and has no cumulative effect when combined with nicergoline

Further experiments were performed to examine whether this inhibitory effect of ATA could also be observed on platelet stimulated in the absence of extracellular Ca^{2+}. In addition, experiments were simultaneously performed to examine whether the inhibitory effect of ATA was cumulative with the inhibitory effect of nicergoline under these conditions. If there is cumulative effect of these two inhibitors used together is greater than the effect of either inhibitor used alone, it would indicate they are working through distinct pathways, such that we could rule out the possibility that kinesins are the targets

of nicergoline. However if the effect of either inhibitor alone was similar in magnitude to that observed when both inhibitors are used together then this would indicate that these inhibitors could be working through inhibiting the same part of the Ca^{2+} signalling pathway.

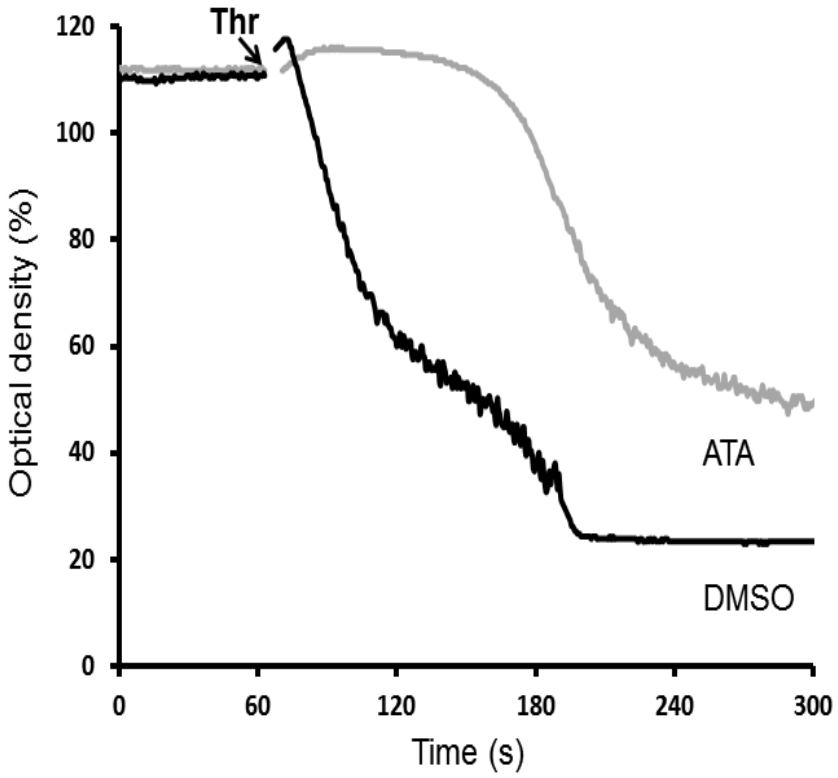

Fig. 3.15: ATA inhibits thrombin-evoked platelet aggregation. Washed platelets were resuspended in supplemented HBS and incubated with either 30 μM ATA or an equivalent volume of DMSO at 37℃ for 10 minutes under continuous magnetic stirring. $CaCl_2$ was added to raise it to a final concentration of 1 mM. Platelets were then stimulated with 0.5 U/mL thrombin.

Initially Fura-2-loaded human platelets were pretreated with either 30 µM ATA, or an equivalent volume of its vehicle (DMSO) for 10 minutes at 37°C under continuous magnetic stirring, and then further treated with either 100 µM nicergoline or an equivalent volume of DMSO for a further 10 minutes under the same conditions. In line with our previous findings, pretreatment with nicergoline alone significantly inhibited thrombin-evoked rises in $[Ca^{2+}]_{cyt}$ compared to double DMSO-treated cells (75.2 ± 2.4% of double DMSO-treated cells, n = 5, *P* < 0.05; **Fig 3.16B**; Walford *et al*., 2016). Interestingly, cells pretreated with ATA alone inhibited thrombin-evoked rises in $[Ca^{2+}]_{ext}$ more than nicergoline (33.9 ± 10.8% of double DMSO-treated cells (n = 5, *P* < 0.05 against both nicergoline- and DMSO-treated cells, **Fig 3.16C**). When platelets were pre-treated with ATA followed by nicergoline, the inclusion of nicergoline elicited no additional inhibitory effect compared to cells treated with ATA alone (35.8 ± 4.9 % of double DMSO-treated control cells; n = 5; P > 0.05; **Fig 3.16D**). These data therefore suggest the possibility that nicergoline could have its inhibitory effects through partially inhibiting kinesin activity.

3.4.4 ATA inhibits thrombin-evoked rises in $[Ca^{2+}]_{ext}$ and thrombin-evoked decreases in $[Ca^{2+}]_{st}$ in human platelets

To confirm these findings, further experiments were performed to examine the effect of ATA and nicergoline alone and in combination; on the thrombin-evoked rise in $[Ca^{2+}]_{ext.}$ Washed platelets were suspended in supplemented HBS and treated with either 30 µM ATA or an equivalent volume of DMSO for 10 minutes, and then followed by

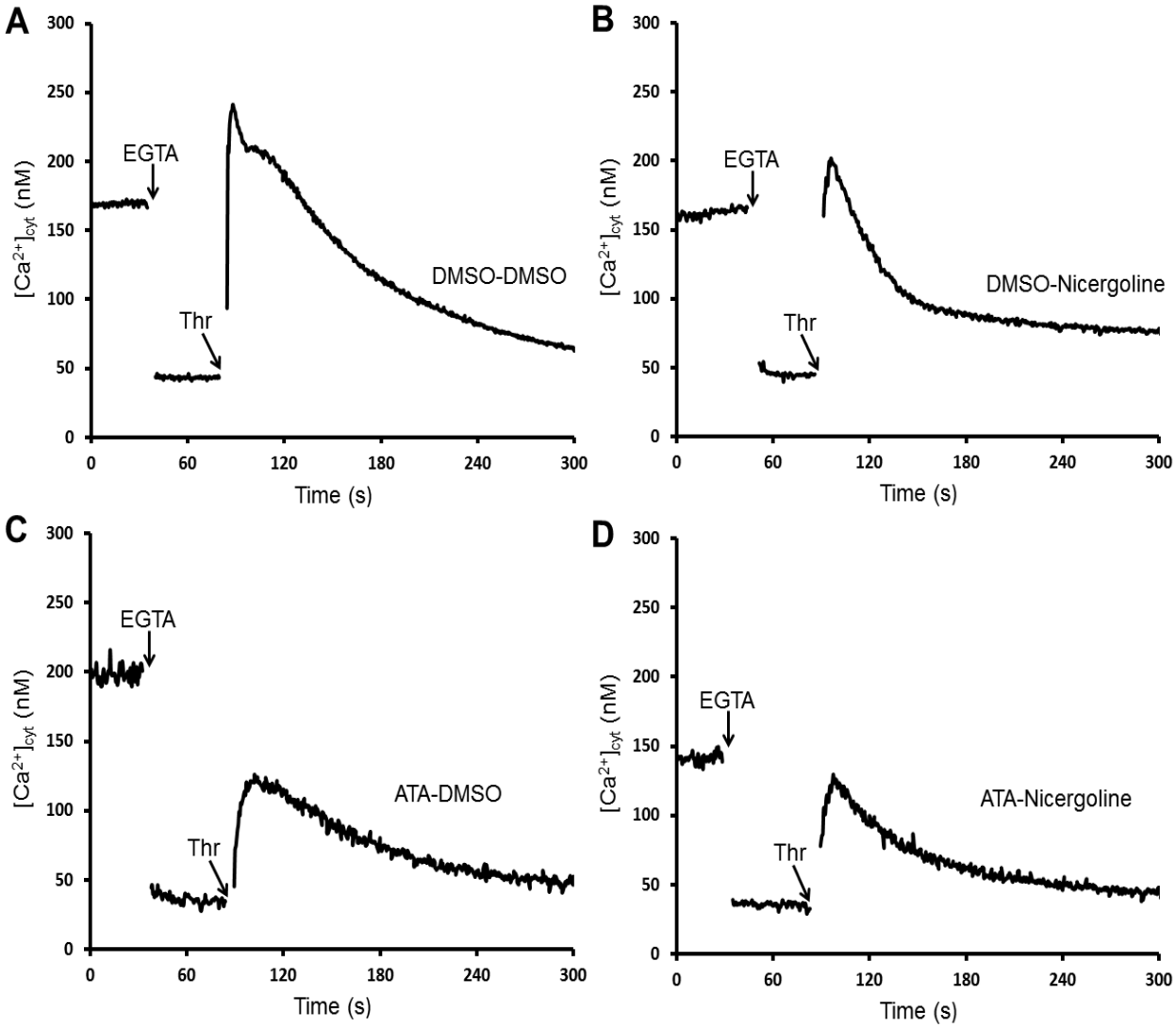

Fig. 3.16: ATA inhibits thrombin-evoked rises in $[Ca^{2+}]_{cyt}$ in human platelets stimulated in the absence of extracellular Ca^{2+}, and has no cumulative effect when combined with nicergoline. Fura-2-loaded human platelets were resuspended in supplemented HBS, and incubated with either 30 µM ATA (C,D) or an equal volume of its vehicle, DMSO (A,B) for 10 minutes at 37C under continuous magnetic stirring. This was followed by a further incubation of cells for 10 minutes with either 100 µM Nicergoline (B,D) or an equal volume of its vehicle, DMSO (A,C) under identical conditions. 1 mM EGTA was added at the start of the experiment to chelate all extracellular Ca^{2+}. Cells were then stimulated 1 minute later by the addition of 0.5 U/mL thrombin.

a further 10 minutes incubation with either 100 μM Nicergoline or an equivalent volume of DMSO at 37℃ under continuous magnetic stirring. Fluo-4 K^+ salt was then added immediately before the start of the experiment to allow thrombin-evoked rises in the Ca^{2+} concentration of the extracellular medium to be measured. Consistent with our previous findings, cells treated with nicergoline alone showed a significant reduction in thrombin-evoked rises in $[Ca^{2+}]_{ext}$ to 49.0 ± 7.0% of double DMSO-treated cells (n = 6, *P* < 0.05; **Fig. 3.17B**). A similar inhibition was also obtained in cells pretreated with ATA (55.0 ± % of double DMSO-treated cells; n = 6, *P* < 0.05; **Fig. 3.17C**). Pretreatment with both ATA and nicergoline also inhibited the reduction in $[Ca^{2+}]_{ext}$ rises to 33.9 ± 7.9% of control, although this was not significantly different from either treatment alone (n = 6, *P* < 0.05 compared to control; P > 0.05 for both single drug treatments; **Fig. 3.17D**).

In addition, the same experiment was also conducted with Fluo-5N-loaded human platelets to examine how ATA and nicergoline affect thrombin-evoked Ca^{2+} release from intracellular stores when cells were stimulated in the absence of extracellular Ca^{2+}. As can be seen in **Fig 3.18**, pretreatment with either ATA or nicergoline alone significantly inhibited the thrombin-evoked reduction in intracellular store Ca^{2+} concentration to 31.5 ± 11.1% and 72.3 ± 3.6% of double DMSO treated control cells for ATA- and nicergoline-treated cells respectively (both n = 6; both P < 0.05 compared to control). In addition, cells treated with both compounds were found to have a reduction in the thrombin-evoked fall in $[Ca^{2+}]_{st}$ to 43.5 ± 6.8% of control (n =6; P < 0.05). Treatment with both ATA and nicergoline was found not to be significantly different from treatment with ATA alone (P > 0.05), in line with these compounds could be working via a common mechanism.

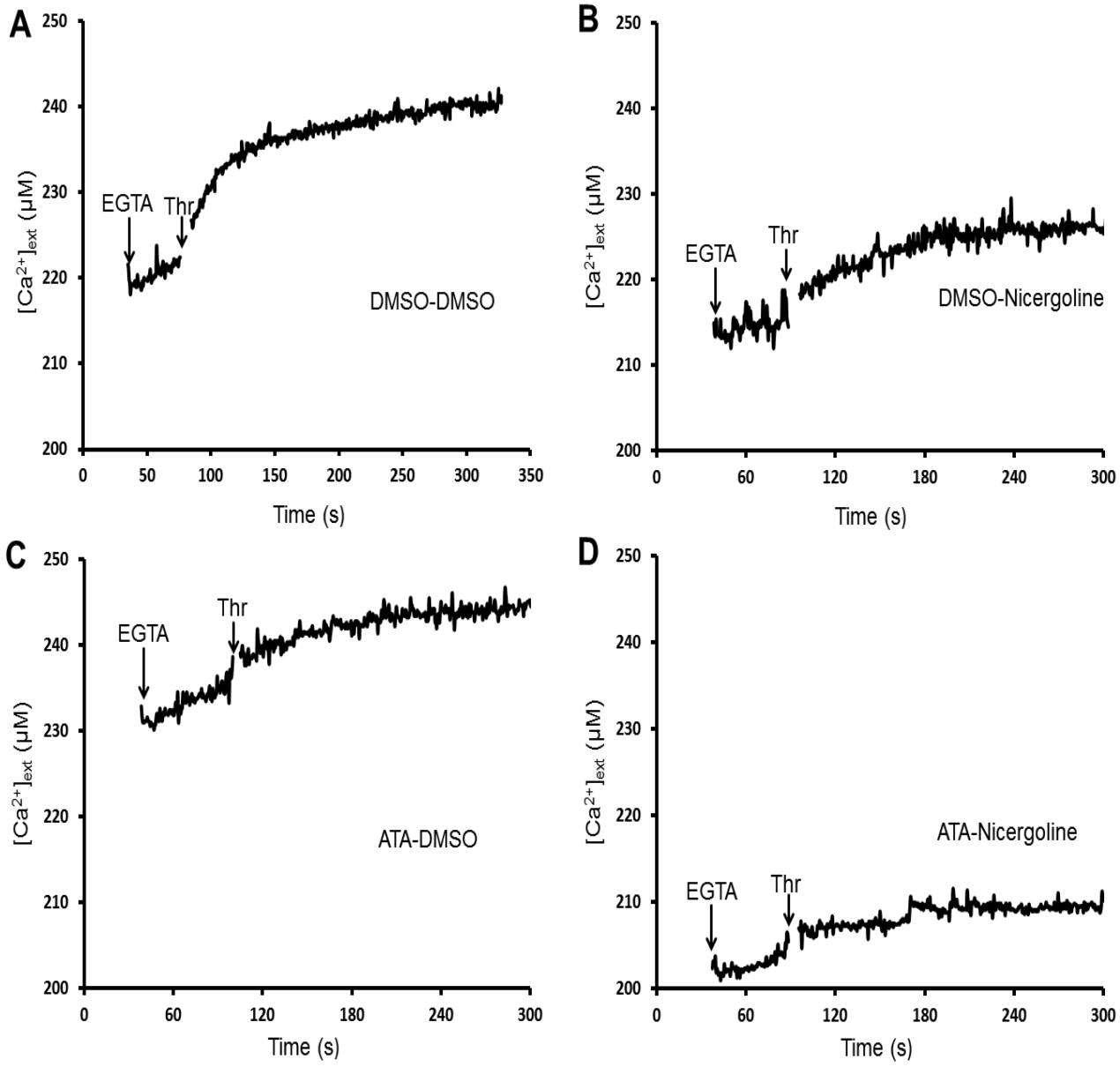

Fig.3.17: ATA inhibits thrombin-evoked rises in $[Ca^{2+}]_{ext}$ in human platelets stimulated in the absence of extracellular Ca^{2+}, and has no cumulative effect when combined with nicergoline. Washed human platelets were resuspended in supplemented HBS and incubated with either 30 μM ATA (C,D) or an equivalent volume of DMSO (A,B) for 10 minutes, followed by additional incubation with either 100 μM Nicergoline (B,D) or an equivalent volume of DMSO (A,C) for another 10 minutes at 37℃. 2.5 μM Fluo-4 salt was added to the cells just prior the start of experiment. 1 mM EGTA was then added at the start of the experiment to chelate extracellular Ca^{2+}, followed 1 minute later by the stimulation of cells with 0.5 U/mL thrombin.

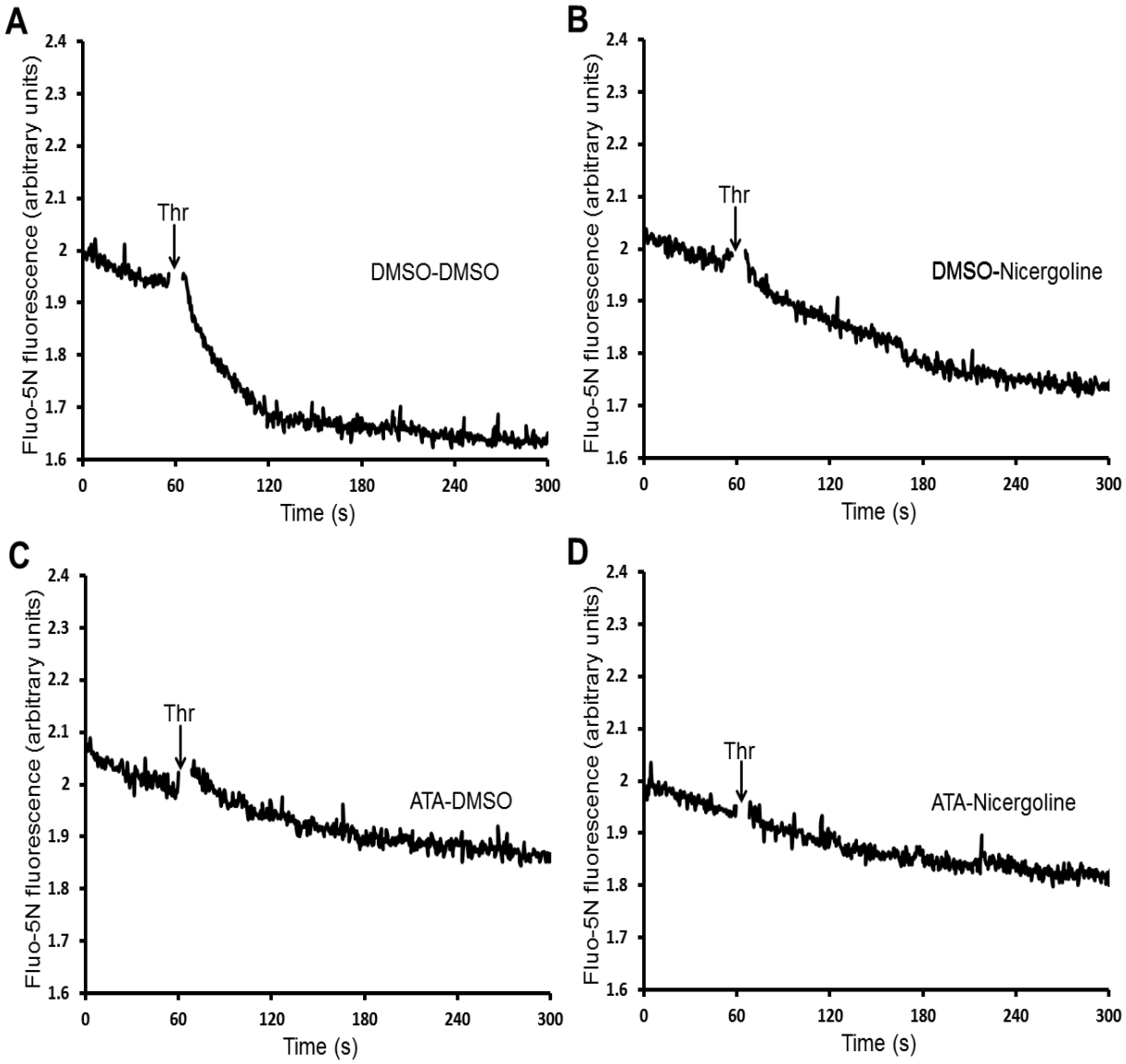

Fig. 3.18 ATA inhibits thrombin-evoked reductions in $[Ca^{2+}]_{st}$ in human platelets stimulated in the absence of extracellular Ca^{2+}, and has no cumulative effect when combined with nicergoline Fluo-5N-loaded human platelets were resuspended in supplemented HBS and incubated at 37°C with either 30 µM ATA (C,D) or an equivalent volume of DMSO (A,B) for 10 minutes. Stirred platelet samples were further incubated with either 100 µM Nicergoline (B,D) or an equivalent volume of DMSO (A,C) for a further 10 minutes. 1 mM EGTA was then added to cells prior to the start of experiment. Cells were then stimulated with 0.5 U/mL thrombin 1 minute later.

3.4.5 ATA inhibits thrombin-evoked shape change

To examine whether the inhibition of Ca^{2+} signalling by ATA elicited concomitant changes in platelet functionality, experiments were performed to examine if platelet shape change elicited in the absence of extracellular Ca^{2+} was affected by pre-treatment with this drug. Washed human platelets suspended in supplemented HBS were preincubated for 10 minutes with either 30 μM ATA or an equivalent volume of its vehicle, DMSO at 37℃ under continuous magnetic stirring. EGTA was then added to chelate the extracellular Ca^{2+} prior the monitoring of samples in an aggregometer at 37°C. As can be seen in **Fig. 3.19**, pretreatment with ATA significantly inhibited the magnitude of platelet shape change observed. A mean light transmittance decrease of 10.0 ± 2.0% of maximum light transmittance was observed in DMSO-treated cells, compared to a mean decrease of 1.8 ± 0.9% of maximum light transmittance in ATA-treated cells ($n = 7$; $P < 0.05$). These data suggest that ATA pretreatment interferes with the normal shape change response of human platelets, as previously suggested by Diagouraga *et al*., (2014).

3.4.6 Incubation with ATA significantly inhibited the thrombin-evoked increase F-actin content in human platelets.

Previous studies have been reported the importance of the actin cytoskeleton in the platelet shape that is elicited upon agonist stimulation (White & Burris, 1984; Johnson *et al*., 2007). In addition previous studies have also demonstrated that the actin cytoskeleton plays a key role in modulating platelet Ca^{2+} signalling (Harper & Sage,

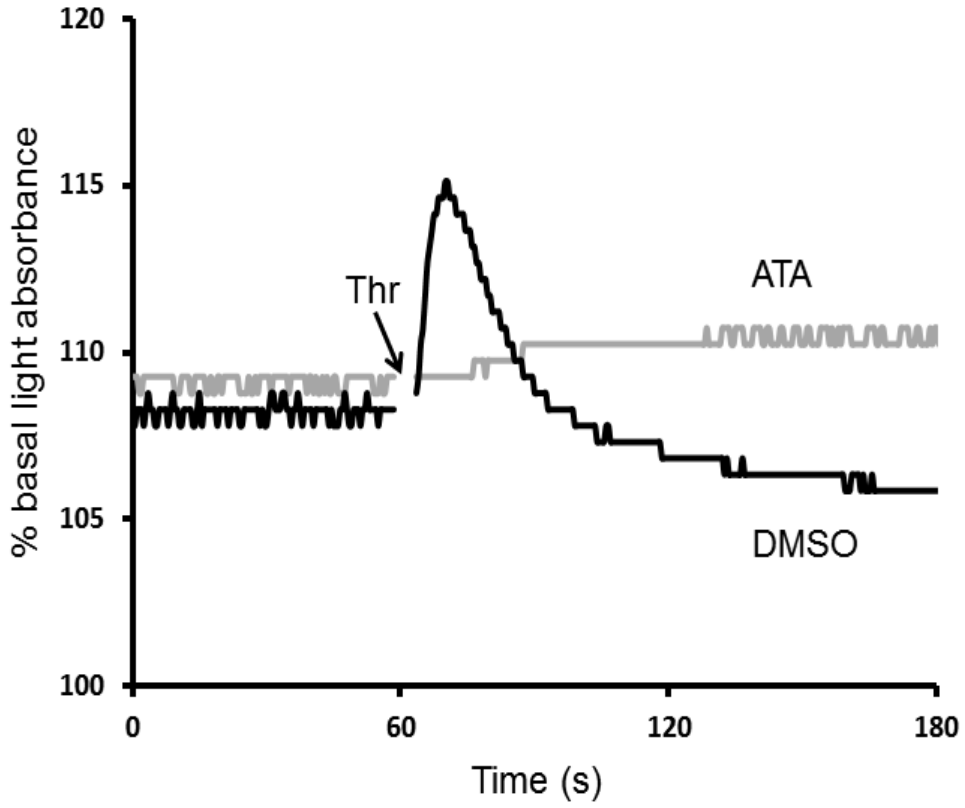

Fig 3.19 ATA inhibits thrombin-evoked shape change. Washed human platelets were resuspended in supplemented HBS and incubated at 37℃ with either 30 μM ATA or an equivalent volume of its vehicle, DMSO for 10 minutes. EGTA was then added at 1 mM just before the start of the experiment. Cells were then stimulated with 0.5 U/mL thrombin.

2006; Harper & Sage, 2007; Rosado & Sage, 2000). Therefore, additional experiments were performed to identify if ATA treatment is able to affect platelet Ca^{2+} signalling by either altering the distribution of the cortical actin cytoskeleton in resting platelets or the amount of F-actin in resting and thrombin-stimulated human platelets. Resting platelets or platelets stimulated with thrombin for 1 minute were fixed and labelled with iFluor555-labelled phalloidin. Cells were then washed and fluorescence from phalloidin-tagged F-actin was monitored using a microplate reader. Each individual measurement was the mean of 3 fluorescence readings obtained from different samples of the labelled platelets. Under these conditions, ATA had no significant effect on the F-actin content of resting platelets (129.0 ± 14.0 % of control; n = 6; *P* = 0.09). These results were supported by analysis of these platelets by fluorescence microscopy after loading onto poly-L-lysine coverslips. Assessment showed that ATA-treated platelets appear more rounded – similar to nicergoline-treated platelets (Walford *et al.*., 2016). The cortical actin ring appeared unaffected in ATA-treated cells. Measurements were made of the thickness of the cortical actin ring using Image J analysis of the recorded pictures, and there was found to be no significant difference in the thickness of the cortical ring in both ATA- (819 ± 48.nm; n = 56 cells) and DMSO-treated platelets (802 ± 33.nm; n = 58 cells; *P* > 0.05; **Fig 3.20**). These data therefore suggest that despite the ATA-induced coiling of the cortical microtubule bundles in resting platelets (Diagouraga *et al*., 2013), there is no associated change in the distribution of F-actin in resting platelets. However upon thrombin stimulation in the absence of extracellular Ca^{2+}, F-actin content of ATA-treated platelets showed significantly less increase in the F-actin content compared to DMSO-treated cells (44.3 ± 18.8% of control; n = 6, *P* < 0.05).

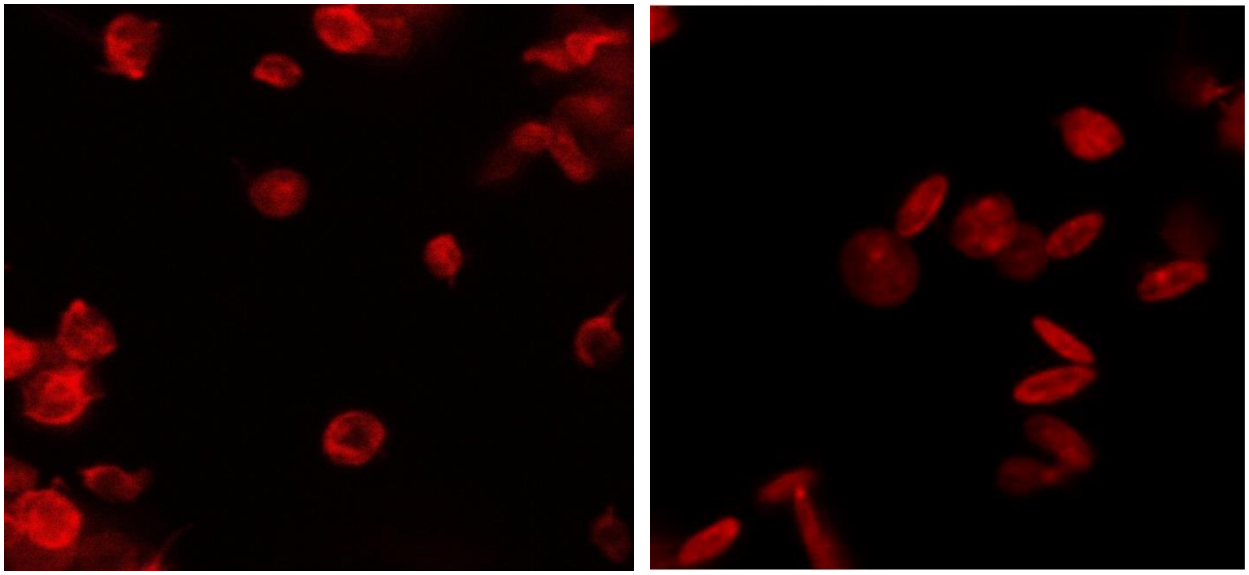

Fig. 3.20: The cortical F-actin ring appears unaffected in ATA-treated platelets. Platelets were treated with either 30 μM ATA (left panel) or DMSO (right panel) at 37ºC for 10 minutes under constant magnetic stirring. Cells were then fixed, permeabilised and labelled with phalloidin iFluor 555 dye. Platelets were then washed and loaded onto poly-L-lysine coated slides and cells left for 5 minutes to settle. Excess platelet suspension was then pipetted out and the slides were washed with PBS. Cells were then monitored for F-actin fluorescence using an Olympus Fluoview FV1200 confocal microscope. The results were obtained from cells from two different donors.

As blocking F-actin polymerization with cytochalasin D has been shown to potentiate thrombin-evoked cytosolic Ca^{2+} signals under the same stimulatation conditions (Harper & Sage, 2006), these data therefore suggest the possibility that the ATA-induced impairment of the thrombin-evoked rise in cytosolic Ca^{2+} may prevent normal reorganization of the F-actin cytoskeleton.

3.4.7 ATA inhibits thrombin-evoked dense granule secretion in human platelets

Our previous studies have demonstrated that nicergoline inhibited platelet functionality at least in part through an inhibitory effect on dense granule secretion (Walford *et* al., 2016). Therefore experiments were performed to examine whether ATA was able to elicit a similar inhibitory effect on this parameter here. Washed human platelets were resuspended in supplemented HBS and incubated at 37°C with 30 µM ATA or an equal volume of its vehicle, DMSO for 10 minutes under continuous magnetic stirring. EGTA and luciferin-luciferase was then added to the cells prior to thrombin stimulation. All values were normalized to the maximum luminescence values obtained at the end of each run by addition of 10 µM ATP to each sample. Thrombin-evoked dense granule secretion was found to be significantly inhibited in ATA-pretreated cells compared to control cells. Thrombin stimulation of DMSO-treated cells was found to elicit an increase in fluorescence of 7.4 ± 2% of maximum ATP secretion, whereas ATA-treated cells only elicited an increase of 0.8 ± 0.3% of maximum ATP secretion ($n = 6$; $P < 0.05$; **Fig. 3.21**). These data therefore are consistent with kinesin being a potential molecular target of nicergoline in platelets.

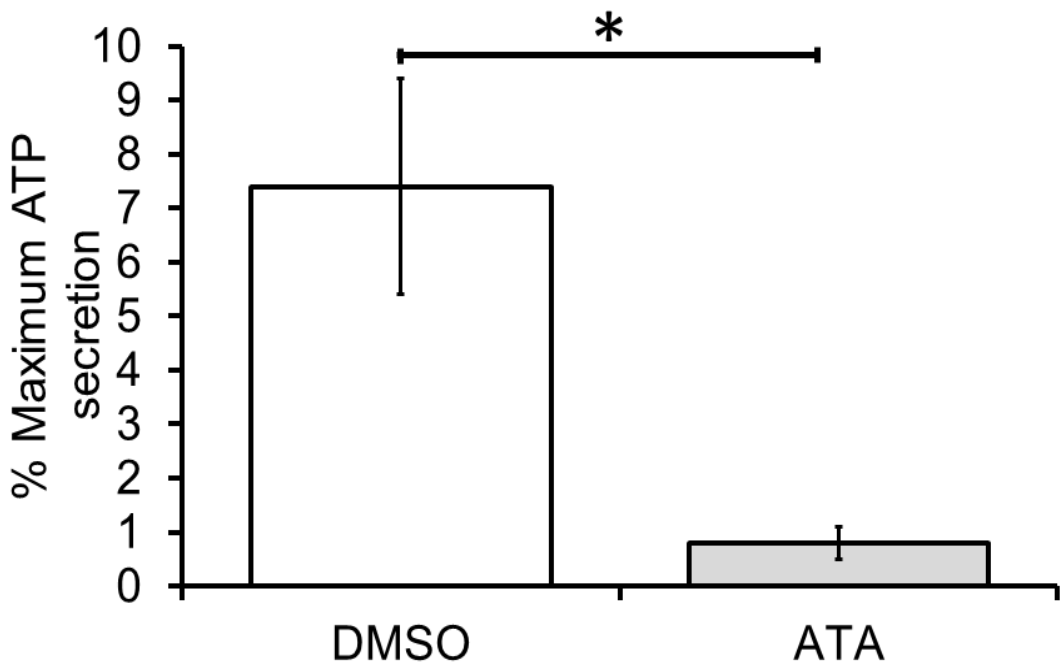

Fig. 3.21: ATA inhibits thrombin-evoked dense granule secretion in human platelets. Washed human platelets were resuspended in supplemented HBS, and incubated at 37°C with 30 µM ATA or an equal volume of DMSO for 10 minutes at 37°C. EGTA was then added to cells followed by the addition of Luciferin-luciferase prior the start of experiment. Cells were then monitored before and after stimulation with 0.5 U/mL thrombin. All results normalized to a maximum value measured after the addition of 10 µM ATP to the sample at the end of the experiment. * = $P < 0.05$

3.4.8 ATA inhibits the generation of pericellular Ca^{2+} signalling in human platelets.

Previous studies have demonstrated that it is possible to observe pericellular Ca^{2+} signals in single, thrombin-stimulated human platelets (Sage *et al*., 2013; Walford *et al*., 2016). These pericellular Ca^{2+} rises were found to occur within an extracellular space found within the interior of the cell, consistent with their creation in the OCS. In addition,

they were found to originate within a specific sub-region of the cell – which has been shown to be likely created by the membrane complex (Sage *et al*., 2013; Walford *et al*., 2016). If kinesin inhibition alters the normal positioning of the DTS in human platelets, it would be expected that it would disrupt the membrane complex and thus reduce the number of pericellular Ca^{2+} rises observed in ATA-treated cells. Therefore, experiments were performed to examine whether the creation of pericellular Ca^{2+} hotspots was reduced in ATA pretreated cells. Thrombin stimulation evoked pericellular Ca^{2+} hotspots in 77.1 ± 5.0% of DMSO-treated control cells, whilst these Ca^{2+} signals were only observed in 41.0 ± 13.6% of ATA-treated cells taken from the same 5 donors ($P < 0.05$; **Fig 3.22**). These data are consistent with our previous findings in which nicergoline significantly reduced the proportion of cells producing these signals (Walford *et al*., 2016). Therefore, these data further support the hypothesis that kinesin may be the target of nicergoline's action in human platelets.

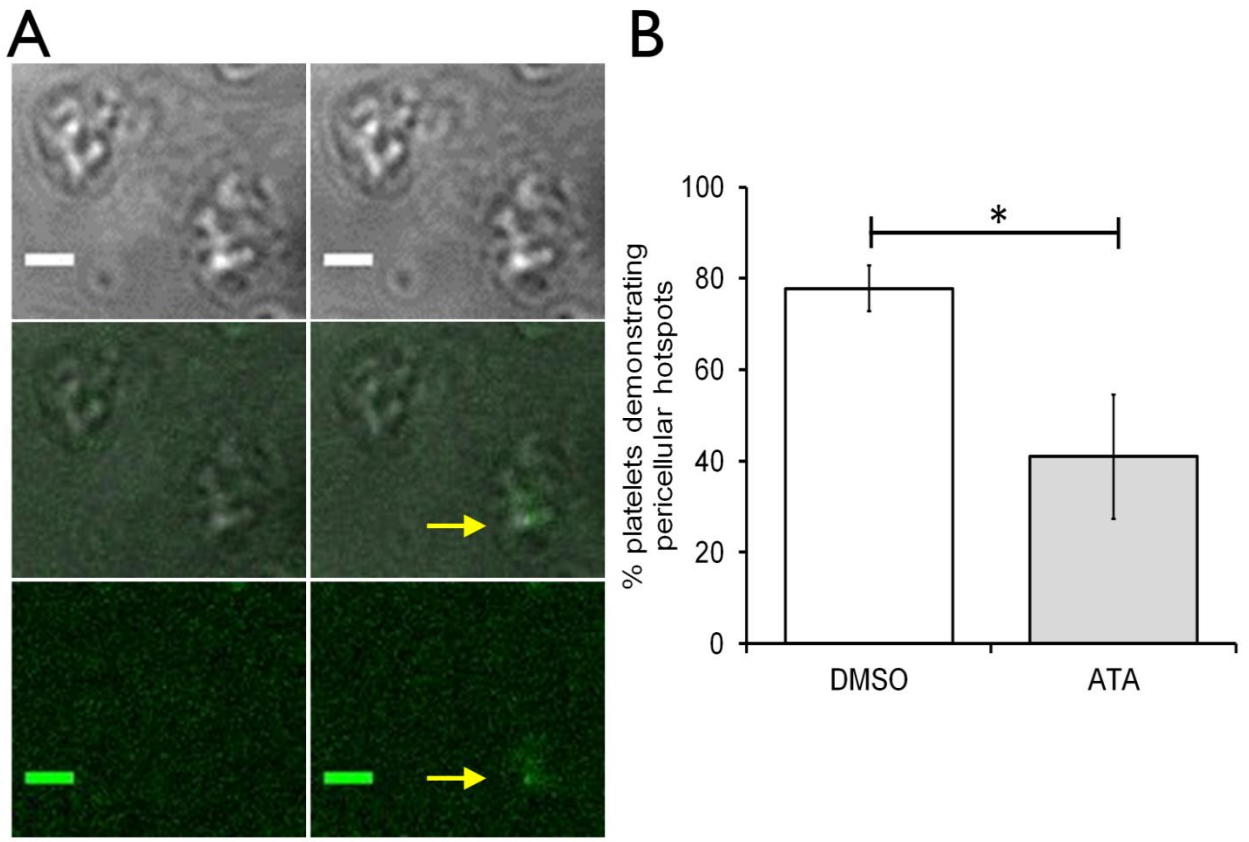

Fig. 3.22: ATA significantly inhibited the generation of the pericellular Ca^{2+} hotspots in thrombin activated human platelets.. Washed platelets were resuspended in supplemented HBS. Samples of platelet suspension were then preincubated with either 30 µM ATA or an equivalent volume of DMSO for 10 minutes at 37°C. Samples were then treated with 1 mM EGTA before they were loaded onto poly-L-lysine coated chambered coverslides and left to settle for 5 minutes prior to imaging. Fluo-4 salt was then added and mixed gently immediately prior to imaging. Cells were imaged before and 5 minutes after the addition of 0.5 U/mL thrombin by confocal microscopy.

4. Assessment of CD34$^+$-cultured human megakaryocytes as a model system in which to study the effect of nicergoline on human platelets

4.1 Characterization of human CD34$^+$ cell culture undergoing megakaryocytic differentiation.

Initial experiments were performed to establish whether it was possible to successfully elicit megakaryocytic differentiation of CD34$^+$ cells in culture using a previously published methodology (Pinault *et al*., 2013). To do this CD34$^+$ cells were plated into 24-well plates and cultured in SFEM-II^{TM} culture media with a cytokine cocktail containing Interleukin-6 (IL-6), Interleukin-9 (IL-9), Thrombopoietin (TPO) and Stem Cell Factor (SCF). Cells were examined for up to 14 days by light and fluorescence microscopy. Initial results found that the largest cells were observable from days 7-9, and that cells often disappeared after this time point often with the appearance of cell fragments observable in the culture. These may have represented the production of proplatelets, but further examination will be required to assess this.

Initial light microscopy experiments were performed to examine changes in cell morphology and colony formation on days 2 and 7 of the culture. As shown in **Fig. 4.1A**, by day 2 cells could be seen to clump into colonies within the liquid cultures. Closer examination showed the cells on day 2 to have a uniform circular shape, with only one nucleus, visible as a central dark area surrounded by a narrow, very light and transparent rim of cytoplasm indicative of an undifferentiated CD34$^+$ cell (**Fig. 4.1B**). At day 7, cells started to appear to have signs of megakaryocytic development recognizable by their irregular, larger size (**Fig 4.1C**, blue arrow).

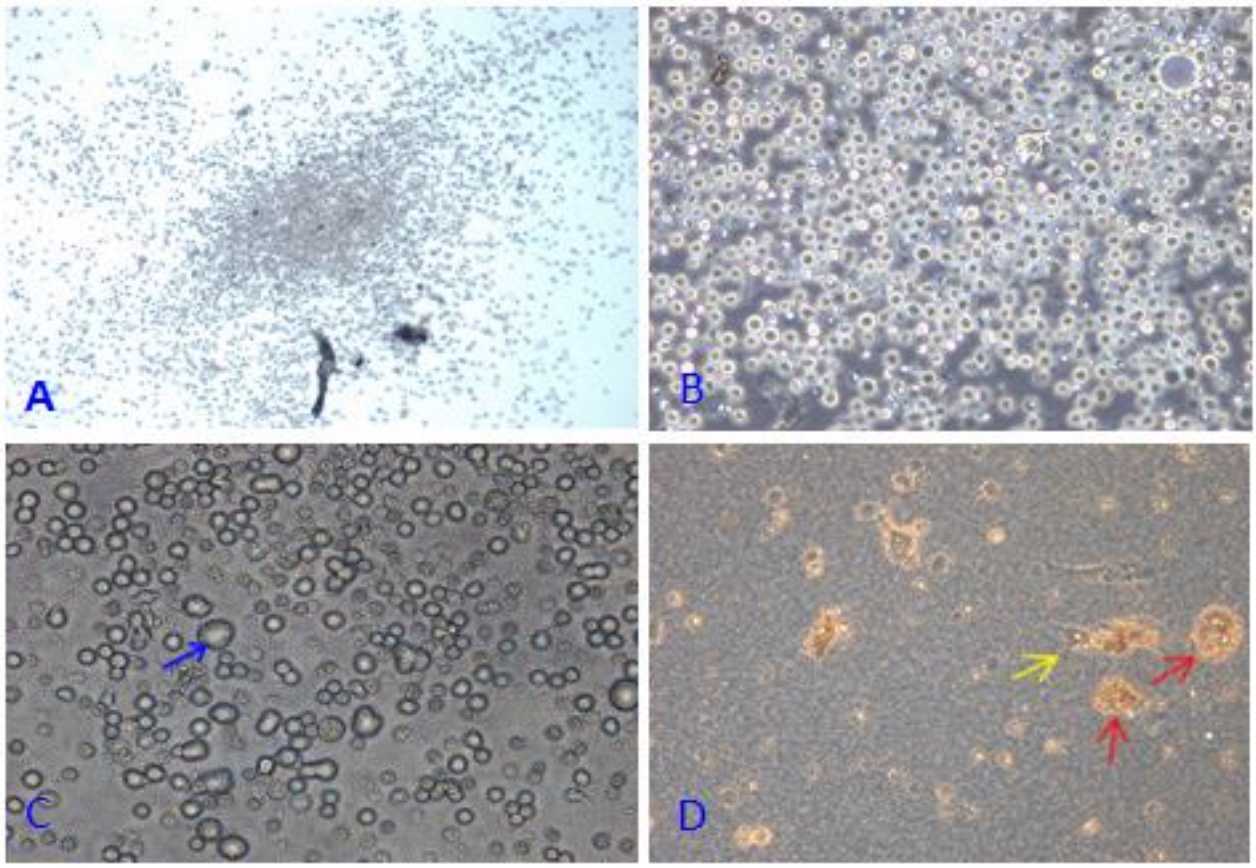

Fig. 4.1: Light microscopy showing different stages of CD34$^+$ cell growth and differentiation during the 14 day tissue culture. (A) Colony of CD34$^+$ cells at an early stage of growth (Day 2, X4 magnification). (B) Cells are starting a megakaryocytic differentiation (Day 2, X 20). (C) Cells are in an advanced stage of megakaryocytic maturation recognizable by their irregular larger size (blue arrow; day 7, X 20). (D) Cells at their late stages of megakaryocytic maturation showing cells with distorted large size and markedly indented and lobed nucleus (red arrows) with cytoplasmic protrusions which might possibly be pro-platelets (yellow arrow; day 11, X 20).

At day 11 (**Fig. 4.1D**) cells at the end stage of maturation showing the distorted large size of mature megakaryocyte with a markedly indented and lobed nucleus (red arrows), as well as cytoplasmic protrusions which might possibly be pro-platelets were present (yellow arrow). There were also less overall cells and a number of cellular fragments suggesting that megakaryocyte differentiation towards a platelet-shedding phenotype was occurring.

Cultured $CD34^+$ cells were also examined fluorescently for megakaryocytic differentiation on the same days. Cells were loaded with Hoechst 33342 to allow us to observe the nucleus and Fluo-5N to allow us to identify intracellular Ca^{2+} stores. The loaded cell suspension was then placed in a Poly-L-lysine-coated chambered coverslide and suspended in a supplemented HBS in which Rhod-5N tripotassium salt was added just before the start of imaging. The high Ca^{2+} present in the supplemented HBS allowed the Rhod-5N low-affinity fluorescent Ca^{2+} indicator to be used to indicate the presence of the extracellular fluid within the lumen of the demarcation membrane system (DMS; an invagination of the megakaryocyte plasma membrane) as has been previously shown by other groups (Mahaut-Smith *et al*., 2003).

On day 2 of culture, cells had a uniform circular shape with single nucleus (blue) suggesting these cells had yet to undergo significant megakaryocytic maturation (**Fig. 4.2A**). The nucleus was surrounded by cytosol in which there was a fine structure of intracellular Ca^{2+} stores (green), suggesting no specific polarization of the stores in these cells . There was no red Rhod-5N fluorescence observed inside of the surface membrane indicating that the DMS had yet to develop in these cells.

On day 7 of culture, cells had a larger and completely irregular shape. In addition, fluorescent staining indicated that the cell nucleus could be seen to be multi-lobular indicative of endomitosis found during megakaryocytic differentiation of the cells (Blue; Kaushansky *et al.,* 2010). In addition, the Rhod-5N fluorescence demonstrates the presence of a DMS, therefore further supporting the megakaryocytic differentiation of the cells (**Fig. 4.2B**). Intracellular Ca^{2+} stores could still be seen over most of the cell, however there were puncta of bright spots observed suggesting that these are more localized in these cells.

4.2 Quantitative assessment of the megakaryocytic maturation of $CD34^{+}$ cells in the *in vitro* liquid culture system.

In order to assess the extent of megakaryocyte differentiation we scored all imaged cells from day 2 and day 7 for presence of known markers of platelet maturation (Kaushansky *et al.,* 2010). The cells were assessed for cell diameter, nuclear lobulation and presence of DMS (**Fig. 4.3**). Mature megakaryocytes show diameters of between 20-40 μm in diameter, presence of an extensive DMS and multi-lobular nuclei in-line with the presence of endomitosis (Kaushansky *et al.,* 2010). Therefore these parameters were measured in each of the day 2 and day 7 cultures and compared. Cells showing no megakaryocytic marker were classified as megakaryocyte lineage cells, whereas those showing 1 or more megakaryocytic markers were classified as developing cells. The data therefore showed that day 2 and day 7 cultured cells showed no significant difference in any of these markers. All of these factors were significantly improved in the developing cells compared to the megakaryocyte lineage cells on day 2

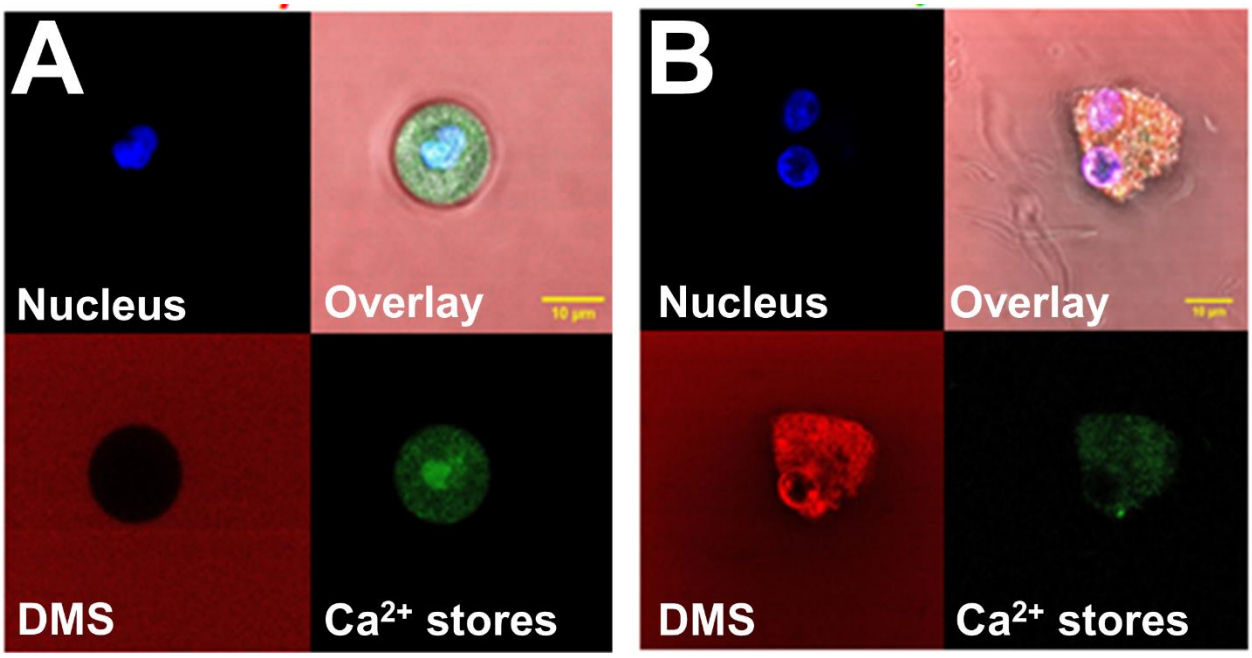

Fig. 4.2: Confocal microscopy of CD34$^+$ cells showing the differences between day 2 and day 7 megakaryocytic cell differentiation. CD34$^+$ cells collected on day 2 (A) and day 7 (B) of megakaryocyte culture were incubated with Hoechst 33342 and Fluo-5N dye for 2 hours at 37°C. Cells were then resuspended in supplemented HBS and loaded onto chambered coverglass and left for 30 minutes to settle. Rhod-5N dye was added just before the start of imaging the cells using laser-scanning confocal microscopy.

and day 7 indicating that a small subpopulation of day 7 cells had not responded to the culture conditions at all (around 15%). Interestingly there was no significant difference in nuclear lobulation or DMS presence in day 2 and day 7 developing cells, but there was a difference in cellular size. These data therefore indicate that prolonged culture is required to allow $CD34^+$ to expand to the same size as the mature megakaryocytes. Despite this our cultures did not show a large proportion of large diameter megakaryocytes, indicating that further refinement of our cultures may be required in the future. Overall these data indicated that in our hands it is possible to develop megakaryocytic lineage cells from $CD34^+$ cells, but that the final stages of maturation either do not occur or are transient and so are not observed here.

Lastly we examined the images for possible presence of the MC. By overlaying the Fluo-5N and Rhod-5N data (after filtration of background fluorescence) it was possible to observe areas in which the two membrane systems coalesced suggesting the possible presence of a MC-like structure in these cells. These results therefore suggest the possibility that these cells may provide a potential model in which to study the platelet MC.

4.3 Quantitative measurement of megakaryocyte maturation by the assessment of expression of cell surface markers of this lineage

To further analysis the maturity of our megakaryocytes we performed single cell analysis of the expression of known cell-surface markers of mature megakaryocytes – CD42b (part of the integrin αIIbβ3 complex, a platelet receptor for fibrinogen) and CD41a (the GPIb antigen for binding vWF; Pineault *et al*., 2013). Cells were fixed on day 2 and day

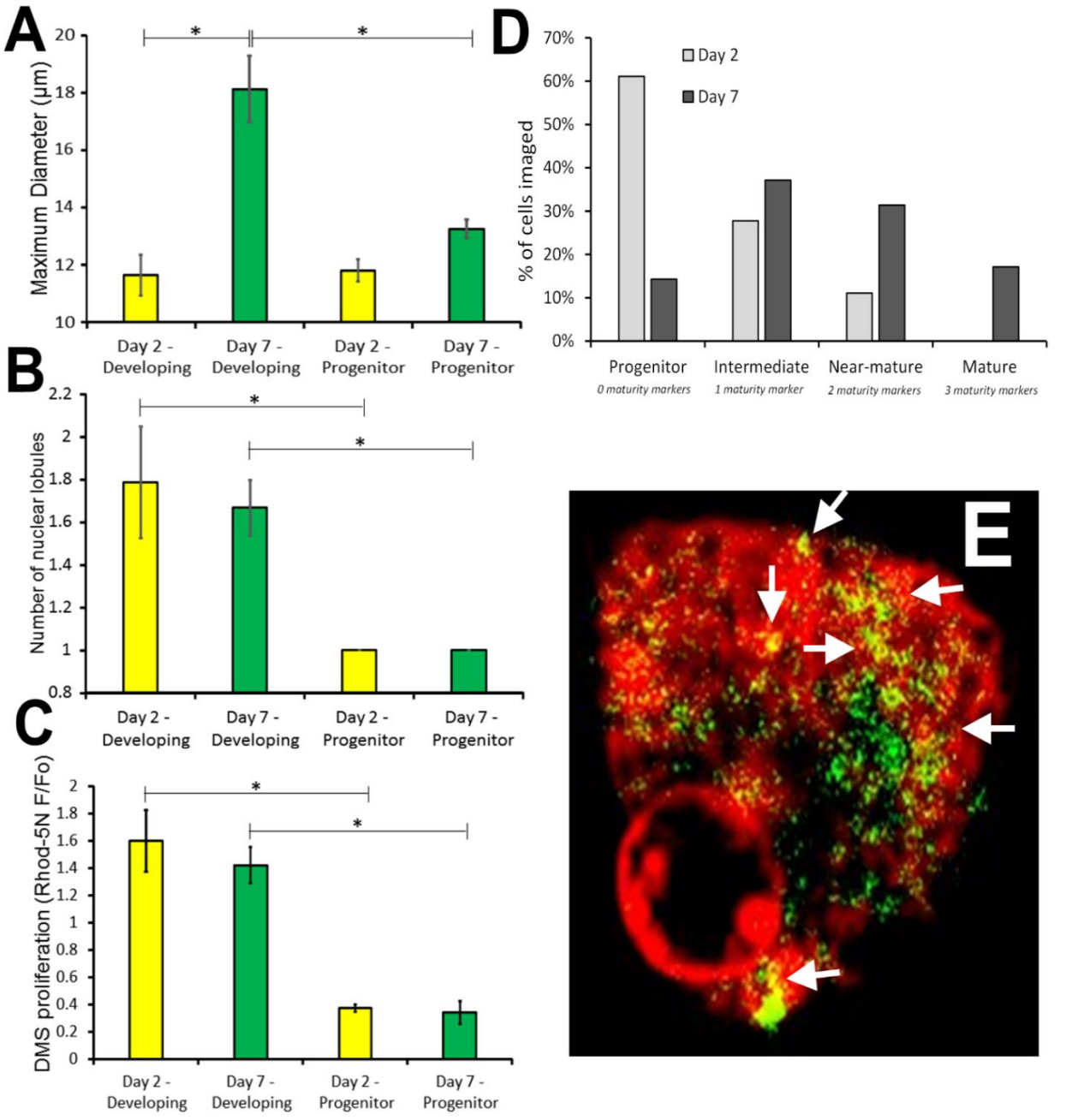

Fig. 4.3: Day 7 cells show an increase in megakaryocytic markers, and formation of a membrane complex-like structure. (A-D) The progress of maturation was judged by a special scale of parameters including cell diameter (A), nuclear lobulation (B) and DMS development (C). Cells are representative of cells taken from 4 different cultures covering 35 and 36 cells for day 2 and 7 respectively. (D) Each cell in the culture observed was scored for each of the 3 maturation markers identified in A-C, the proportion of cells showing 0, 1, 2 or 3 of these indices is shown. Overlaid fluorescence shows the presence of foci of co-localisation of DMS and intracellular Ca^{2+} stores (white arrows) which are indicative of structures potentially analogous to the MC (E).

7 of the culture and incubated with APC-labelled CD41a and FITC-labelled CD42b antibodies. Initial attempts were made to use flow cytometry to assess the maturation status of the culture, but due to the financial requirement to keep cell numbers low in each experiment, this was found to not be feasible. Therefore we examined the expression by fluorescent microscopy (**Fig. 4.4**). Only 23.4% of cells were found to stain positive for both markers on day 2 of the culture, whilst 83.8% of the cells were found to stain on day 7. Mean fluorescence for CD41a was found to be 1261 ± 180 arbitrary units for day 7 cells (n = 38) and 31 ± 21 for day 2 cells (n = 14; $P < 0.05$). Similar results were found for CD42b-labelling with mean fluorescence of 1221 ± 177 for day 7 cells and 41 ± 28 for day 2 cells ($P < 0.05$). These data therefore confirmed that day 7 cells are megakaryocytic in lineage.

4.4 Nicergoline does not elicit a reorganisation of intracellular Ca^{2+} stores in $CD34^{+}$-derived cultured human megakaryocytes

Our previous work has indicated that nicergoline induces a microtubule-dependent redistribution of intracellular Ca^{2+} stores in human platelets (Walford *et al*., 2016). To examine whether similar structural effects are observed in human megakaryocytes, we examined whether treatment of day 7 $CD34^{+}$-derived human megakaryocytes with 100 μM nicergoline altered the distribution of the intracellular Ca^{2+} stores. As can be seen in **Fig. 4.5**, treatment of cells with nicergoline elicited a loss of the bright puncta of

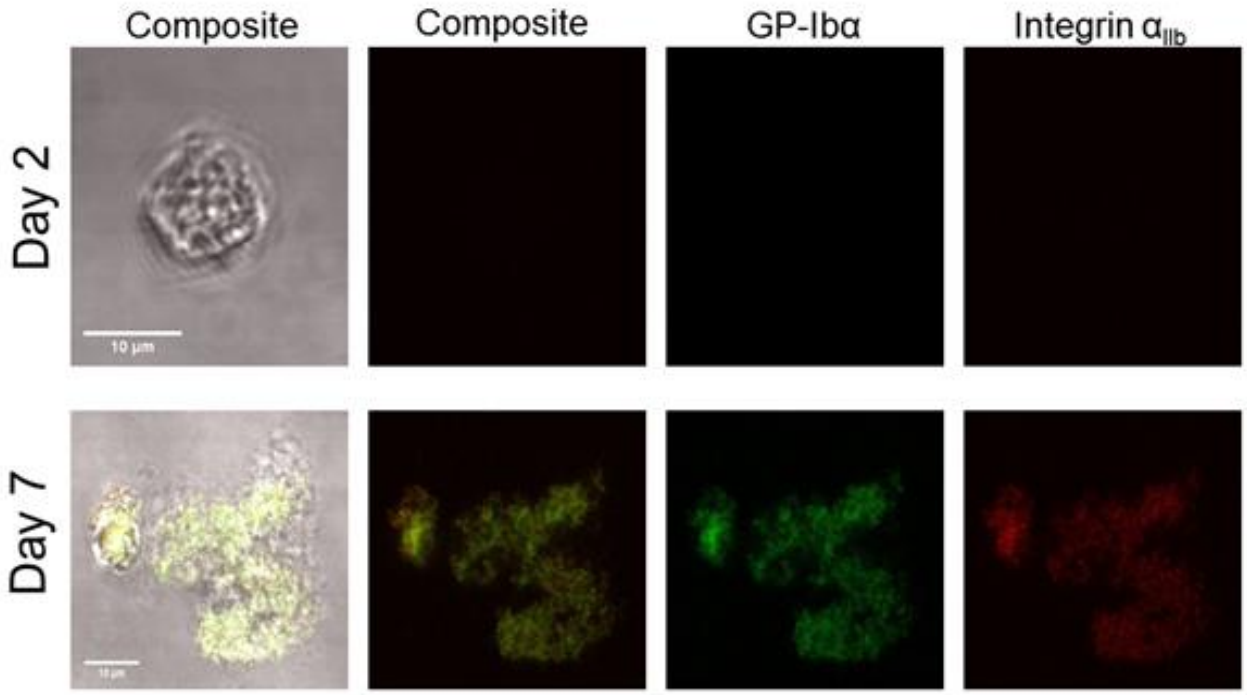

Fig. 4.4 Expression of cell surface markers of megakaryocyte lineage is greater on day 7 cells. $CD34^+$ cells were harvested on day 2 (upper panels) and 7 (lower panels) of megakaryocyte culture and fixed in formaldehyde solution. Fixed cells were then labelled with fluorescently-labelled antibodies to the megakaryocyte cell surface markers, CD41a and CD42b. The labelled cells were then analyzed by confocal microscopy. *P < 0.05, n = 14 and 38 cells for day 2 and day 7, respectively. Cells are representative of 3 different $CD34^+$ cultures.

intracellular Ca^{2+} stores observed in the cell prior to treatment, with the store distribution appearing more homogenous. Numerical analysis of the distribution of Fluo-5N fluorescence across the cell indicated no significant difference in the mean fluorescence across the cells (598 ± 88 arbitrary units and 580 ± 82 before and after nicergoline treatment respectively; n = 11; P > 0.05). Analysis of the variance of pixel fluorescence also indicated no significant difference before and after nicergoline treatment (standard deviation of pixel fluorescence was 525 ± 31 arbitrary units and 474 ± 38 before and after nicergoline treatment respectively; n = 11; P = 0.24). These results therefore indicate that nicergoline does not significantly alter the distribution of the intracellular Ca^{2+} stores across the megakaryocyte. This may be due to the endoplasmic reticulum and other Ca^{2+} stores behaving differentially to nicergoline treatment. Further experiments using a more specific endoplasmic reticulum marker, the fluorescently-labelled anti-KDEL antibody used during our previous study may help address this more effectively (Walford *et al*., 2016).

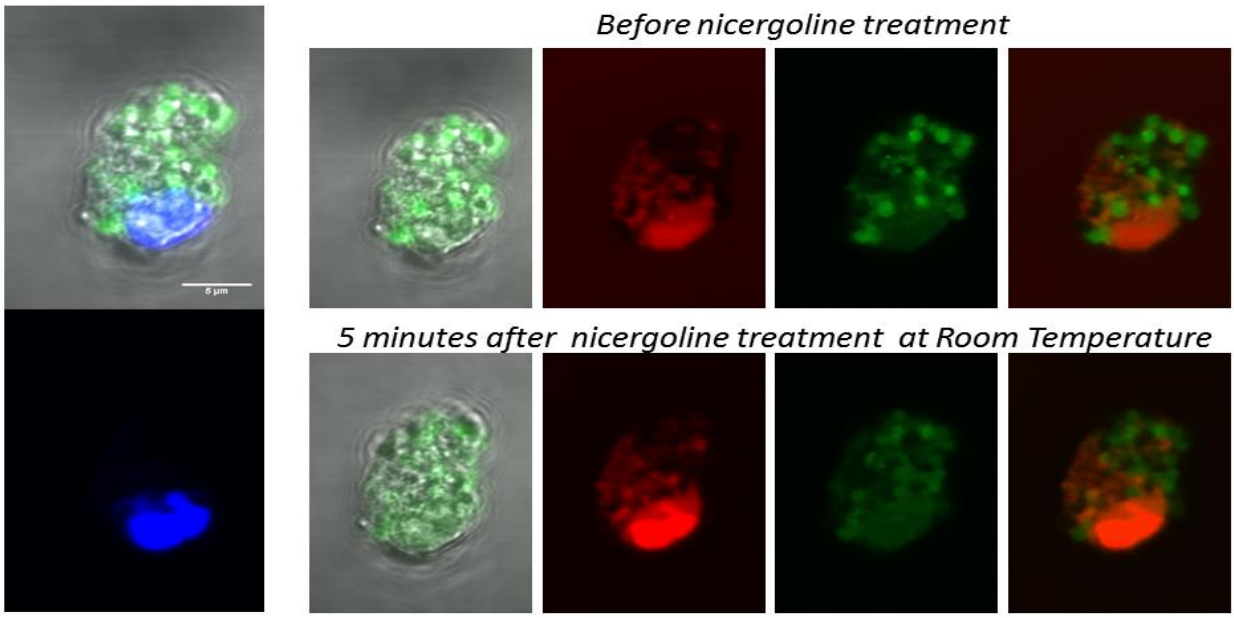

Fig. 4.5: Nicergoline does not induce a reorganisation of Fluo-5N-labelled intracellular Ca^{2+} stores. Day 7 cultured $CD34^{+}$ cells were stained with Hoechst 33342 (nucleus; blue) and Fluo-5N (intracellular Ca^{2+} stores; green). Cells were the resuspended into a supplemented HBS containing Rhod-5N salts to label the demarcation membrane system (red). Cells were then loaded onto a poly-L-lysine-coated chambered cover slide and examined under the Olympus Fluoview confocal microscope (upper panel). Cells were reexamined 5 minutes later after the addition of 100 µM nicergoline (lower panel).

4.5 Nicergoline appears to inhibit thrombin-evoked pericellular Ca^{2+} accumulation in thrombin-stimulated $CD34^{+}$-derived human megakaryocytes.

Previous experiments on human platelets showed that nicergoline disrupts thrombin-evoked Ca^{2+} signalling by inhibiting pericellular Ca^{2+} recycling (Le Menn *et al*., 1979; Parker *et al*., 1993; Sage *et al*., 2013). Experiments were therefore performed to examine if nicergoline pre-treatment could inhibit thrombin-evoked rises in cytosolic and pericellular Ca^{2+} concentration in the $CD34^{+}$-derived human megakaryocytes. Day 9 cultured megakaryocyte cells were co-loaded with Hoechst and Fluo-2 dyes, washed and preincubated with either 100 µM nicergoline or an equivalent volume of DMSO.

The cells were then allowed to adhere to a poly-L-lysine-coated chambered coverslide in supplemented HBS containing 5 µM Rhod-5N salt. Fluorescence readings for Fluo-2 were taken continuously before and after stimulation with 0.5 U/mL thrombin to assess changes in cytosolic Ca^{2+} concentration, whereas images of Rhod-5N were taken before thrombin stimulation and at the end of the 5 minute recording period to assess changes in the pericellular Ca^{2+} concentration. Unfortunately it was not possible to measure changes in cytosolic Ca^{2+} concentration as Fluo-2 fluorescence was found to photobleach rapidly through the recording period, making interpretation of the data difficult. The Rhod-5N fluorescence measurements showed that control cells demonstrated an increase in the pericellular Ca^{2+} concentration after thrombin stimulation (120.7 ± 6.1% of pre-stimulation fluorescence; n = 16), which was decreased by pretreatement with nicergoline (103.4 ± 5.9% of pre-stimulation fluorescence; n = 11). However this effect was not statistically significant (P = 0.058). Further experiments will be required to confirm this preliminary finding. If confirmed, this effect is consistent

with the possibility of megakaryocytes utilizing a pericellular Ca^{2+} recycling system in a similar manner to human platelets (Sage *et al*., 2013; Walford *et al*., 2015).

4.6 Nicergoline may inhibit thrombin-evoked rises in $[Ca^{2+}]_{cyt}$ in $CD34^{+}$-derived human megakaryocytes

Our previous studies have shown that nicergoline is able to inhibit thrombin-evoked rises in $[Ca^{2+}]_{cyt}$ (Walford *et al*., 2016). Experiments were therefore performed to find out whether nicergoline can exhibit a similar inhibitory action on the Ca^{2+} signals in cultured megakaryocytes upon stimulation with thrombin. Therefore, cultured human megakaryocyte cell samples were harvested on day 7-9 of the culture and loaded with Fura-2, and thrombin-evoked changes in $[Ca^{2+}]_{cyt}$ were then assessed using a fluorescence microplate reader. Preliminary findings indicated that pretreatment with nicergoline elicited a consistent reduction in cytosolic Ca^{2+} signalling in cells stimulated in the presence of extracellular Ca^{2+}. However these effects are not significant at this time (25.3 ± 13.1% of control; n = 5; P = 0.25; **Fig 4.6**). These results suggesting that the inhibitory effect of nicergoline on Ca^{2+} signalling in human platelets is also seen in human $CD34^{+}$-derived human megakaryocytes, although further experiments will be required to complete these preliminary findings.

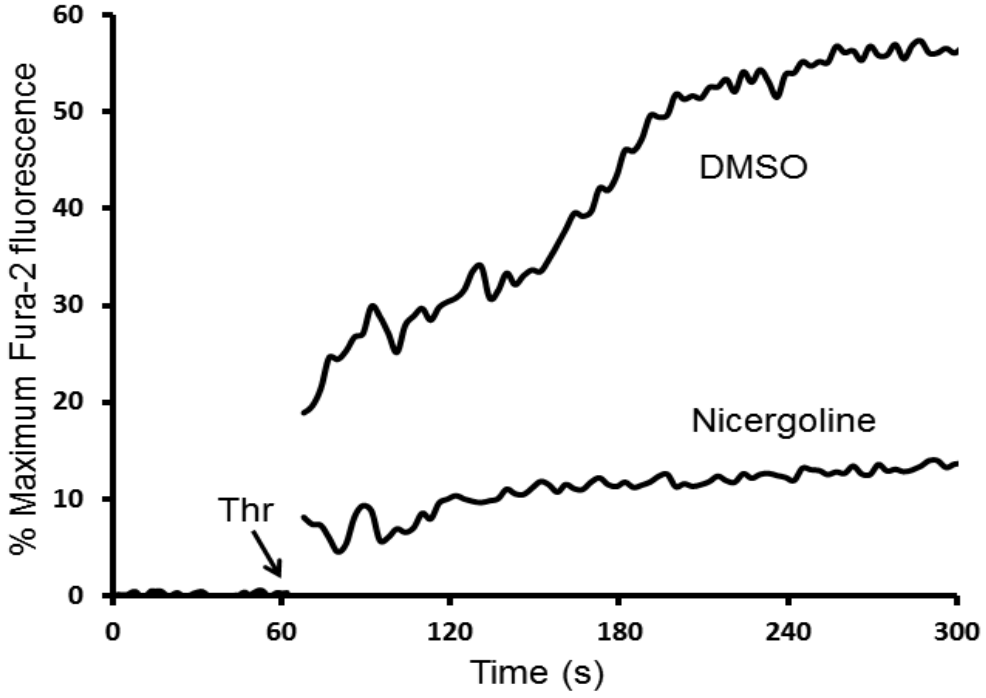

Fig 4.6: Nicergoline may inhibit thrombin-evoked rises in $[Ca^{2+}]_{cyt}$ in $CD34^{+}$-derived human megakaryocytes. Fura-2-loaded cultured human megakaryocyte cells were resuspended in supplemented HBS, and treated with either 100 µM nicergoline or an equal volume of its vehicle, DMSO. Extracellular Ca^{2+} was then raised to 1 mM immediately prior to the start of the experiments. Fura-2 fluorescence was then monitored using a microplate reader before and after stimulation with 0.5 U/mL thrombin.

5. Discussion

Previous work in our lab has demonstrated that nicergoline exerts its inhibitory effect on Ca^{2+} signalling in human platelets through triggering reorganisation of the cortical microtubule bundle (Walford *et al*., 2016). Based on the structural observations previously observed by Walford *et al*. (2016), the study authors suggested the possibility of an effect of this drug on either a change in the post-translational modifications of the cortical microtubule bundle or an alteration in the activity of microtubule-dependent motor proteins. In this project, experiments have been performed to attempt to examine each of these hypothesised mechanisms, with the aim of identifying the molecular mechanisms by which nicergoline exerts its inhibitory effect on human platelets.

5.1 Does nicergoline inhibit platelet Ca^{2+} signalling through an effect on the acetylation status of platelet microtubules?

Our studies of the effect of inhibiting microtubule deacetylation with the deacetylase inhibitor, trichostatin A, have demonstrated that this compound has minimal effect on both platelet Ca^{2+} signalling and platelet function. In addition, this drug has no direct effect on mitigating the effect of nicergoline when platelets are incubated with both drugs. These findings therefore suggest that microtubule acetylation is unlikely to be the target of nicergoline.

These findings are interesting as previous studies in human platelets have demonstrated that inhibition of the main microtubule deacetylase, HDAC6, is able to inhibit collagen-evoked aggregation (Aslan *et al*., 2013). This is distinct from our findings

here with thrombin where we find that inhibitors of this enzyme have no significant effect on platelet Ca^{2+} signalling or aggregation. These results therefore suggest that thrombin- and collagen-evoked signalling pathways are differentially affected by this inhibitor. Further studies should investigate whether microtubule acetylation affects collagen-evoked Ca^{2+} signalling through the PLCγ pathway in a distinct manner from the PLCβ-mediated thrombin-evoked signalling.

Whilst our findings rule out microtubule acetylation as a potential target of nicergoline, it is worth noting that there are many other post-translational modifications of tubulin that have not been explored in this study. Currently acetylation is the best studied, with minimal study of other post-translational modifications such as detyrosination, (poly)glutamylation and (poly)glycylation. Therefore additional studies of the existence and functional significance of these pathways may provide future areas of study.

5.2 Does nicergoline inhibit platelet Ca^{2+} signalling through an effect on platelet myosin?

Our attempts to assess the potential role of myosin as the target of nicergoline have been hampered by the autofluorescent properties of its specific inhibitor, blebbistatin. Due to interference with the readings obtained from all of the major fluorescent Ca^{2+} indicators we could use, this has prevented us from assessing the effect of blebbistatin and nicergoline in combination. However we have been able to assess the effect of blebbistatin alone on platelets. Previous studies showed that blebbistatin was able to abolish internal contraction at doses between 10-25 μM after 30 seconds of exposure to

this drug (Johnson *et al*., 2007). Therefore after 10 minutes of preincubation, the 10 and 30 µM doses should provide significant inhibition of myosin activity in these cells. This is consistent with our shape change data in which 30 µM blebbistatin abolished thrombin-evoked shape change (**Fig. 3.5**), consistent with the known role of myosin in this platelet response (Paul *et al*., 1999). However whilst shape change was inhibited there was no effect of this treatment on thrombin-evoked aggregation or Ca^{2+} signalling elicited in the presence of extracellular Ca^{2+}. This is a distinct pharmacological profile from the effect of nicergoline, and therefore provides strong evidence that nicergoline isn't working through inhibition of myosin in human platelets.

The inhibitory effect of blebbistatin on thrombin-evoked Ca^{2+} signalling in the absence of extracellular Ca^{2+} is similar to that seen with nicergoline (Walford *et al*., 2016). These results could indicate an effect on Ca^{2+} release, possibly by inhibiting pericellular Ca^{2+} recycling (Sage *et al*., 2013). However this result appear inconsistent with those on Ca^{2+} entry as impaired Ca^{2+} release should also block Ca^{2+} entry, via inhibition of store-operated Ca^{2+} entry (Berna-Erro *et al*., 2016). Therefore this indicates the possibility that these results may be the result of the effect of the blebbistatin quenching the Fura-2 fluorescence in an inconsistent manner, such that calibrating in the presence of the drug is not able to compensate for this. Further studies will be needed to examine if this is a *bone fide* effect of the drug or an artefactual effect of the autofluorescent properties of the drug. Future work should be able to assess this using a highly soluble, non-fluorescent blebbistatin derivative which has recently been reported (Várkuti et al., 2016). These should provide us with a definitive conclusion regarding the role myosin plays in controlling platelet Ca^{2+} signalling. However the lack of effect of blebbistatin on

platelet aggregation indicates that nicergoline is unlikely to be working via an effect on myosin.

5.3 Does nicergoline inhibit platelet Ca^{2+} signalling through an effect on platelet dyneins?

Our initial findings demonstrated that dyneins appear to play a role in negatively regulating Ca^{2+} release from intracellular stores as thrombin-evoked rises in $[Ca^{2+}]_{cyt}$ elicited in the absence of extracellular Ca^{2+} are enhanced when dyneins are inhibited. This was consistent with the effect of this drug in potentiating thrombin-evoked depletion of intracellular stores as well as rises in extracellular Ca^{2+} concentration under similar conditions. These results therefore suggested the possibility that nicergoline could work by acting as an activator of dyneins. However further studies examining the effect of co-incubation of ciliobrevin A with nicergoline suggested that this wasn't the case, as this treatment lead to no reversal of the inhibitory effect of nicergoline. Thus these results suggest that whilst dyneins may have an inhibitory effect on Ca^{2+} signalling these are not the molecular targets of nicergoline in human platelets.

Previous studies in primate cells has demonstrated that dyneins can play a key role in positioning of the endoplasmic reticulum through triggering rapid movement towards the centre of the cell (Wozniak *et al*., 2009). Given that platelet activation has been shown to trigger increased dynein activity, leading to the coiling of the platelet microtubule bands (Diagouraga *et al*., 2014), there is a possibility that dyneins have an inhibitory effect by rapid reorganization of the DTS which reduces its sensitivity to IP_3 signals.

Indeed previous studies have described rapid, Ca^{2+}-dependent change in the DTS ultrastructure, which would be consistent with a role for dyneins (Ebbeling *et al*., 1992). Future studies assessing this effect may therefore provide novel findings on how Ca^{2+} signalling is controlled in human platelets.

The tendency towards an inhibitory effect of ciliobrevin A on thrombin-evoked Ca^{2+} signals when platelets were stimulated in the presence of extracellular Ca^{2+} suggests that Ca^{2+} entry pathways must be partially inhibited by this treatment to counter the effect of the increased Ca^{2+} release from intracellular Ca^{2+} stores. However this effect must be a mild one as no effect of this drug is observed on platelet aggregation in the same conditions. Further studies will need to more fully characterise the effect of ciliobrevin A on Ca^{2+} signalling in the platelet to understand this effect further.

5.4 Does nicergoline inhibit platelet Ca^{2+} signalling through an effect on platelet kinesins?

The data presented here examining the effect of the kinesin inhibitor, aurin tricarboxylic acid, showed a pharmacological profile consistent with the effects of nicergoline on platelet Ca^{2+} signalling – with a similar inhibition of thrombin-evoked rise in $[Ca^{2+}]_{cyt}$, depletion of intracellular Ca^{2+} stores, inhibition of pericellular Ca^{2+} rises, platelet aggregation and dense granule secretion (Lanza *et* al., 1986; Walford *et al*., 2016). Furthermore the effect of ATA and nicergoline was not cumulative suggesting that they may be working through a related signalling pathway. Interestingly ATA was a more potent inhibitor of Ca^{2+} signalling in human platelets than nicergoline - therefore

suggestive that if nicergoline does work via this mechanism, it may only work through partially inhibiting kinesins in platelets. However further experiments will need to directly assess the impact of nicergoline on platelet kinesin activity before we can definitively conclude this. Previous studies by Diagouraga *et al*., (2013) have demonstrated the impact of ATA on microtubule structure. They demonstrated that this drug induces activation-independent coiling of the platelet microtubules, which appears to produce a similar partial disruption of the cortical bundle seen in a large proportion of the nicergoline-treated cells (Walford *et al*., 2016). These data therefore suggest that nicergoline may disrupt the normal structure of the microtubule bundle not through dismantling it, but through its ability to induce microtubule folding by a dynein-dependent mechanism (Diagouraga *et al*., 2013). As the DTS is attached to these microtubules (Behnke, 1965) this will likely induce its redistribution across the cell through an indirect effect on the microtubules. The previous demonstration that nicergoline's effect could be prevented by pre-treating with taxol to stabilise the cortical microtubules, would be consistent with this being the method by which nicergoline induces the reorganisation of the intracellular stores. Further experiments will be required to examine if ATA's effect on Ca^{2+} signalling can also be prevented by prior treatment with taxol.

Kinesins also play a role in directly moving intracellular organelles around the cell through their motor activity directed towards the plus end of microtubules (Wells *et al*., 1999; Marx *et al*., 2009). Interestingly, kinesins have previously been shown to play a significant role in regulating the granule motility in platelets (Cerecedo *et al*., 2010). Given that our previous study demonstrated a secondary microtubule-independent

effect of nicergoline on dense granule secretion (Walford *et al*., 2016) which was not related to the dismantling the membrane complex, it is possible that both the microtubule-dependent and -independent effects could both be mediated via inhibition of kinesins – with kinesin inhibition triggering coiling of the microtubule bundle to disrupt the membrane complex (Diagouraga *et al*., 2013; Walford *et al*., 2016), as well as separately interfering with the normal kinesin-mediated distribution of dense granules in the cell, such that dense granule secretion is inhibited. Consistent with this possibility we find that dense granule secretion is inhibited by ATA pretreatment. This possibility is an interesting one and therefore provides us with further circumstantial evidence that suggests that kinesin inhibition may be the target of nicergoline.

Whilst our results suggest that nicergoline may partially inhibit kinesin activity, future work will also need to examine whether this is a direct effect of this drug on kinesin activity, or whether it is an indirect interaction with the systems that regulate kinesin activity (Gibbs *et al*., 2015). For instance, nicergoline has previously been shown to stimulate PKC activity, which could directly regulate kinesin activity (Gibbs *et al*., 2015) as well as trigger cleavage of the amyloid precursor protein, which acts as an adaptor protein to assist kinesin interaction with the organelles (Cedazo-Minguez *et al*., 1999; Gibbs *et al*., 2015). Understanding this mechanism of action of nicergoline better will help guide future drug development of anti-platelet agents to mimic the effect of nicergoline, by identifying the precise effect of this drug on platelets.

5.5 Are $CD34^+$-derived megakaryocytes a model system in which we can study the mechanism of action of nicergoline in human platelets?

One of the major limitations of our current studies into how nicergoline may work is the difficulty of working with human platelets. Due to our inability to genetically modify these cells we are reliant on the presence of accessible pharmacological agents to target our pathways of interest – however as can be seen in this report, many drugs have issues surrounding solubility or autofluorescence which make them problematic to work with. The ability to genetically knockdown particular proteins in the nucleate megakaryocytic cell would provide us with another method in which to confirm our findings. In this project, attempts were made to establish a $CD34^+$-derived cell culture system in which to generate human megakaryocytic cells in which we could investigate the effect of nicergoline.

These pilot studies using previously published methodology (Pineault *et al*., 2013), demonstrated that it was possible to create human megakaryocytes, although it was difficult to capture a significant proportion of them at the sizes expected of a fully-matured cells. Further work optimising the culturing conditions may facilitate this better. However cells could still be observed to possess membrane complex-like structures made up of the apposition of the demarcation membrane system and intracellular Ca^{2+} store (**Fig 4.3**). Recent work has also identified the close apposition between the DMS and the DTS-like, smooth endoplasmic reticulum (Eckly *et al*., 2014) – thus suggesting that we might be observing these structures in our cells. These initial results therefore

suggested that these cells could be useful for modelling nicergoline-induced changes in the platelet ultrastructure. However our initial studies to assess this further demonstrated that nicergoline did not significant delocalise the intracellular Ca^{2+} stores in human platelets, with similar distributions of Fluo-5N fluorescence observed in cells before and after nicergoline treatment. This is different from our findings in human platelets in which the Fluo-5N could be found to be significantly more homogenously distributed across the cell after nicergoline treatment (Walford *et al*., 2016). One possibility is that the Fluo-5N is not selective solely for the smooth endoplasmic reticulum and so disruption of the membrane complex structure may still occur in these cells, but is not observed due to the positioning of other Ca^{2+}-storing organelles not being disrupted by this treatment. Further studies utilising more specific probes for the endoplasmic reticulum may clarify this possibility.

Initial studies examining the effect of nicergoline on the thrombin-evoked Ca^{2+} signals in these cells indicated the possibility that this drug also inhibited rises in cytosolic and extracellular Ca^{2+} concentration, although these results had not quite reached statistical significance. Further work will be required to complete these pilot studies and investigate if they are responsive to reversal by taxol pre-treatment to prevent microtubule remodelling as we saw in the original paper (Walford *et al*., 2016).

At this time it is not possible to conclude on whether $CD34^{+}$-derived megakaryocytes are a good model for studying the effect of nicergoline in human platelets, however our initial data suggest that they may at least provide a system in which we could study the formation of the membrane complex.

5.6 Conclusion

In this study we have demonstrated a key role for motor proteins in controlling thrombin-evoked Ca^{2+} signalling and changes in human platelet function. These data have indicated that the most likely target for nicergoline's ability to block platelet Ca^{2+} signalling is the ability to interfere with kinesin activity in the resting platelet. This effect could explain the microtubule-dependent reorganization of the dense tubular system's distribution in the platelets, as well as the potential for interfering with granule secretion in platelets. Interestingly the effect of ciliobrevin A in potentiating Ca^{2+} signalling in human platelets, suggests the possibility that Ca^{2+} release may be differentially controlled by the antagonistic action of these two molecular motors. Future work will be required to assess whether nicergoline can directly affect kinesin activity, or works via an indirect effect on a regulatory signalling pathway or an adaptor for kinesin transport. This study has expanded our understanding of the known anti-platelet effect of nicergoline. By further refining our understanding of the direct molecular target of nicergoline we may be able to design novel anti-platelet agents which can specifically target the mechanisms controlling the normal positioning of the dense tubular system within the platelet, and as such downregulate agonist-evoked Ca^{2+} signalling.

6. References

Akhmanova A & Hammer JA (2010). Linking molecular motors to membrane cargo. *Curr Opin Cell Biol* ***22***: 479-487.

Alexander WS, Roberts AW, Nicola NA, Li R & Metcalf D (1996). Deficiencies in progenitor cells of multiple hematopoietic lineages and defective megakaryocytopoiesis in mice lacking the thrombopoietic receptor c-Mpl. *Blood* **87:** 2162-2170.

Alexander, JE, Hunt DF, Lee MK, Shabanowitz J, Michel H, Berlin SC, Macdonald TL, Sundberg RJ, Rebhun LI & Frankfurter A (1991). Characterization of posttranslational modifications in neuron-specific class III beta-tubulin by mass spectrometry. *Proc Nat Acad Sci* **88**: 4685-4689.

Andrews NC, Erdjument-Bromage H, Davidson MB, Tempst P & Orkin SH (1993). Erythroid transcription factor NF-E2 is a haematopoietic-specific basic-leucine zipper protein. *Nature* **362**: 722-728.

Andrews RK & Fox JEB (1996). Identification of a region from the cytoplasmic domain of the platelet membrane GP Ib-IX complex that binds to purified actin-binding protein*. J Biol Chem* **267**: 18605-18611.

Arce CA, Rodriguez JA, Barra HS & Caputto R (1975). Incorporation of l-Tyrosine, l-Phenylalanine and l-3, 4-Dihydroxyphenylalanine as Single Units into Rat Brain Tubulin. *European Journal of Biochemistry* **59**: 145-149.

Aslan JE, Phillips KG, Healy LD, Itakura A, Pang J & McCarty OJ (2013). Histone deacetylase 6-mediated deacetylation of α-tubulin coordinates cytoskeletal and signaling events during platelet activation. *Am J Physiol-Cell Physiol* **305**: 1230-1239.

Authi KS, Crawford N (1985). Inositol 1,4,5-trisphosphate-induced release of sequestered Ca^{2+} from highly purified human platelet intracellular membranes. *Biochem J* **230**: 247–253.

Azzam K, Cisse-Thiam M & Drouet L (1996). The antithrombotic effect of aurin tricarboxylic acid in the guinea pig is not solely due to its interaction with the von Willebrand factor-GPIb axis. *Thromb Haemost* ***75***: 203-210

Behnke O (1965). Further studies on microtubules. A marginal bundle in human and rat thrombocytes. *J Ultrastruct Res* **13**: 469–477.

Behnke O (1967). Electron microscopic observations on the membrane systems of the rat blood platelet. *Anat Rec* **158**: 121–137.

Behnke O (1968) Electron microscopical observations on the surface coating of human blood platelets. *J Ultrastruct Res* **24**: 51–69.

Bennett JS (2005). Structure and function of the platelet integrin $\alpha_{IIb}\beta_3$. *J Clin Inv* **115**: 3363.

Bentfeld-Barker ME & Bainton DF (1982). Identification of primary lysosomes in human megakaryocytes and platelets. *Blood* **59:** 472-481.

Bergmeier W, Oh-Hora M, McCarl CA, Roden RC, Bray PF & Feske S (2009). R93W mutation in Orai1 causes impaired calcium influx in platelets. *Blood* **113**: 675–678.

Berna-Erro A, Jardín I, Smani T & Rosado JA (2016). Regulation of Platelet Function by Orai, STIM and TRP. In *Calcium Entry Pathways in Non-excitable Cells* pp157-181. Springer International Publishing.

Berridge MJ, Lipp P & Bootman MD (2000). The versatility and universality of calcium signalling. *Nat Rev Mol Cell Biol* **1**: 11–21.

Bers DM, Patton CW & Nuccitelli R (2010). A Practical Guide to the Preparation of Ca^{2+} Buffers.*Methods Cell Biol* **99**: 1-26.

Bieback K, Hec A, Ker A, Kocaomer Lannert H, Schallmoser K, Strunk D & Kluter H (2009). Human alternatives to fetal bovine serum for the expansion of mesenchymal stromal cells from bone marrow. *Stem Cells* **27**: 2331-2341.

Bobe R, Bredoux R, Wuytack F, Quarck R, Kovacs T, Papp B, Corvazier E, Magnier C & Enouf J (1994). The rat platelet 97-kDa Ca^{2+} ATPase isoform is the sarcoendoplasmic reticulum Ca^{2+} ATPase 3 protein. *J Biol Chem* **269**: 1417–1424.

Born GV (1972). Current ideas on the mechanism of platelet aggregation. *Ann N Y Acad Sci* **201**: 4–12.

Brass LF & Joseph SK (1985). A role for inositol triphosphate in intracellular Ca^{2+} mobilization and granule secretion in platelets. *J Biol Chem* **260**: 15172–15179.

Brass LF, Stalker TJ, Zhu L & Woulfe DS (2006). Signal transduction during platelet plug formation. In: *Platelets*, 2nd Edn ,eds Michelson AD (Burlington, VT: Academic Press), 1376.

Brass LF, Wannemacher KM, Ma P & Stalker TJ (2011). Regulating thrombus growth and stability to achieve an optimal response to injury. *J Thromb Haemost* **9**: 66-75.

Brass LF (2003). Thrombin and platelet activation. *CHEST Journal* **124**: 18-25.

Braun A, Varga-Szabo D, Kleinschnitz C, Pleines I, Bender M, Austinat M, Bosl M, Stoll G, Nieswandt B (2009). Orai1 (CRACM1) is the platelet SOC channel and essential for pathological thrombus formation. *Blood* **113**: 2056–2063.

Breton-Gorius J & Guichard J (1972). Ultrastructural localization of peroxidase activity in human platelets and megakaryocytes. *Am J Pathol* **66**: 277-293.

Breton-Gorius J & Reyes F (1975). Ultrastructure of human bone marrow cell maturation. International review of cytology **46**: 251-321.

Brownlow SL & Sage SO (2005). Transient receptor potential protein subunit assembly and membrane distribution in human platelets. *Thromb Haemost* **94:** 839-845.

Brunner D, Frank J, Appl H, Schoffl H, Pfaller W & Gstraunthaler G (2010). Serum-free cell culture:the serum-free media interactive online database. *ALTEX* **27**: 53-62.

Burkhart JM, Vaudel, M., Gambaryan S, Radau S., Walter U, Martens L, Geiger J, Sickmann A & Zahedi RP (2012). The first comprehensive and quantitative analysis of human platelet protein composition allows the comparative analysis of structural and functional pathways. *Blood* **120**: 73-82.

Cai D, McEwen DP, Martens JR, Meyhofer E & Verhey KJ (2009). Single molecule imaging reveals differences in microtubule track selection between Kinesin motors. *PLoS Biol*, **7**: 1000216.

Canizares C, Vivar N & Grijalva J (1990), Thrombocytopathy due to a defect of the platelet membrane complex. *Acta Haematol* **83**: 99-104.

Castellot JJ, Favreau LV, Karnovsky MJ & Rosenberg RD (1982). Inhibition of vascular smooth muscle cell growth by endothelial cell-derived heparin. Possible role of a platelet endoglycosidase. *J Biol Chem* **257**: 11256–11260.

Cavallini L, Coassin M & Alexandre A (1995). Two classes of agonist-sensitive Ca^{2+} stores in platelets, as identified by their differential sensitivity to 2,5-di-(tert-butyl)-1,4-benzohydroquinone and thapsigargin. *Biochem J* **310**: 449-52.

Cedazo-Minguez A, Bonecchi L, Winblad B, Post C, Wong EHF, Cowburn RF & Benatti, L (1999). Nicergoline stimulates protein kinase C mediated α-secretase processing of the amyloid precursor protein in cultured human neuroblastoma SH-SY5Y cells. *Neurochem int* **35**: 307-315.

Cerecedo D, Cisneros B, Mondragón R, González S & Galván IJ (2010). Actin filaments and microtubule dual-granule transport in human adhered platelets: the role of α-dystrobrevins. *Br J Haematol* **149**: 124-136.

Chakraborti S, Natarajan K, Curiel J, Janke C & Liu J (2016). The emerging role of the tubulin code: from the tubulin molecule to neuronal function and disease. *Cytoskeleton*, **73**: 521-550.

Chu CW, Hou F, Zhang J, Phu L, Loktev AV, Kirkpatrick DS, Jackson PK, Zhao Y & Zou H (2011). A novel acetylation of β-tubulin by San modulates microtubule polymerization via down-regulating tubulin incorporation. *Mol Biol Cell* **22**: 448-456.

Civin CI, Strauss LC, Brovall C, Fackler MJ, Schwartz JF & Shaper JH (1984). Antigenic analysis of hematopoiesis. III. A hematopoietic progenitor cell surface antigen defined by a monoclonal antibody raised against KG-1a cells. *J Immunol* **133**: 157-165.

Cohen I, Gerrard JM & White JG (1982). Ultrastructure of clots during isometric contraction. *J Cell Biol* **93**: 775-787.

Cortin V, Garnier A, Pineault N, Lemieux R, Boyer L & Proulx C (2005). Efficient in vitro megakaryocyte maturation using cytokine cocktails optimized by statistical experimental design. *Exp Hematol* **33**: 1182–1191.

Coxon CH, Lewis AM, Sadler AJ, Vasudevan SR, Thomas A, Dundas KA, Taylor L, Campbell RD, Gibbins JM, Churchill GC & Tucker KL (2012). NAADP regulates human platelet function. *Biochem J* **441**: 435-442.

Cutler L, Rodan G & Feinstein MB (1978). Cytochemical localization of adenylate cyclase and of calcium ion, magnesium ion-activated ATPases in the dense tubular system of human blood platelets. *Biochim Biophys Acta* **542**: 357-371.

Daniel JL, Molish IR, Rigmaiden M & Stewart G (1984). Evidence for a role of myosin phosphorylation in the initiation of the platelet shape change response. *J Biol Chem* **259**: 9826-9831.

De Bruyn C, Delforge A, Martiat P & Bron D (2005). Ex vivo expansion of megakaryocyte progenitor cells: cord blood versus mobilized peripheral blood. *Stem Cells Dev* **14**: 415-424.

Debili N, Robin C, Schiavon V, Letestu R, Pflumio F, Mitjavila-Garcia MT, Coulombel L. & Vainchenker W (2001). Different expression of CD41 on human lymphoid and myeloid progenitors from adults and neonates. *Blood* **97**: 2023-2030.

Deutsch VR & Tomer A (2006). Megakaryocyte development and platelet production. *Br J Haematol* **134**: 453-466.

Diagouraga B, Grichine A, Fertin A, Wang J, Khochbin S & Sadoul K (2014). Motor-driven marginal band coiling promotes cell shape change during platelet activation. *J Cell Biol* **204**: 177-185.

Dolzhanskiy A, Basch R & Karpatkin S (1997). The development of human megakaryocytes. 3. Development of mature megakaryocytes from highly purified committed progenitors in synthetic culture media and inhibition of thrombopoietininduced polyploidization by interleukin-3. *Blood* **89**: 426-434.

Dompierre JP, Godin JD, Charrin BC, Cordelieres FP, King SJ, Humbert S & Saudou F (2007). Histone deacetylase 6 inhibition compensates for the transport deficit in Huntington's disease by increasing tubulin acetylation. *J Neurosci* **27**: 3571-3583.

Downing KH & Nogales E (1998). Tubulin and microtubule structure. *Curr Opin Cell Biol* **1**: 16-22.

Drachman J G (2000). Role of thrombopoietin in hematopoietic stem cell and progenitor regulation. *Current Opin Hematol* **7**: 183-190.

Ebbe S & Stohlman F (1965). Megakaryocytopoiesis in the Rat. *Blood* **26:** 20–35.

Ebbeling L, Robertson C, McNicol A & Gerrard JM (1992). Rapid ultrastructural changes in the dense tubular system following platelet activation. *Blood* **80**: 718-723.

Eckly A, Heijnen H, Pertuy F, Geerts W, Proamer F, Rinckel JY & Gachet C (2014). Biogenesis of the demarcation membrane system in megakaryocytes. Blood **123**: 921-930.

Edde B, Rossier J, Gros F, Denoulet P & Desbruyeres E (1990). Posttranslational Glutamylation of (alpha)-Tubulin. *Science* **247**: 83.

Enyedi A, Paszty K, Kovacs T, Sarkadi B, Gardos G, Magnier C, Wuytack F & Enouf J (1992). Simultaneous presence of two distinct endoplasmic-reticulum-type calcium-pump isoforms in human cells. Characterization by radio-immunoblotting and inhibition by 2,5-di-(t-butyl)-1,4-benzohydroquinone. *Biochem, J* **288**: 297–302.

Estacion M, Sinkins WG, Jones SW, Applegate MA & Schilling WP (2006). Human TRPC6 expressed in HEK 293 cells forms non-selective cation channels with limited Ca^{2+} permeability. *J Physiol* **572**: 359–377.

Ezerman EB & Ishikawa H (1967). Differentiation of the sarcoplasmic reticulum and t system in developing chick skeletal muscle in vitro. *J Cell Biol* **2**: 405–420.

Feghhi S & Sniadecki NJ (2011). Mechanbiology of platelets: techniques to study fluid flow and platelet retraction forces at the micro- and nanoscale. *Int J Mol Sci* **12**: 9009-9030.

Feghhi S, Munday AD, Tooley WW, Rajsekar S, Fura AM, Kulman JD, López JA & Sniadecki NJ (2016). Glycoprotein Ib-IX-V complex transmits cytoskeletal forces that enhance platelet adhesion. *Biophysical Journal*, **111**: 601-608.

Feng Y, Zhang L, Xiao Z J, Li B, Liu B, Fan CG & Han ZC (2005). An effective and simple expansion system for megakaryocyte progenitor cells using a combination of heparin with thrombopoietin and interleukin-11. Exp Hematol **33**: 1537-1543.

Firestone AJ, Weinger JS, Maldonado M, Barlan K, Langston LD, O'Donnell M, Gelfand, VI, Kapoor TM & Chen JK (2012). Small-molecule inhibitors of the AAA+ ATPase motor cytoplasmic dynein. *Nature* **484**: 125-129.

Flaumenhaft R (2003). Molecular basis of platelet granule secretion. *Arterioscl Thromb Vasc Biol* **23**: 1152-1160.

Fox JE (1993). The platelet cytoskeleton. *Thromb Haemost* **70**: 884-93.

Fox JE, Boyles JK, Reynolds CC & Phillips DR (1984). Actin filament content and organization in unstimulated platelets. *J Cell Biol* **98**: 1985-1991.

Fujiki H, Kimura T, Minamiguchi H, Harada S, Wang J, Nakao M & Sonoda Y (2002). Role of human interleukin-9 as a megakaryocyte potentiator in culture. *Exp Hematol* **30**: 1373-1380.

Fung CY, Cendana C, Farndale RW & Mahaut-Smith MP (2007). Primary and secondary agonists can use P_{2X1} receptors as a major pathway to increase intracellular Ca^{2+} in the human platelet. *J Thromb Haemost* **5**: 910–917.

Furie B & Furie BC (2008). Mechanism of thrombus formation. *N Engl J Med* **359**: 938-949

Gear AR & Camerini D (2003) Platelet chemokines and chemokine receptors: linking hemostasis, inflammation, and host defense. *Microcirculation* **10**: 335-50.

George JN, Caen JP & Nurden AT (1990). Glanzmann's thrombasthenia: the spectrum of clinical disease. *Blood* **75**: 1383–1395.

George JN & Shattil SJ (1991). The clinical importance of acquired abnormalities of platelet function. *N Engl J Med* **324**: 27-39.

Gerrard J M, White JG & Peterson DA (1978). The platelet dense tubular system: its relationship to prostaglandin synthesis and calcium flux. *Thromb Haemost* **40**: 224–231.

Gerrard JM, White JG, Rao GH & Townsend D (1976). Localization of platelet prostaglandin production in the platelet dense tubular system. *Am J Pathol* **83**: 283-298.

Gibbins JM (2004) Platelets and Megakaryocytes, New Jersey, Humana press Inc.

Gibbs KL, Greensmith L & Schiavo G (2015). Regulation of axonal transport by protein kinases. *Trends Biochem Sci* **40**: 597-610

Gordon MY, Bearpark AD, Clarke D & Dowding CR (1990). Haemopoietic stem cell subpopulations in mouse and man: discrimination by differential adherence and marrow repopulating ability. *Bone Marrow Transplant* **5**: 6–8.

Green D, Ts'ao CH, Cohen I & Rossi EC (1981). Haeorrhagic thrombocytopathy associated with dilatation of the platelet-membrane complex. *Br J Haematol* **48**: 595-600.

Grette K (1962). Studies on the mechanism of thrombin-catalyzed hemostatic reactions in blood platelets. *Acta Physiol Scand* **195**: 1-93.

Grynkiewicz G, Poenie M & Tsien RY (1985). A new generation of Ca^{2+} indicators with greatly improved fluorescence properties. *J Biol Chem* **260**: 3440-3450.

Gurney AL, Carver-Moore K, de Sauvage FJ & Moore MW (1994). Thrombocytopenia in c-mpl-deficient mice. *Science* **265**: 1445–1447.

Hagopian M & Spiro D (1967). The sarcoplasmic reticulum and its association with the t system in an insect. *J Cell Biol* **3**: 535–545.

Hallak ME, Rodriguez JA, Barra HS & Caputto R (1977). Release of tyrosine from tyrosinated tubulin. Some common factors that affect this process and the assembly of tubulin. *FEBS letters* **73**: 147-150.

Handagama PJ, George M, Shuman R, McEver R & Bainton DF (1987). Incorporation of circulating protein into megakaryocyte and platelet granules. *Proc Natl Acad Sci U. S. A* **84**: 861–865.

Harper AGS, Mason MJ & Sage SO (2009). A key role for dense granule secretion in potentiation of the Ca^{2+} signal arising from store-operated calcium entry in human platelets.*Cell Calcium* **45**: 413-420.

Harper MT, Mason MJ, Sage SO & Harper AGS (2010). Phorbol ester-evoked Ca^{2+} signaling in human platelets is via autocrine activation of P_{2X1} receptors, not a novel noncapacitative Ca^{2+} entry*. J. Thromb. Haemost* **8**: 1604–1613.

Harper AGS & Sage SO (2007). A key role for reverse Na^{+}/Ca^{2+} exchange influenced by the actin cytoskeleton in store-operated Ca^{2+} entry in human platelets: evidence against the de novo conformational coupling hypothesis. *Cell Calcium* **42**: 606-617.

Harper MT & Sage SO (2006). Actin polymerisation regulates thrombin-evoked Ca^{2+} signalling after activation of PAR-4 but not PAR-1 in human platelets. *Platelets* **17***:* 134-142.

Harrison P & Cramer EM (1993) Platelet alpha-granules. *Blood Rev* **7**: 52-62.

Hassock S, Zhu MX, Trost C, Flockerzi V & Authi KS (2002). Expression and role of TRPC proteins in human platelets: evidence that TRPC6 forms the store-independent calcium entry channel. *Blood* **100**: 2801-2811.

Hechler B, Lenain N, Marchese P, Vial C, Heim V, Freund M & Gachet C (2003). A role of the fast ATP-gated P2X1 cation channel in thrombosis of small arteries *in vivo*. *J Exp Med* **198**: 661-667.

Heemskerk JWM, Mattheij NJA, Cosemans JMEM (2013). Platelet-based coagulation: different population, different function. *J Thromb Haemost* **11**: 2-11.

Heijnen HF, Debili N, Vainchencker W, Breton-Gorius J, Geuze HJ & Sixma JJ (1998). Multivesicular bodies are an intermediate stage in the formation of platelet alpha granules. *Blood* **91**: 2313–2325.

Heptinstall S (1976). The use of a chelating ion-exchange resin to evaluate the effects of the extracellular calcium concentration on adenosine diphosphate induced aggregation of human blood platelets. *Thromb Haemost* **36**: 208–220.

Hickey MJ, Hagen FS, Yagi M & Roth GJ (1993). Human platelet glycoprotein V: characterization of the polypeptide and the related Ib-V-IX receptor system of adhesive, leucine-rich glycoproteins. *Proc Natl Acad Sci U.S.A.* **90:** 8327-8331.

Hopkins SC, Vale RD & Kuntz ID (2000). Inhibitors of kinesin activity from structure-based computer screening. *Biochemistry* **39**: 2805-2814.

Hubbert C, Guardiola A, Shao R, Kawaguchi Y, Ito A, Nixon A, Yoshida M, Wang XF & Yao TP (2002). HDAC6 is a microtubule-associated deacetylase. *Nature* **417**: 455-458.

Huizing M, Helip-Wooley A, Westbroek W, Gunay-Aygun M & Gahl WA (2008). Disorders of Lysosome-Related Organelle Biogenesis: Clinical and Molecular Genetics. *Annu Rev Genomics Hum Genet* **9**: 359–386.

Ignarro LJ, Buga GM, Wood KS, Byrns RE & Chaudhuri G (1987). Endothelium-derived relaxing factor produced and released from artery and vein is nitric oxide. *Proc Natl Acad Sci U S A* **84**: 9265-9269.

Italiano JE, Lecine P, Shivdasani RA & Hartwig JH (1999). Blood platelets are assembled principally at the ends of proplatelet processes produced by differentiated megakaryocytes. *J Cell Biol* **6**: 1299-1312.

Italiano JJ & Shivdasani RA (2003). Megakaryocytes and beyond: the birth of platelets. *J Thromb Haemost* **1:** 1174-1182.

Jackson S P, Nesbitt WS & Kulkarni S (2003). Signaling events underlying thrombus formation. *J Thromb Haemost* **1:** 1602-1612.

Jackson SP & Schoenwaelder SM (2010). Procoagulant platelets: are they necrotic?. *Blood* **116**: 2011-2018.

Janke C & Bulinski JC (2011). Post-translational regulation of the microtubule cytoskeleton: mechanisms and functions. *Nat Rev Mol Cell Biol* **12**: 773-786.

Janke C & Kneussel M (2010). Tubulin post-translational modifications: encoding functions on the neuronal microtubule cytoskeleton. *Trends Neurosci* **33**: 362-372.

Johansson JS & Haynes DH (1988). Deliberate quin2 overload as a method for *In Situ* characterization of active calcium extrusion systems and cytoplasmic calcium binding: application to the human platelet. J. Membr. Biol **104**: 147-163.

Johnson CP, Tang HY, Carag C, Speicher DW & Discher DE (2007). Forced unfolding of proteins within cells. *Science* **317***:* 663-666.

Jones S, Solomon A, Sanz-Rosa D, Moore C, Holbrook L, Cartwright EJ, Neyes L & Emerson M (2010). The plasma membrane calcium ATPase modulates calcium homeostasis, intracellular signaling events and function in platelets. *J Thromb Haemost* **8**: 2766–2774.

Kahn ML, Zheng YW, Huang W, Bigornia V, Zeng D, Moff S, Farese RV, Jr Tam C, Coughlin SR (1998). A dual thrombin receptor system for platelet activation. *Nature* **394**: 690–694.

Karki S & Holzbaur EL (1999). Cytoplasmic dynein and dynactin in cell division and intracellular transport. *Curr Opin Cell Biol* **11**: 45-53.

Kaser-Glanzmann R, Jakabova M, George JN, Luscher EF (1978). Further characterization of calcium-accumulating vesicles from human blood platelets. *Biochim Biophys Acta* **512**: 1-12.

Kaushansky K, Broudy VC, Lin N, Jorgensen MJ, McCarty J, Fox N, Zucker-Franklin D & Lofton-Day C (1995). Thrombopoietin, the Mp1 ligand, is essential for full megakaryocyte development. *Proc Natl Acad Sci USA* **92**: 3234–3238.

Kaushansky K, Lichtman MA, Kipps TJ, Prchal J (2010). Williams Hematology, Eighth Edition Hardcover. McGraw-Hill Medical.

Kaushansky K. (1999). Thrombopoietin and hematopoietic stem cell development. *Ann. NY Acad. Sci.* **872**: 314–319.

Kessinger A, Armitage JO & Landmark JD (1988). Autologous peripheral hematopoietic stem cell transplantation restores hematopoietic function following marrow ablative therapy. *Blood* **71**: 723–727.

Knight DE & Scrutton MC (1984). Cyclic nucleotides control a system which regulates Ca^{2+} sensitivity of platelet secretion. *Nature* **309**: 66–68.

Knight DE, Niggli V & Scrutton MC (1984). Thrombin and activators of protein kinase C modulate secretory responses of permeabilised human platelets induced by Ca^{2+}. *Eur J Biochem* **143**: 437–446.

Kobayashi M, Laver JH, Kato T, Miyazaki H & Ogawa M (1996). Thrombopoietin supports proliferation of human primitive hematopoietic cells in synergy with steel factor and}or interleukin-3. *Blood* **88**: 429–436.

Kovacs T, Berger G, Corvazier E, Paszty K, Brown A, Bobe R, Papp B, Wuytack F, Cramer EM & Enouf J (1997). Immunolocalization of the multi-sarco/endoplasmic reticulum Ca^{2+} ATPase system in human platelets. *Br J Haematol* **97**: 192–203.

Kovács M, Tóth J, Hetényi C, Málnási-Csizmadia A & Sellers JR (2004). Mechanism of blebbistatin inhibition of myosin II. *J Biol Chem* **279**: 35557-35563.

Kulkarni S & Jackson SP (2004) Platelet factor XIII and calpain negatively regulate integrin alphaIIbbeta3 adhesive function and thrombus growth. *J Biol Chem* **279**: 30697-30706.

Kulkarni S, Dopheide SM, Yap CL, Ravanat C, Freund M, Mangin P, Heel KA, Street A, Harper IS, Lanza F & Jackson SP (2000). A revised model of platelet aggregation. *J Clin Invest* **105**: 783-791.

Lages B & Weiss HD (1999). Secreted dense granule adenine nucleotides promote calcium influx and the maintenance of elevated cytosolic calcium levels in stimulated human platelets. *Thromb Haemost* **81**: 286-292.

LaIuppa JA, Papoutsakis ET & Miller WM (1998). Oxygen tension alters the effects of cytokines on the megakaryocyte, erythrocyte, and granulocyte lineages. *Exp Hematol* **26**: 835–843.

Lanza F, Cazenave JP, Beretz A, Sutter-Bay A, Kretz JG & Kieny R (1986). Potentiation by adrenaline of human platelet activation and the inhibition by the alpha-adrenergic

antagonist nicergoline of platelet adhesion, secretion and aggregation. *Agent Action* **18**: 586-595.

Le Menn R, Migne J & Probst-Djovakovich RJ (1978). Ultrastructural study on the effect of an inhibition of platelet aggregation. *Arzneimittelforschung* **29**: 1278-1282.

Lecine P, Italiano JE, Kim SW, Villeval JL & Shivdasani RA (2000). Hematopoietic-specific beta 1 tubulin participates in a pathway of platelet biogenesis dependent on the transcription factor NF-E2. *Blood* **96**: 1366-1373.

Lesurtel M, Graf R, Aleil B, Walther DJ, Tian Y, Jochum W, Gachet C, Bader M & Clavien PA (2006). Platelet-derived serotonin mediates liver regeneration. *Science* **312**: 104-107.

Lewis SA, Gu W & Cowan NJ (1987) Free intermingling of mammalian beta-tubulin isotypes among functionally distinct microtubules. *Cell* **4**: 539-48.

L'Hernault SW & Rosenbaum JL (1985). Chlamydomonas alpha-tubulin is posttranslationally modified by acetylation on the epsilon-amino group of a lysine. *Biochemistry* **24**: 473-478.

Long MW, Williams N & Ebbe S (1982). Immature megakaryocytes in the mouse: physical characteristics, cell cycle status, and in vitro responsiveness to thrombopoietic stimulatory factor. *Blood* **59**: 569–575.

Lopez JJ, Redondo PC, Salido GM, Pariente JA & Rosado JA (2006). Two distinct Ca^{2+} compartments show differential sensitivity to thrombin, ADP and vasopressin in human platelets. *Cell Signal* **18**: 373–381.

Luft T, Pang KC, Thomas E, Bradley CJ, Savoia H, Trapani J, Cebon J (1998). A serum-free culture model for studying the differentiation of human dendritic cells from adult $CD34^{+}$ progenitor cells. *Exp Hematol* **26:** 489-500.

Mackenzie AB, Mahaut-Smith MP & Sage SO (1996). Activation of receptor-operated cation channels via P_{2X1} not P_{2T} purinoceptors in human platelets. *J Biol Chem* **271**: 2879–2881.

Mahaut-Smith MP (2004). Emerging roles for P_{2X1} receptors in platelet activation. *Platelets* **15**: 131–44.

Mahaut-Smith MP, Thomas D, Higham AB, Usher-Smith JA, Hussain JF, Martinez-Pinna J, Skepper JN & Mason MJ (2003). Properties of the demarcation membrane system in living rat megakaryocytes. *Biophys J* **84**: 2646-2654.

Marcus AJ, Broekman MJ & Pinsky DJ (2002). COX inhibitors and thromboregulation. *N Engl J Med* **347**: 1025-1026.

Marcus AJ, Broekman MJ, Drosopoulos JH, Olson KE, Islam N, Pinsky DJ & Levi R (2005). Role of CD39 (NTPDase-1) in thromboregulation, cerebroprotection, and cardioprotection. *Semin Thromb Hemost* **31**: 234-246.

Marcus AJ, Zucker-Franklin D, Safier LB & Ullman HL (1966). Studies on human platelet granules and membranes. *J Clin Invest* **45**: 14-28.

Markello T, Chen D, Kwan JY, Horkayne-Szakaly I, Morrison A, Simakova O5, Maric I, Lozier J, Cullinane AR, Kilo T, Meister L, Pakzad K, Bone W, Chainani S, Lee E, Links A, Boerkoel C, Fischer R, Toro C, White JG, Gahl WA & Gunay-Aygun M (2015). York platelet syndrome is a CRAC channelopathy due to gain-of-function mutations in STIM1. *Mol Genet Metab* **114**: 474-482.

Martin JH, Carson FL & Race GJ (1974). Calcium-containing platelet granules. *Cell Biology* **60**: 775-777.

Marx A, Hoenger A & Mandelkow E (2009). Structures of kinesin motor proteins. *Cytoskeleton* **66**: 958-966.

Matsunaga T, Tanaka I, Kobune M, Kawano Y, Tanaka M, Kuribayashi K, Iyama S, Sato T, Sato Y, Takimoto R, Takayama T, Kato J, Ninomiya T, Hamada H & Niitsu Y (2006). Ex vivo large-scale generation of human platelets from cord blood $CD34^+$ cells. *Stem Cells* **24**: 2877-2887.

Maynard DM, Heijnen HF, Horne MK, White JG & Gahl WA (2007). Proteomic analysis of platelet alpha-granules using mass spectrometry. *J Thromb Haemost* **5**: 1945-1955.

Mazzucato M, Pradella P, Cozzi MR, de Marco L & Ruggeri ZM (2002). Sequential cytoplasmic calcium signals in a 2-stage platelet activation process induced by the glycoprotein Ib alpha mechanoreceptor. *Blood* **100**: 2793-2800.

McNicol A & Israels SJ (1999) Platelet dense granules: structure, function and implications for haemostasis. *Thromb Res* **95**: 1-18.

McRedmond J (2007) Finding drug targets through analysis of the platelet transcriptome. *Curr Pharm* **13**: 2662–2667.

Meiamed I, Djaldetti M, Joshua H & Seligsohn (1984). Association of the hemophilia a carrier state and hemorrhagic Thrombocytopathy with dilatation of the platelet membrane complex. *Acta Haematol* **71**: 381-387.

Merdes A, Ramyar K, Vechio JD & Cleveland DW (1996). A complex of NuMA and cytoplasmic dynein is essential for mitotic spindle assembly. *Cell* **87**: 447-458.

Misceo D, Holmgren A, Louch WE, Holme PA, Mizobuchi M, Morales RJ, De Paula AM, Stray-Pedersen A, Lyle R, Dalhus B, Christensen G, Stormorken H, Tjønnfjord GE & Frengen E (2014). A Dominant STIM1 Mutation Causes Stormorken Syndrome.*Hum. Mutat* **35**: 556-564.

Morita Y, Iseki A, Okamura S, Suzuki S, Nakauchi H & Ema H. (2011). Functional characterization of hematopoietic stem cells in the spleen. *Exp Hematol* **39**: 351–359.

Mostafa S S, Papoutsakis ET & Miller WM (2001). Oxygen tension modulates the 27 expression of cytokine receptors, transcription factors, and lineage-specific markers in 28 cultured human megakaryocytes, *Exp Hematol* **29:** 873–883.

Mostafa SM., Papoutsakis ET & Miller WM (2000). Oxygen tension has significant effects on human megakaryocyte maturation*. Exp. Hematol* **28**: 1498.

Nakamura S, Nakagawa Y, Nakajima M, Endo H, Dohda T, Takayama N, Nakauchi H, Arai F, Fukuda T & Eto K (2013).Two differential flows in a bioreactor promoted platelet generation from human pluripotent stem cell-derived megakaryocytes. *Exp Haematol* **41**: 742-748.

Nakao K & Angrist AA (1968) Membrane surface specialization of blood platelet and megakaryocyte. *Nature* **217**: 960–961.

Nesbitt WS, Giuliano S, Kulkarni S, Dolpheide SM, Harper IS & Jackson SP (2003). Intercellular calcium communication regulates platelet aggregation and thrombus growth. *J Cell Biol* **160**: 1151-1161.

Ogawa D (1993). Differentiation and proliferation of haematopoietic stem cells. *Blood* **81**: 2844-2853.

Onohara N, Nishida M, Inoue R, Kobayashi H, Sumimoto H, Sato Y, Mori Y, Nagao T & Kurose H (2006). TRPC3 and TRPC6 are essential for angiotensin II-induced cardiac hypertrophy. *EMBO J* **25**: 5305–5316.

Oury C, Toth-Zsamboki E, Thijs C, Vermylen J, & Hoylaerts MF (2001). The ATP-gated P_{2X1} ion channel acts as a positive regulator of platelet responses to collagen. *Thromb Haemost* **86**:1264-1271

Owens MR & Holme S (1996). Aurin tricarboxylic acid inhibits adhesion of platelets to subendothelium. *Thromb Res* **81**: 177-185.

Painter RG & Ginsberg MH (1984). Centripetal myosin redistribution in thrombin-stimulated platelets: relationship to platelet factor 4 secretion. *Exp Cell Res* **155***:* 198-212.

Palazzo A, Ackerman B & Gundersen GG (2003). Tubulin acetylation and cell motility. *Nature* **421**: 230-230.

Palmer RMJ, Ferrige AG & Moncada S (1987). Nitric oxide release accounts for the biological activity of endothelium-derived relaxing factor. *Nature* **327**: 524-526.

Papp B, Enyedi A, Kovacs T, Sarkadi B, Wuytack F, Thastrup O, Gardos G, Bredoux R, Levy-Toledano S & Enouf J (1991). Demonstration of two forms of calcium pumps by thapsigargin inhibition and radioimmunoblotting in platelet membrane vesicles. *J. Biol. Chem* **266**: 14593–14596.

Parker RI, Bray GL, McKeown LP & White JG (1993). Failure to mobilise intracellular calcium in response to thrombin in a patient with familial thrombocytopathy characterized by macrothrombocytopenia and abnormal platelet membrane complex. *J Lab Clin Med* **122**: 441-449.

Patel SR, Hartwig JH & Italiano JE Jr (2005). The biogenesis of platelets from megakaryocyte proplatelets. *J Clin Invest* **115**: 3348-3354.

Patel-Hett S, Richardson J.L., Schulze, H., Drabek, K., Isaac, N.A., Hoffmeister, K., Shivdasani, R.A., Bulinski JC, Galjart N, Hartwig JH & Italiano JE (2008). Visualization of microtubule growth in living platelets reveals a dynamic marginal band with multiple microtubules. *Blood* **111**: 4605-4616.

Paul BZ, Daniel JL & Kunapuli SP (1999). Platelet shape change is mediated by both calcium-dependent and-independent signaling pathways Role of p160 Rho-associated coiled-coil-containing protein kinase in platelet shape change. *J Biol Chem* **274**: 28293-28300.

Paulus JM, Bury J & Grosdent JC (1979). Control of platelet territory development in megakaryocytes*. Blood* Cells **5**: 59.

Phillips MD, Moake JL, Nolasco L & Turner N (1988). Aurin tricarboxylic acid: a novel inhibitor of the association of von Willebrand factor and platelets. *Blood* **72**: 1898-1903.

Pineault N, Boucher JF, Cayer MP, Palmqvist L, Boyer L, Lemieux R & Proulx C (2008).Characterization of the effects and potential mechanisms leading to increased megakaryocytic differentiation under mild hyperthermia. *Stem Cells Dev* **17**: 483–493.

Pineault N, Robert A, Cortin V & Boyer L (2013). *Ex vivo* differentiation of cord blood stem cells into megakaryocytes and platelets. *Methods Mol Biol* **946**: 205-224.

Piperno G, LeDizet M & Chang XJ (1987). Microtubules containing acetylated alpha-tubulin in mammalian cells in culture. *J Cell Biol* **104**: 289-302.

Proulx C, Boyer L, Humanen D R & Lemieux R (2003). Preferential ex vivo expansion of megakaryocytes from human cord blood $CD34^+$-enriched cells in the presence of thrombopoietin and limiting amounts of stem cell factor and Flt-3 ligand. *J Hematother Stem Cell Res* **12**: 179–188.

Proulx C, Dupuis N, St-Amour I, Boyer L & Lemieux R (2004). Increased megakaryopoiesis in cultures of $CD34^+$-enriched cord blood cells maintained at 39 degrees C. *Biotechnol Bioeng* **88**: 675–680.

Qudenrijn SVD, Bruin M & Folman CC (2000). Mutations in the thrombopoietin receptor, Mpl, in children with congenital amegakaryocytic thrombocytopenia. *Br J Hematol* **110**: 441–448.

Radley JM & Haller CJ (1982). The demarcation membrane system of the megakaryocyte: a misnomer*? Blood* **60**: 213–219.

Ramanathan G, Gupta S, Thielmann I, Pleines I, Varga-Szabo D, May F, Mannhalter C, Dietrich A, Nieswandt B & Braun A (2012). Defective diacylglycerol-induced Ca^{2+} entry but normal agonist-induced activation responses in TRPC6-deficient mouse platelets. *J Thromb Haemost* **10**: 419-429.

Redeker V, Levilliers N, Schmitter JM & Le Caer JP (1994). Polyglycylation of tubulin: a posttranslational modification in axonemal microtubules. *Science* **266***:* 1668.

Redeker V, Melki R, Promé D, Le Caer JP & Rossier J (1992). Structure of tubulin C-terminal domain obtained by subtilisin treatment The major α and β tubulin isotypes from pig brain are glutamylated. *FEBS letters* **313**: 185-192.

Reed NA, Cai D, Blasius TL, Jih GT, Meyhofer E, Gaertig J & Verhey KJ (2006). Microtubule acetylation promotes kinesin-1 binding and transport. *Curr Biol* **16**: 2166–2172.

Reed GL (2007). Platelet Secretion. In: Michelson AD, editor. Platelets. San Diego: *Elsevier Science* 181–195.

Reems JA, Pineault N & Sun S (2010) In vitro megakaryocyte production and platelet biogenesis: state of the art. *Transfus Med Rev* **24**: 33–43.

Richardson JL, Shivdasani RA, Boers C, Hartwig JH, Italiano JR (2005). Mechanisms of organelle transport and capture along proplatelets during platelet production. *Blood* **106**: 4066–4075.

Rink TJ & Sage SO (1990) Calicum signalling in human platelets. *Annu Rev Physiol* **52**: 429-447.

Rittenhouse SE & Allen CL (1982). Synergistic activation by collagen and 15-hydroxy-9 alpha,11-alpha-peroxidoprosta-5,13-dienoic acid (PGH2) of phosphatidylinositol metabolism and arachidonic acid release in human platelets. *J Clin Invest* **70**: 1216–1224.

Robert A, Cortin V, Garnier A & Pineault N (2012). Megakaryocyte and platelet production from human cord blood stem cells. *Methods Mol Biol* **788**: 219-247.

Roberts DE, Matsuda T, & Bose R (2012). Molecular and functional characterization of the human platelet Na^{+}/Ca^{2+} exchangers. *Br J Pharmacol* **165**: 922-936.

Rosado JA, Brownlow SL & Sage SO (2002). Endogenously expressed Trp1 is involved in store-mediated Ca^{2+} entry by conformational coupling in human platelets. *J Biol Chem* **277**: 42157–42163.

Rosado JA, Jenner S & Sage SO (2000). A role for the actin cytoskeleton in the initiation and maintenance of store-mediated calcium entry in human platelets. Evidence for conformational coupling. *J Biol Chem* **275:** 7527-7533.

Rosado, JA & Sage SO (2000). The actin cytoskeleton in store-mediated calcium entry. *The Journal of Physiology* **526**: 221-229.

Ruas M, Chuang KT, Davis LC, Al-Douri A, Tynan PW, Tunn R, Teboul L, Galione A & Parrington J (2014). TPC1 has two variant isoforms, and their removal has different effects on endo-lysosomal functions compared to loss of TPC2. *Mol Cell Biol* **34**: 3981-3992.

Ruas M, Davis LC, Chen CC, Morgan AJ, Chuang KT, Walseth TF, Grimm C, Garnham C, Powell T, Platt N, Platt FM, Biel M, Wahl-Schott C, Parrington J & Galione A (2015). Expression of Ca^{2+}-permeable two-pore channels rescues NAADP signalling in TPC-deficient cells. *EMBO J* **34**: 1743-1758.

Ruiz FA, Lea CR, Oldfield E & Docampo R (2004). Human platelet dense granules contain polyphosphate and are similar to acidocalcisomes of bacteria and unicellular eukaryotes. *J Biol Chem* **279**: 44250-44257.

Sadoul K, Wang J, Diagouraga B, Vitte AL, Buchou T, Rossini T, Polack B, Xi X, Matthias P & Khochbin S (2012). HDAC6 controls the kinetics of platelet activation. *Blood* **120**: 4215-4218.

Sage SO, Pugh N, Mason MJ & Harper AGS (2011). Monitoring the intracellular Ca^{2+} concentration in agonist-stimulated, intact human platelets using Fluo-5N. *J Thromb Haemost* **9**: 540–551.

Sage SO, Pugh N, Farndale RW & Harper AGS (2013). Pericellular Ca^{2+} recycling potentiates thrombin-evoked Ca2+ signals in human platelets. *Physiol Rep* **1**: e00085.

Schatten G, Simerly C, Asai DJ, Szöke E, Cooke P & Schatten H (1988). Acetylated α-tubulin in microtubules during mouse fertilization and early development. *Dev Biol* **130**: 74-86.

Schattner M, Lefebvre P, Mingolelli SS, Goolsby CL, Rademaker A, White JG & Cohen I (1996). Thrombopoietin-Stimulated ex Vivo Expansion of Human Bone Marrow Megakaryocytes. *Stem Cells* **14**: 207-214.

Schulze H, Korpal M, Hurov J, Kim SW, Zhang J, Cantley LC, Graf T & Shivdasani RA (2006). Characterization of the megakaryocyte demarcation membrane system and its role in thrombopoiesis. *Blood* **107:** 3868–3875.

Schulze E, Asai DJ, Bulinski JC & Kirschner M (1987). Posttranslational modification and microtubule stability. *J Cell Biol* **105**: 2167-2177.

Schwer HD, Lecine P, Tiwari S, Italiano JE, Hartwig JH & Shivdasani RA (2001). A lineage-restricted and divergent beta-tubulin isoform is essential for the biogenesis, structure and function of blood platelets. *Curr Biol* **11**: 579-586.

Sehgal S & Storrie B (2009). Evidence that differential packaging of the major platelet granule proteins von Willebrand factor and fibrinogen can support their differential release. *J Thromb Haemost* **5**: 2009-2016.

Sidney LE, Branch MJ, Dunphy SE, Dua HS & Hopkinson A (2014). Concise review: evidence for CD34 as a common marker for diverse progenitors. *Stem Cells* **32**: 1380-1389.

Sitnicka E, Lin N, Priestle, GV, Fox N, Broudy VC, Wolf NS & Kaushansky K (1996). The effect of thrombopoietin on the proliferation and differentiation of murine hematopoietic stem cells. *Blood* **87**: 4996-5005.

Song Y & Brady ST (2015). Post-translational modifications of tubulin: pathways to functional diversity of microtubules. *Trends Cell Biol **25***: 125-136.

Sullivan KF (1988). Structure and utilization of tubulin isotypes. *Annu Rev Cell Biol* **4**: 687-716.

Suzuki-Inoue K, Hughes CE, Inoue O, Kaneko M, Cuyun-Lira O, Takafuta T, Watson SP & Ozaki Y (2007). Involvement of Src kinases and PLCγ2 in clot retraction. *Thromb Res* **120**: 251-258.

Szyk A, Deaconescu AM, Spector J, Goodman B, Valenstein ML, Ziolkowska NE, Kormendi V, Grigorieff N & Roll-Mecak A (2014). Molecular basis for age-dependent microtubule acetylation by tubulin acetyltransferase. *Cell* **157**: 1405-1415.

Takiguchi Y, Shimazawa M and Nakashima M (1996). A comparative study of the antithrombotic effect of aurintricarboxylic acid on arterial thrombosis in rats and guinea-pigs. *Br J Pharmacol* **118**: 1633-1638.

Tavassoli M (1980). Megakaryocyte--platelet axis and the process of platelet formation and release. *Blood* **55**: 537-545.

Tronik-Le Roux D, Roullot V, Schweitzer A, Berthier R &Marguerie G (1995). Suppression of erythro-megakaryocytopoiesis and the induction of reversible thrombocytopenia in mice transgenic for the thymidine kinase gene targeted by the platelet glycoprotein αIIb promoter. *J Exp Med* **181**: 2141–2151.

Valant PA, Adjei PN & Haynes DH (1992). Rapid Ca^{2+} extrusion via the Na^{+}/Ca^{2+} exchanger of the human platelet*. J Membr Biol* **130**: 63–82.

Van Breemen C, Fameli N, Evans AM (2013). Pan-junctional sarcoplasmic reticulum in vascular smooth muscle: nanospace Ca^{2+} transport for site-and function-specific Ca^{2+} signaling. *J Physiol* **591**: 2043-2054.

van Gestel MA, Heemskerk JW, Slaaf DW, Heijnen VVT, Sage SO & Reneman RS (2003). Real-time detection of activation patterns in individual platelets during thromboembolism in vivo: differences between thrombus growth and embolus formation. *J Vasc Res* **39**: 534-543.

van Nispen tot Pannerden H, de Haas F, Geerts W, Posthuma G, van Dijk S, Heijnen HF (2010). The platelet interior revisited: electron tomography reveals tubular alpha-granule subtypes. *Blood* **116**: 1147-1156.

Vanhaecke T, Papeleu P, Elaut G & Rogiers V (2004). Trichostatin A-like hydroxamate histone deacetylase inhibitors as therapeutic agents: toxicological point of view. *Curr Med Chem* **11**: 1629-1643.

Varga-Szabo D, Authi KS, Braun A, Bender M, Ambily A, Hassock SR, Gudermann T, Dietrich A & Nieswandt B (2008). Store-operated Ca(2+) entry in platelets occurs independently of transient receptor potential (TRP) C1. *Pflugers Arch* **457**: 377-87.

Varga-Szabo D, Braun A & Nieswandt B (2009). Calcium signaling in platelets. *J Thromb Haemost* **7**: 1057-1066.

Várkuti BH, Képiró M, Horváth IÁ, Végner L, Ráti S, Zsigmond Á, Hegyi G, Lenkei Z, Varga M & Málnási-Csizmadia A (2016). A highly soluble, non-phototoxic, non-fluorescent blebbistatin derivative. *Sci Rep* **6**: 26141.

Varma D, Monzo P, Stehman SA & Vallee RB (2008). Direct role of dynein motor in stable kinetochore-microtubule attachment, orientation, and alignment. *J Cell Biol* **182**: 1045-1054.

Vu TK, Hung DT, Wheaton VI & Coughlin SR (1991). Molecular cloning of a functional thrombin receptor reveals a novel proteolytic mechanism of receptor activation. *Cell* **64**: 1057-1068.

Walford T, Musa FI & Harper AGS (2016). Nicergoline inhibits human platelet Ca^{2+} signalling through triggering a microtubule-dependent reorganization of the platelet ultrastructure. *Br J Pharmacol* **173**: 234-247.

Wang D, Villasante A, Lewis SA, Cowan NJ (1986). The mammalian beta-tubulin repertoire: hematopoietic expression of a novel, heterologous beta-tubulin isotype. *J Cell Biol* **103:** 1903-1910.

Watson SP, Reep B, McConnell RT & Lapetina EG (1985). Collagen stimulates [3H]inositol trisphosphate formation in indomethacin-treated human platelets. *Biochem J* **226**: 831–837.

Weiss H J, Baumgartner HR, Tschopp TB, Turitto VT & Cohen D (1978). Correction by factor VIII of the impaired platelet adhesion to subendothelium in von Willebrand disease. *Blood* **51**: 267-279.

Wells AL, Lin AW, Chen LQ, Safer D, Cain SM, Hasson T, Carragher BO, Milligan RA & Sweeney HL (1999). Myosin VI is an actin-based motor that moves backwards. *Nature* **401**: 505-508.

White JG & Burris SM (1984). Morphometry of platelet internal contraction. *Am. J. Pathol* **115**: 412–417.

White JG & Krivit W (1967). An ultrastructural basis for the shape changes induced in platelets by chilling. *Blood* **30**: 625-35.

White JG & Rao GH (1998). Microtubule coils versus the surface membrane cytoskeleton in maintenance and restoration of platelet discoid shape. *Am J Pathol* **152**: 597–609..

White JG (1968a). Effects of colchicine and Vinca alkaloids on human platelets. I. Influence on platelet microtubules and contractile function. *Am J Pathol* **53**: 281-91.

White JG (1968b). The substructure of human platelet microtubules. *Blood* **32:** 638-48.

White JG (1969). The submembrane filaments of blood platelets. *Am J Pathol* **56**: 267-77.

White JG (1972). Interaction of membrane systems in blood platelets. *Am J Pathol* **66**: 295-312.

White JG (1973). Identification of platelet secretion in the electron microscope. *Ser Haematol* **6**: 429-59.

White JG (1974). Electron microscopic studies of platelet secretion. *Prog Hemost Thromb* **2**: 49-98.

White JG (1993). Anatomy and structural organization of the platelets, in hemostasis and thrombosis. Basic principles and clinical practice, 3rd ed, edited by Colman RW, Hirsh J, Marder VJ, Salzman EW. JB Lippincott, *Philadelphia* 397.

Woźniak MJ, Bola B, Brownhill K, Yang YC, Levakova V & Allan VJ (2009). Role of kinesin-1 and cytoplasmic dynein in endoplasmic reticulum movement in VERO cells. *J Cell Sci* **122**: 1979-1989.

Wuytack F, Papp B, Verboomen H, Raeymaekers L, Dode L, Bobe R, Enouf J, Bokkala S, Auth, KS & Casteels R (1994). A sarco/endoplasmic reticulum Ca^{2+}-ATPase 3-type Ca^{2+} pump is expressed in platelets, in lymphoid cells, and in mast cells. *J. Biol. Chem* **269**: 1410–1416.

Yamada E (1957). The fine structure of the megakaryocyte in the mouse spleen. *Acta Anat* **29**: 267–290.

Yang J, Wu J, Jiang H, Mortensen R, Austin S, Manning DR, Woulfe D & Brass LF (2002). Signaling through Gi family members in platelets. Redundancy and specificity in the regulation of adenylyl cyclase and other effectors. *J Biol Chem* **277:** 46035-46042.

Zhang ZG, Zhang L, Tsang W, Goussev A, Powers C, Ho KL,Morrisc D, Smythe S, Collere S & Choppet BS (2001). Dynamic platelet accumulation at the site of the occluded middle cerebral artery and in downstream microvessels is associated with loss of microvascular integrity after embolic middle cerebral artery occlusion. *Brain Research* **912**: 181–194.

Zhu MX, Evans AM, Ma J, Parrington J, Galione A (2010). Two-pore channels for integrative Ca signaling. *Common Integr Biol*. **1**:12-7.

Zucker-Franklin D & Petursson S (1984). Thrombocytopoiesis--analysis by membrane tracer and freeze-fracture studies on fresh human and cultured mouse megakaryocytes. *J Cell Biol* **99**: 390-402.

Zucker-Franklin D (1981). Megakaryocytes and Platelets. In: Atlas of Blood Cells D Zucker-Franklin, M. F Greaves, C E. Grossi, and A M Marmont, editors Lea At Febiger, Philadelphia. Chap. 10

Zucker-Franklin D (1989). The relationship of alpha granules to the membrane systems of platelets and megakaryocytes. *Blood Cells* **15**: 73-79.

Zucker-Franklin D (1997). Platelet Structure and Function. Thrombopoiesis and Thrombopoietins. *Humana Press*.